1985

Geochemistry and petrology of the Lake Vermilion Formation, Ely Greenstone Belt, northeastern Minnesota

Scott E. Robinson
University of North Dakota

GEOCHEMISTRY AND PETROLOGY OF THE LAKE VERMILION FORMATION, ELY GREENSTONE BELT, NORTHEASTERN MINNESOTA

by
SCOTT E. ROBINSON

Bachelor of Science, University of Minnesota, Duluth, 1979
Bachelor of Arts, University of Minnesota, Duluth, 1980

A Thesis

Submitted to the Graduate Faculty

of the

University of North Dakota

in partial fulfillment of the requirements

for the degree of

Master of Science

Grand Forks, North Dakota

November
1985

This thesis submitted by SCOTT E. ROBINSON in partial fulfillment of the requirements for the Degree of Master of Science from the University of North Dakota is hereby approved by the Faculty Advisory Committee under whom the work has been done.

_____

_____

_____

This thesis meets the standards for appearance and conforms to the style and format requirements of the Graduate School of the University of North Dakota, and is hereby approved.

_____

Title GEOCHEMISTRY AND PETROLOGY OF THE LAKE VERMILION FORMATION, ELY GREENSTONE BELT, NORTHEASTERN MINNESOTA

Department Geology

Degree Master of Science

In presenting this thesis in partial fulfillment of the requirements for a graduate degree from the University of North Dakota, I agree that the Library of this University shall make it freely available for inspection. I further agree that permission for extensive copying for scholarly purposes may be granted by the professor who supervised my thesis work or, in his absence, by the Chairman of the Department or the Dean of the Graduate School. It is understood that any copying or publication or other use of this thesis or part thereof for financial gain shall not be allowed without my written permission. It is also understood that due recognition shall be given to me and to the University of North Dakota in any scholarly use which may be made of any material in my thesis.

Signature _____

Date _____

TABLE OF CONTENTS

LIST OF TABLES

LIST OF ILLUSTRATIONS

Figure

Dedication

This thesis is dedicated to my mother, who, though she never held the finished product, saw it and greeted it from afar.

ABSTRACT

Alteration in the Lake Vermilion Formation took place at low water/rock ratios. Calculations using the method of Grescens (1967) indicate that the amount of open-system elemental exchange was slight. During secondary alteration, Ca, Na, K, Rb, Sr, and Ba were very mobile; Mg and Fe were less mobile; Si, Al, Ti, Zr, Y, and Ni were slightly mobile. Chemically the rocks resemble modern spilites and keratophyres.

The dacites and basalts are depleted in Ti, Zr, and Y relative to Tertiary igneous rocks of similar composition. The Lake Vermilion Formation basalts display a volcanic arc basalt trend of constant TiO_2 with increasing Zr, similar to low-K tholeiites of the island arc tholeiitic series. The few Lower Ely basalt samples are similar. The Upper Ely samples display a trend of increasing TiO_2 with increasing Zr, similar to ocean-floor basalts.

The Vermilion igneous rocks' Ti-Zr-Y systematics are of the convergent plate-margin "Andean" type of Pearce and Norry (1979). Partial melting of mantle peridotite could produce the Ti-Zr-Y covariations observed in the basalts. Partial melting of amphibolite or eclogite with biotite in the residuum could produce the Ti-Zr-Y trend observed in the dacites.

The graywackes of the Lake Vermilion Formation have compositions resembling the dacites and are derived from them.

The chloritic facies graywackes may be equivalents of the biotitic graywackes which have been subjected to retrograde metamorphism. The slates and many graywackes are higher in Fe_2O_3T, MgO, Ni, and Cr than the dacites, indicating the presence of mafic components or derivation from intermediate (andesitic) volcanics. No evidence for plutonic components in the LVF graywackes was found.

The Vermilion igneous and sedimentary rocks closely resemble rocks formed in young ensimatic island arcs in their chemistry, mineralogy, and abundance of rock types. Formation of the district by an accretionary-tectonic mechanism could explain its structural and geochemical characteristics.

Acknowledgements

Lo, these are but the outskirts of His ways,
and how small a whisper do we hear of Him!
Job 26:14

I am greatly indebted to Dr. Richard W. Ojakangas for providing the initial focus for this study, and for many helpful discussions. I am indebted to Dr. David Southwick for providing a much-needed initiation to the Vermilion District. Thanks to Kyle Harriss, Chris Robinson, Laird Eklund, and my father, Mr. W. T. Robinson, for their assistance during fieldwork. I am grateful to Dr. Robert Stevenson for his patience and guidance, especially during the analytical phases of this study. I would like to thank my committee, Dr. Dexter Perkins, Dr. Will Gosnold, and Dr. Frank Karner, for their thorough and insightful comments. Dr. Richard W. Ojakangas and Dr. Gilbert N. Hanson reviewed the manuscript, and their help is gratefully acknowledged.

My family has given me invaluable moral support and material aid throughout the duration of this project, and I thank them for their faith in me. Special thanks go to Penny Palmer, a very special friend who drafted many of the figures and typed the bibliography, and who never failed to encourage me.

Lastly, and most importantly, I acknowledge the Lord for showing me how faithful He really can be! I thank Him for picking me up and dusting me off many times, and keeping me on the path (Proverbs 3:5-6).

LIST OF ABBREVIATIONS USED IN THE TEXT

CAB -- Calc-alkaline basalt (synonymous with IAB)

CSB -- Carolina Slate Belt

Fm -- Total Fe as Fe_2O_3+MgO+MnO

FeO* -- Total Fe as FeO

Fe_2O_3T -- Total Fe as Fe_2O_3

FV -- Felsic volcaniclastic member of Lake Vermilion Formation

HFS -- High field strength elements (generally Ti, Y, and Zr)

HREE -- Heavy rare-earth elements

IAB -- Island arc basalt (synonymous with CAB)

KLG -- Knife Lake Group

LKT -- Low-K tholeiite

LREE -- Light rare-earth elements

LVF -- Lake Vermilion Formation

MORB -- Mid-ocean ridge basalt

mybp -- Million years before present

OFB -- Ocean-floor basalt

PNG -- Papua New Guinea

REE -- Rare earth elements

WPB -- Within-plate basalt, i.e., ocean island basalt

XRD -- X-ray diffractometry

INTRODUCTION AND BACKGROUND

Geologic Setting

The discussion which follows is largely drawn from Sims (1976) plus references in the Minnesota Geological Survey's centennial volume (Sims and Morey, 1972).

The Vermilion District of northeastern Minnesota is an extension of the Shebandowan volcanic-plutonic belt. It is typical of Archean granite-greenstone terranes of the Canadian Shield. The district consists of a nearly linear belt 10 to 30 km wide and more than 160 km long, The belt is made up of metavolcanic-metasedimentary rock units which represent the complexly folded and faulted remnants of many volcanic centers with intervening small sedimentary basins, all of which have been intruded and isoclinally folded by synorogenic trondhjemitic and granitic plutons (Figure 1). Volcanism, sedimentation, and plutonism all took place within 50 myr from 2750 to 2700 m.y.b.p. (Goldich, 1972). The Ely Greenstone belt is synformal, and has been offset by a number of strike-slip faults of what is termed the Vermilion Fault System. This faulting has imparted an imbricate pattern to the rock units of the district, producing its beltlike geometry. The belt is truncated on the north by the Vermilion Granite-Migmatite Massif along the Vermilion Fault, which brings amphibolite grade rocks on the north into contact with greenschist grade rocks on the south. The belt is bounded to the south by the Giants Range batholith, which truncates

Fig. 1 -- Geologic map of the Vermilion District and surrounding regions (Sims, 1973).

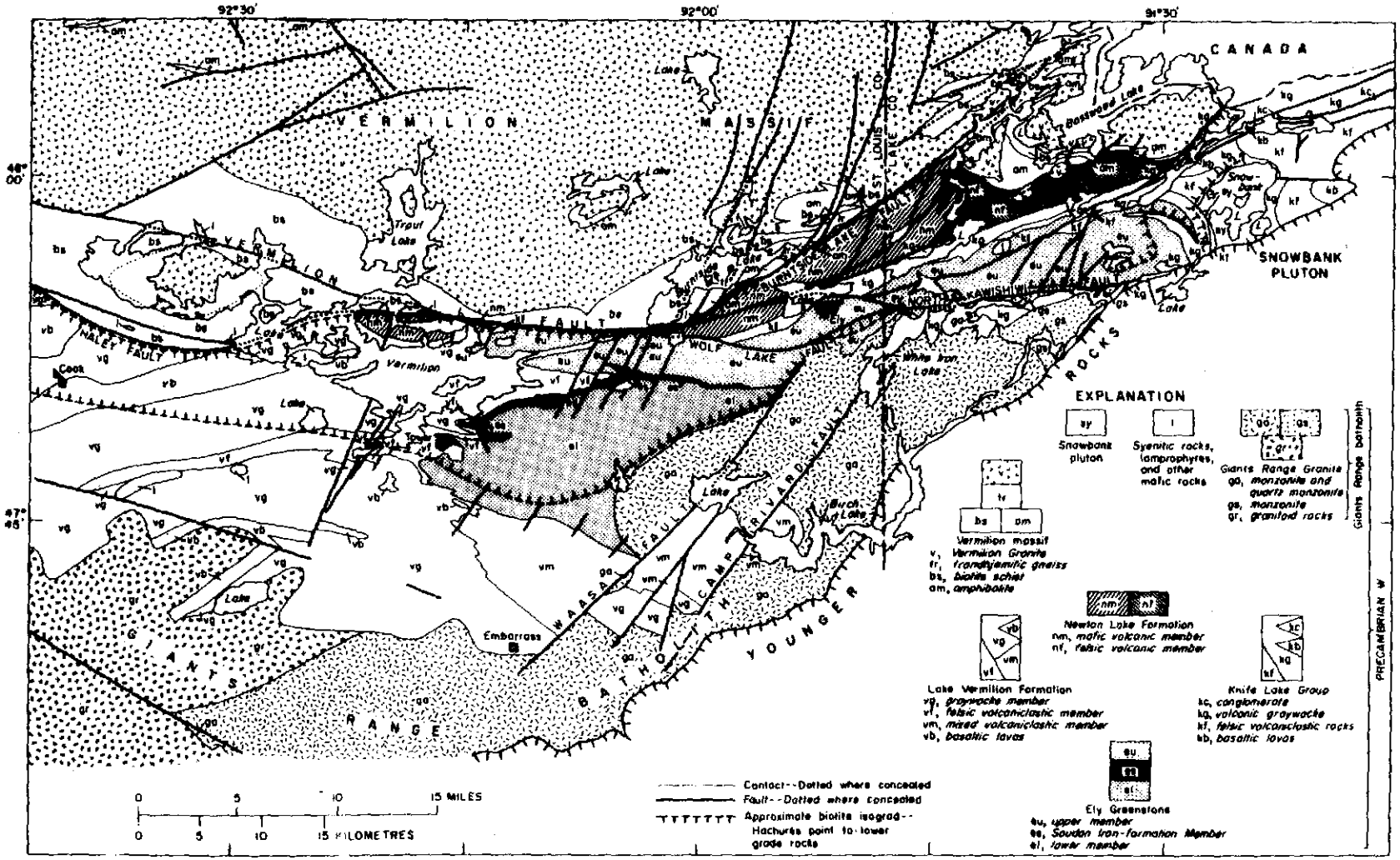
92°30'
92°00'
91°30'
48° 00'
47° 45'
CANADA
VERMILION
MASSIF
SNOWBANK
PLUTON
ROCKS
GIANTS
RANGE
BATHOLITH
YOUNGER
Trout Lake
Basswood Lake
Snow-Bank Lake
White Iron Lake
Birch Lake
Vermilion
Cook
Embarrass
Lake
ST. LOUIS CO.
LAKE CO.
NORTH KAWISHIWI
NORTH KAWISHIWI FAULT
ELBOW LAKE FAULT
WOLF LAKE FAULT
NAILEY FAULT
WAASA FAULT
CAMP RIVARD FAULT
EXPLANATION
Snowbank pluton
Syenitic rocks, lamprophyres, and other mafic rocks
Giants Range Granite
gq, monzonite and quartz monzonite
gs, monzonite
gr, granitoid rocks
Giants Range batholith
Vermilion massif
v, Vermilion Granite
fr, tromdhjemitic gneiss
bs, biotite schist
am, amphibolite
Newton Lake Formation
nm, mafic volcanic member
nf, felsic volcanic member
Lake Vermilion Formation
vg, graywacke member
vf, felsic volcaniclastic member
vm, mixed volcaniclastic member
vb, basaltic lavas
Knife Lake Group
kc, conglomerate
kg, volcanic graywacke
kf, felsic volcaniclastic rocks
kb, basaltic lavas
Ely Greenstone
eu, upper member
ee, Soudan Iron-formation Member
el, lower member
PRECAMBRIAN W
0 5 10 15 MILES
0 5 10 15 KILOMETRES
Contact--Dotted where concealed
Fault--Dotted where concealed
Approximate biotite isograd--Hachures point to lower grade rocks

the base of the volcanic-sedimentary pile. To the east the belt extends into Canada where it is bounded in part by the Saganaga batholith.

The supracrustal rocks of the district consist mainly of diabasic metabasalt, intercalated iron formation, andesitic to dacitic flows, dikes and tuffs, and dacitic graywackes and slates (Sims, 1976). The rocks of the district have been subdivided into four formations based on dominant lithologic characteristics (Table 1). The units are listed in stratigraphic order in table 1. No contacts have been found between the Knife Lake Group and the Lake Vermilion Formation, and for this reason they have been given separate formational status (Morey, et al., 1970).

Hooper and Ojakangas (1971) and Sims (1976) distinguished three generations of folding in the area around Tower. They have been further studied and described by Hudleston (1976) and Bauer (1985). Bauer has shown that the Ely Greenstone Belt and the Vermilion Granite-Migmatite Complex shared a common tectonic evolution since earliest stages of folding. Two sets of folds are present in the eastern part of the district (Gruner, 1941). Three sets of faults postdate the folding in the district. Longitudinal strike-slip faults are the major faults of the district, with right-lateral displacements up to 19 km. Two sets of dip-slip faults postdate the longitudinal faults (Sims, 1976).

Metamorphism and Alteration

The rocks of the district have been affected to varying degrees by seawater alteration and metasomatism, as well as later regional metamorphism. Original textures and structures have been obliterated or in large part obscured in many cases, especially in rocks of the Lake

Table 1
Stratigraphy of the Vermilion District supracrustal rocks

Newton Lake Formation (northeastern Vermilion District)	
Mafic member	Pillowed to massive felsic to mafic flows, gabbros, diabases, iron formations.
Felsic member	Felsic to intermediate pyroclastic rocks, felsic lavas.
Knife Lake Group (eastern end of district only)	
	Felsic to intermediate pyroclastic rocks, dacitic sandstones, slates, some conglomerates or agglomerates, iron formations, mafic lavas.
Lake Vermilion Formation (western end of district only)	
Graywacke member	Dacitic metagraywacke, felsic to intermediate pyroclastics, iron formations. Chloritic subfacies concentrated around eastern end of Lake Vermilion. Biotitic subfacies makes up remainder of member.
Felsic volcaniclastic member	Tuff, volcanic sandstone, slate, conglomerate, iron formation, basaltic lavas.
Mixed volcaniclastic member	Felsic to intermediate tuff breccia, conglomerates, dacitic sandstone, basaltic lavas.
Basaltic lavas	Pillowed, massive, diabasic, and gabbroic.
Ely Greenstone (around Ely)	
Upper member	Dominantly pillowed basalts.
Soudan Iron Formation Member	Dominantly iron-formation, also basalts and tuffs.
Lower Member	Dominantly massive basalts and diabase, pillowed basalts.

Vermilion Formation. Sericitization and saussuritization of plagioclase are common (Green, 1970; Ojakangas, 1972a,b). Secondary calcite can be an abundant mineral in these rocks (Green, 1970). Recrystallization (accompanied by the growth of chlorite and epidote) is usually indicated

by a pronounced greenish cast to the rocks. The assemblage consisting of epidote and chlorite, along with sericite and clear, untwinned albite, occurs in most of the altered rocks. Rocks of the Lake Vermilion Formation are typical of the district in that bleaching and veining vary from minor to major from place to place. Fresh samples are gray or gray-black (Ojakangas, 1972a).

The sedimentary rocks of the Gabbro Lake quadrangle are chemically similar to spilites (Green, 1970). Schulz (1977) noted wide ranges for Na_2O and K_2O on Harker-type scatter diagrams of Vermilion igneous rock analyses. He assumed Ti to be a relatively immobile component, and found that relative to TiO_2 the abundances of SiO_2, CaO, MnO, Rb, Sr, and Nb were highly variable, while FeOT and MgO were moderately variable, and Al_2O_3, P_2O_5, Zr, and Y were only slightly variable. He concluded that the major elements were not extensively remobilized because chemical classifications for the rocks for the most part agreed with each other and with petrographic evidence of rock type.

Most of the supracrustal rocks of the district have been metamorphosed to greenschist facies or higher. The metamorphism is characterized by disequilibrium textures and disequilibrium mineral assemblages (Griffin and Morey, 1969). In general, biotite grade rocks occur near to the bounding plutons and greenschists away from them. Amphibolite facies rocks occur in narrow zones less than 3,000 feet in width adjacent to the batholiths and stocks of the region, and adjacent to some faults (Sims, 1976). An exception to this overall pattern is in the western end of the district, where amphibolite facies rocks occur in a zone up to 8 miles wide around the Giants Range batholith. These are

in turn surrounded by an extensive region of biotite grade graywacke in the graywacke member of the Lake Vermilion Formation, suggesting that plutonic rocks underlie the area near the surface (Griffin and Morey, 1969). In some places, later prehnite-pumpellyite facies metamorphism has overprinted the rocks.

Geochemistry and Petrogenetic Modeling

Very few geochemical studies had been conducted in the Vermilion District prior to 1972 when Sims (1972b) summarized all available major element analyses on Vermilion igneous rocks. Since 1972, further geochemical studies of the rocks of the Vermilion District have been published. Hanson and Goldich (1972) first examined major element and REE data on the Saganaga tonalite and Northern Light Gneiss for the purpose of modeling magma genesis. They also analyzed selected units of the Knife Lake Group. They concluded that the tonalite and trondhjemite of the intrusive rocks could not have formed by partial melting of graywacke but could have formed by partial melting of garnet-bearing eclogite or amphibolite at mantle depths. Arth and Hanson (1972, 1975) analyzed major, REE's, and selected trace elements in tonalite, trondhjemite, basalt, and a graywacke composite from the Knife Lake Group, and proposed a model for the origin of the magma types based on their chemical characteristics. Their model is summarized in Table 2. Arth and Hanson (1975) concluded, as had other workers (Jahn and Murthy, 1975), that the Vermilion rocks did not develop on a previously-existing sialic crust, since all igneous rock types in the district have initial Sr^{87}/Sr^{86} ratios less than 0.701.

Table 2

Summary of the Petrogenetic Model of Arth and Hanson (1975)

I. Quartz tholeiite by shallow (<10 kb) melting of mantle peridotite;

II. Fractional crystallization of quartz tholeiite to produce basaltic andesite;

III. Trondhjemite, tonalite, and dacite plutons, dikes, and volcanics by approximately 20% partial melting of eclogite or amphibolite of Archean basalt composition at mantle depths;

IV. Quartz monzonite by partial melting of short-lived graywacke at crustal depths;

V. Syenites and syenodiorites by partial melting of a mixed peridotite-eclogite source at mantle depths.

Jahn et al. (1974) noted similarities between the Vermilion rocks and island arc tholeiites (IATs).

Schulz (1977, 1980) performed a major, minor, and selected trace element study of the mafic volcanic rocks of the western Vermilion District. His sampling corridors traversed the Ely Greenstone and Newton Lake Formations. Schulz suggested that the Lower Ely was composed of dominantly calc-alkaline basalts similar to modern island-arc rocks but with lower Al_2O_3 and Y contents, while the Upper Ely basalts were tholeiitic, with affinities to modern-day island arc tholeiites (IATs) or ocean-floor basalts (OFBs). Schulz discussed two analyses of basalts from the Lake Vermilion Formation as well, and interpreted them to be calc-alkaline basalts similar to those of the Lower Ely member.

Sedimentology

The rocks of the Knife Lake Group have been better studied than those of the Lake Vermilion Formation, principally due to the better exposure and less pervasive alteration prevalent in the Knife Lake Group (Gruner, 1941; Ojakangas, 1972a,b). The eastern part of the Lake Vermilion Formaion has been carefully mapped (Ojakangas, et al., 1978; Sims, et al., 1980). Many mapping and petrographic studies have been done on the Knife Lake Group rocks (e.g., McLimans, 1972; Feirn, 1977; Vinje, 1978; Flood, 1981). Very little geochemical work has been conducted.

Ojakangas (1972a,b) concluded that the Lake Vermilion Formation and Knife Lake Group graywackes had a volcanogenic origin, derived mainly from felsic-intermediate (dacitic) volcanic material deposited by turbidity currents in submarine fans close to their source volcanic cones. He noted that much of the two formations consists of sub-graywacke rather than graywacke. However, graywacke was retained as an imprecise field term, and it will be used in that sense throughout the remainder of this paper. Plagioclase crystals and volcanic rock fragments are the two main constituents of the graywackes, followed by quartz and micaceous matrix. Minor plutonic rock fragments have been noted in the Knife Lake Group graywackes (Ojakangas, 1972a,b; Feirn, 1977). They are traceable to the Saganaga Tonalite. No plutonic rock fragments have been positively identified from the Lake Vermilion Formation. Minor potassium feldspar components are present in graywackes in the east (Ojakangas, 1972a,b; Vinje, 1978), but none have been found in the Lake Vermilion Formation. Mafic rock fragments make up as much as 26% of some Knife Lake Group units (Vinje, 1978) but have

not been recognized thus far in the west (Ojakangas, 1972a,b).

Graded bedding and turbidite sequences (usually only top cut-out sequences) are very common in the district, and shallow-water structures (e. g., ripple marks) are not found, indicating deposition in intermediate to deep water (Ojakangas, 1972a). Such turbidite sequences are indicative of the proximal fan facies of Walker (1984). True volcanic (water-laid) tuffs are rare in the district but do exist (Sims, 1972b). Laharic deposits may also be present, as very thick massive sandstones, or as conglomerates grading laterally into graywackes (Flood, 1981). These olisthostromic units could have been deposited in the proximal region of a turbidite fan, and have been interpreted in that way by workers in the district.

Nature of the Present Study

The rocks of the Lake Vermilion Formation are widespread in the western part of the Vermilion District but have received little attention, mainly due to the lack of exposure and more pervasive alteration of the Lake Vermilion Formation relative to the Knife Lake Group. The igneous rocks of the Lake Vermilion Formation have not previously been studied, except for two samples by Schulz (1977) and one by Grout (1926). The chemistry of the sediments of the district has not previously been studied in any detail. Two chemical analyses of Vermilion graywackes were published by Grout (1933). Geochemical studies of the sediments can be used to answer some questions regarding the provenance of sedimentary rocks in the Lake Vermilion Formation.

Objectives

The objectives of the present study are as follows:

1) to describe and classify the weathering, metasomatic, and metamorphic histories of the Lake Vermilion Formation rocks, and establish as much as possible their original composition;
2) to characterize the rocks of the Lake Vermilion Formation geochemically;
3) to sample stratigraphic sections through the formation wherever possible to look for chemostratigraphic trends;
4) to describe and compare the graywackes and slates of the district geochemically, and to use the geochemical data to constrain the provenance of the sediments, especially to test for plutonic and mafic components;
5) to discuss constraints on petrogenetic models for the Vermilion rocks using Ti, Zr, and Y, which have not been incorporated into models previously;
6) to interpret the tectonic history of the area, with especial reference to finding modern tectonic analogs for the region in the light of recent understanding of modern tectonic environments.

Methods

Two and a half summers were spent obtaining rock samples of all units in the Lake Vermilion Formation. Selected samples were studied petrographically to obtain some idea of how mineral assemblages related to alteration processes. Mineral chemistries were determined by microprobe analysis. Ninety-two samples were analyzed for all major and minor elements and selected trace elements by X-ray fluorescence.

Details of sampling methods, sample preparation, accuracy and precision, and evaluation of potential sources of error are contained in Appendix A. The analytical data is contained in Appendix C, normalized to 100% on an anhydrous basis. Ferrous and ferric iron has been allotted according to the method of Nicholls and Whitford (1976, details in Appendix A). CIPW norms have been calculated for all samples, including the metasediments, and are found in Appendix C. Additional chemical data for Vermilion rocks have been drawn from: Green (1970); Jahn (1972); Sims (1972b); Rogers and McKay (1972); Arth and Hanson (1975); Schulz (1977); and Minnesota Geological Survey unpublished data.

PETROGRAPHY

Samples of all major rock types were examined petrographically, except for the slates and basalts, the former because of their small grain size, and the latter because of the limitation on the number of thin sections which were made.

Mineralogy of the LVF Rocks

Plagioclase and quartz phenocrysts are very abundant in the dacite porphyries, and plagioclase and quartz grains are very abundant in the graywackes and arkoses. Quartz grains in the dacites are rounded to subrounded, and many show resorption features. The plagioclase grains show similar features. Volcanic rock fragments are the dominant component in the graywackes, but only large mineral crystals were analyzed by microprobe, to obtain some control on the chemistry of the major mineral phases.

All the plagioclase grains analyzed by microprobe were normally zoned. Zoning is often outlined by preferential growth of sericite and/or saussurite along zoning boundaries. The plagioclase is generally andesine to labradorite. There is no peristerite gap for these rocks. Anorthite contents of plagioclases range between 40 and 50% in the biotitic graywackes, somewhat higher than the anorthite contents of the FV rocks, which is commensurate with the former's higher grade.

Plagioclase is commonly sericitized, often along zoning boundaries. In some cases of extreme alteration, plagioclase is almost completely replaced by sericite and epidote, and the plagioclase that remains is

Table 3
Representative Mineral Analyses

	Plagioclase				Amphibole	
	204-2	199-1	128-1	42-2	TGB74-1	SSGB120-1
SiO_2	62.51	66.48	55.67	61.05	44.19	41.79
Al_2O_3	22.03	19.92	27.97	22.34	10.87	12.03
FeO	0.00	0.00	0.24	0.00	15.98	18.12
MgO	0.00	0.00	0.13	0.00	10.92	9.84
CaO	2.76	0.19	9.64	3.49	11.77	11.72
Na_2O	9.19	10.65	5.43	9.14	1.55	1.64
K_2O	0.23	0.08	0.19	0.14	0.21	0.64
TiO_2	0.00	0.00	0.00	0.00	0.35	0.57
P_2O_5	0.00	0.00	0.00	0.00	0.00	0.00
MnO	0.00	0.00	0.00	0.16	0.56	0.45
SO_3	0.20	0.00	0.00	0.00	0.00	0.00
BaO	0.00	0.00	0.00	0.00	0.00	0.00
Total	96.92	97.31	95.53	96.33	96.39	96.81

	Biotite		Epidote		Muscovite	
	TGB74-1	128-1	ST74-1a	ST74-1b	TGB74-1	199-1
SiO_2	33.94	34.08	37.39	41.48	60.16	44.56
Al_2O_3	15.61	16.95	24.21	22.88	20.50	35.98
FeO	19.44	16.75	9.93	7.94	0.47	0.64
MgO	14.36	10.76	0.00	0.00	0.00	0.99
CaO	0.00	0.17	22.63	21.01	2.02	0.12
Na_2O	0.43	0.73	0.00	0.00	3.06	0.66
K_2O	7.32	9.82	0.17	0.12	9.67	9.77
TiO_2	1.35	2.25	0.00	0.19	0.28	0.17
P_2O_5	0.00	0.00	0.00	0.00	0.00	0.00
MnO	0.35	0.33	0.27	0.29	0.15	0.00
SO_3	0.11	0.00	0.00	0.18	0.00	0.00
BaO	0.00	0.00	0.00	0.00	1.25	0.00
Total	92.92	91.84	94.61	94.09	97.56	92.89

pure albite having a watery appearance.

The more highly altered, sericitized plagioclases are found in rocks in which large flakes of muscovite are also present. There is abundant

Table 4
Representative Chlorite Analyses

	Chlorite 42-2	Chlorite ST81-1	Chlorite ST68-1
SiO_2	27.66	29.07	27.94
Al_2O_3	18.73	22.00	22.19
FeO	25.05	21.79	18.65
MgO	11.43	11.76	17.39
CaO	0.58	0.09	0.40
Na_2O	0.28	0.65	0.63
K_2O	0.83	1.48	0.00
TiO_2	1.68	0.18	0.00
P_2O_5	0.00	0.00	---
MnO	0.53	0.12	0.36
SO_3	0.00	0.00	---
BaO	0.00	---	---
Total	86.77	87.14	87.56

evidence of shearing in the altered rocks also; even some large plagioclase crystals are cut by veins filled with calcite and muscovite, indicating hydration and some carbonization.

In the biotitic graywackes biotite is euhedral with zircon inclusions. Some biotite grains are slightly chloritized. In the chloritic graywackes, there are pseudomorphs of chlorite after biotite, and the few remaining biotites are chloritized. This may indicate that the chloritic graywackes of the region are biotitic graywackes that have undergone retrograde metamorphism.

Pargasitic hornblende is present in two of the biotitic graywackes, with chemistries that are almost identical to a hornblende given by Deer et al. (1978) from an Idaho tonalite. There are also pseudomorphs of epidote after amphibole in some of the sandstones in the felsic volcaniclastic member, indicating that their source rocks may have been

hornblende-phyric flows or tuffs.

Epidote is present in all the sections in the groundmass. Some sections contain large grains of zoisite and clinozoisite, present as pseudomorphs after other minerals.

Chlorite has formed from amphibole and biotite. The grain whose analysis is tabulated here is ripidolite. Pennite and clinochlore are common alteration minerals. Fine-grained muscovite (sericite) is common, generally as an alteration product of plagioclase. Muscovite is also present as discrete subhedral to euhedral grains.

Petrographic Evidence of Alteration

Evidence of low-grade alteration is abundant in the Vermilion rocks, especially in the rocks of the LVF. Gelinas et al., (1982) have described three stages of progressive alteration by seawater in pillow basalts of the Rouyn-Noranda district of Ontario. The Vermilion rocks correspond to their first stage of alteration, with the lowest fluid/rock ratios. The criteria for classifying the Vermilion rocks as little-altered Stage I rocks include the presence of many mineral phases (as opposed to the small number of mineral phases present in the rocks altered at higher fluid/rock ratios), the low content of hydrous minerals in most of the rocks, the incompletely altered plagioclase (relict plagioclase is present in many rocks), and the patchy alteration. This type of alteration corresponds to spilitization in the basalts or keratophyrization in the more felsic rocks (Hughes, 1972; Gunn and Roobol, 1976).

GEOCHEMISTRY OF ALTERATION IN THE VERMILION DISTRICT

Introduction

The Vermilion rocks, like most greenstone belt suites, contain abundant petrographic evidence of alteration by the processes of alteration by seawater, deuteric alteration, diagenesis, low-grade metamorphism, and hydrothermal alteration. A knowledge of the extent to which alteration has affected the rocks is essential to any discussion of their original chemistries.

Estimation of the chemical changes due to low-grade alteration processes consists of two tasks: 1) Identification of the type(s) of alteration affecting the Vermilion rocks; and 2) Identification of the direction(s) and estimation of the degree (slight, moderate, or high) to which each element has been mobile.

Methods of investigation

The first objective will be pursued by a general comparison of the Vermilion rocks to modern rocks which have undergone alteration by seawater and burial metamorphism. Comparative studies of Cenozoic and Archean seafloor basalts (Baragar, et al., 1979; Dimroth and Lichtblau, 1979) have documented identical mineralogies and textures in the two groups, which argues strongly for similarity of alteration processes in the Archean and Cenozoic.

The second objective, that of identifying, on an element-by-element basis, those elements which have been mobile, would be best accomplished by comparing altered Vermilion rocks with their unaltered equivalents. This is not possible with Archean rocks, for which no unaltered counterparts exist. The problem can be to some extent circumvented in a number of ways, three of which have applicability to the Vermilion rocks:

1) Many workers have used linear correlations of pairs of elements, or the observation that values for an element are within the range of known igneous variation for rocks of comparable type as evidence of relative immobility of an element during secondary processes (e.g., Frey et al., 1968; Cann, 1970; Kay, et al., 1970; Wood, et al., 1976). Usually a rock type with a narrow compositional range must be chosen. An assumption of this method is that alteration results in an essentially random redistribution of the elements it affects. This assumption is not always warranted; rather, groups of elements can behave similarly during lowgrade alteration and be redistributed coherently, yielding patterns which can mimic igneous variation (Hellman, et al., 1977, 1979). Linear correlations may still be of use in cases where elements are known to behave incoherently during low-grade metamorphism, and their absence where expected can be used as an indicator that elemental redistribution has occurred.

2) Many workers have compared Archean altered rocks to an "igneous spectrum" encompassing all compositional variations for a set of elements as they are known to occur in Tertiary or Cenozoic

unaltered igneous rocks (e.g., Beswick and Soucie, 1978). This method assumes that the chemical variation present originally in the Archean rocks was essentially the same as that for the Cenozoic or Tertiary rocks.

3) An approach used by Strong et al., (1979) has been to quantify gains or losses of chemical components between two groups of rocks, one of which seems to have undergone some secondary alteration process not experienced by the other, using the Grescens equation (Grescens, 1967). What is quantified are the chemical changes due to any process which has not affected the "less-altered" of the two groups, or at least not affected it to the same degree as it has the "more-altered" group.

Processes of Alteration in Tertiary and Archean Altered Rocks

Low-grade Alteration Processes

The principal alteration processes affecting seafloor and island arc rocks of the Cenozoic as the result of seawater weathering and burial metamorphism were evidently also operative in the Archean (Dimroth and Lichtblau, 1979; Baragar, et al., 1979). These processes are spilitization, keratophyrization, and poeneitization. The petrographic characteristics of the Vermilion samples which make them similar to Cenozoic rocks that have undergone low-grade alteration were discussed in the section on petrography.

Spilitization (Hughes, 1972) occurs in seafloor basalts as a result of exposure to seawater weathering and subsequent burial and low-grade metamorphism. Spilitization results in a loss of Ca, Mg, Al, K, Rb, Sr,

and Ba with increases in Si, Fe, and Na and H_2O by the rocks (Gunn and Roobol, 1976). The same chemical changes were found by Ludden, et al., (1982) for altered and metamorphosed basalts in the Rouyn-Noranda district of the Canadian Shield. Keratophyrization (Battey, 1955; Hughes, 1972) is the term for roughly the same process as spilitization when it occurs in massive flows, typically andesitic in original composition. Potash-keratophyres are those which are enriched in K as well as Na.

The term 'poeneite' was redefined by Brouwer (1942) to refer to the K-spar-bearing equivalent of a spilite, and has been used in that sense by later workers (Jolly, 1970; Gunn and Roobol, 1976). Poeneitization is similar to spilitization, but is accompanied by sericitization and conversion of some of the plagioclase feldspar to K-spar, with concomitant enrichments in K, Ba, Na, Rb, and Sr (Gunn and Roobol, 1976).

Chemical Changes Accompanying Alteration

The main metasomatic changes accompanying seafloor weathering and zeolite facies metamorphism are a gain of K and Fe by the rock and a loss of Ca and Mg (Gelinas, et al., 1982, and references therein). While Mg is lost at low seawater/rock ratios, it can be gained at high ratios as chlorite content in the rock increases (Humphris and Thompson, 1978a; Mottl, 1983). Other elements are also mobile in seafloor alteration, although no consistent direction of mobilization has been found. Si is unchanged or lost from the rock (Hart, et al., 1974; Aumento, et al., 1976). Na can either be gained or lost, but is generally mobile (Gunn and Roobol, 1976; Melson, 1973). P contents have

been shown to vary in seafloor metamorphosed basic rocks (P addition: Hart, 1970; Miyashiro, et al., 1969; P depletion: Hart and Nalwalk, 1970; Melson, 1973). Ba, Sr, Rb, and Mn are mobile (Hart, et al., 1974; Humphris and Thompson, 1978b; Hart, 1969). Ti and the REEs are immobile during seafloor alteration, as are Zr, Y, Nb, Cr, Ni Cu, Zn and to a lesser extent Sr (Cann, 1970; Nicholls and Islam, 1971; Bloxam and Lewis, 1972; Hart, et al., 1974; Pearce, 1975; Humphris and Thompson, 1978b; Morrison, 1978). A reduction in K/Rb ratios is a well-established effect of spilitization, as is an increase in K and an increase in Rb (Hart, 1969; Hart, et al., 1970; Thompson, 1973; Melson, 1973; Hart, et al., 1974; Humphris and Thompson, 1978a). Ca, Sr and Ba should move coherently, as do K and Rb, since Ca, Sr, and Ba all have similar electron configurations. Sr and Ba were enriched in greenschist facies spilitized basalts of the Rouyn-Noranda district of Ontario (Ludden, et al., 1982), poeneitized rocks of the Limestone Caribbees (Gunn and Roobol, 1976), and seafloor weathered basalts (Hart, et al., 1974). Sr contents in these rocks were more enriched than Ba; Ba showed no consistent trend. The lesser mobility of Ba during low-grade alteration probably arises from the fact that plagioclase can serve as a host for Ba at all stages of alteration, while epidote is the only host for Ca and Sr.

Alteration History of the Vermilion Samples

Elemental Correlations

The data used in this discussion are from the sources listed above in the Introduction. Data from this study can be found in Appendix C.

On Harker-type diagrams of trace elements and oxides of major and minor elements versus SiO_2, the values for the alkalis show considerable scatter, with K_2O showing the most scatter. Values for CaO also show some scatter relative to SiO_2, but less in relation to Fe_2O_3T or MgO. Calcite mineralization may be responsible for some of the CaO scatter. The good correlation of MgO and Fe_2O_3T is an indication of a relatively low degree of open-system metasomatism, since MgO and Fe_2O_3T are generally mobilized in opposite directions during such processes. TiO_2 and MnO show very good correlation, while P_2O_5 is variable.

The wide limits on Ba and Sr contents at a given value of SiO_2 indicate that these elements were mobilized. Some Zr scatter is evident on a Harker-type Zr-SiO_2 diagram, but not enough to significantly affect the classification of the rocks by this element (see fig. 10). The elements Zr, Ti, Cr, Ni and Y show good linear correlations with Fe and Mg. Although linear correlations of these elements could be produced by coherent mobilization (Hellman, et al., 1979), there are many studies which indicate low mobility for these elements during alteration processes (see introduction to this section). There are indications that the metasomatism of the Vermilion rocks took place at low fluid/rock ratios as discussed in the petrography section. The foregoing is evidence that the elements Zr, Ti, Y, Cr and Ni are still present in essentially their original abundances.

Rb correlates very well with K_2O in the Vermilion samples. Given the evidence (the poor correlation of K_2O and SiO_2) that K has been mobilized, it is likely that Rb has also been mobile, and that it has moved in a coherent manner with K.

Comparisons to Modern Rock Suites

References to the Carolina Slate Belt (CSB) are made throughout this section. The CSB is an area of Devonian rocks, mainly basalt, dacite, and associated immature graywackes and tuffs, which are believed to be of island arc origin. The igneous rocks of the CSB are bimodal in silica contents, as are the Vermilion igneous rocks (Seiders, 1978; Whitney, et al., 1978). A comparative discussion of this and other bimodal suites and the Vermilion samples follows in the section on tectonic models.

Hughes (1972) proposed a plot to discriminate spilitized igneous rocks from a normal igneous spectrum using alkali contents. With slight modification for high- and low-K andesites and dacites, the Hughes igneous spectrum is useful for discriminating groups of spilitized and keratophyrized igneous rocks from unaltered igneous rocks (Gunn and Roobol, 1976).

Figure 2 shows the Vermilion rocks plotted on the Hughes alkali plot. The Vermilion dacites show scattered $K_2O/(K_2O+Na_2O)$ values, which is typical of keratophyres (compare fig. 5, Hughes, 1972). Volcanic mudstones (slates) from the CSB have very high $K_2O/(K_2O+Na_2O)$(see figure in Whitney, et al., 1978), as do some of the Vermilion slates and graywackes. The basalts from the Vermilion District plot partly within and partly outside of the spilite field on fig. 2. Many of the basalts which do not plot inside the spilite field do plot outside the igneous spectrum.

LMPR (log mole proportion ratio) plots (Beswick and Soucie, 1978)

Fig. 2 -- Hughes alkali plot (Hughes, 1972) showing Vermilion analyses. The field for the Carolina Slate Belt (CSB) rocks is also shown.

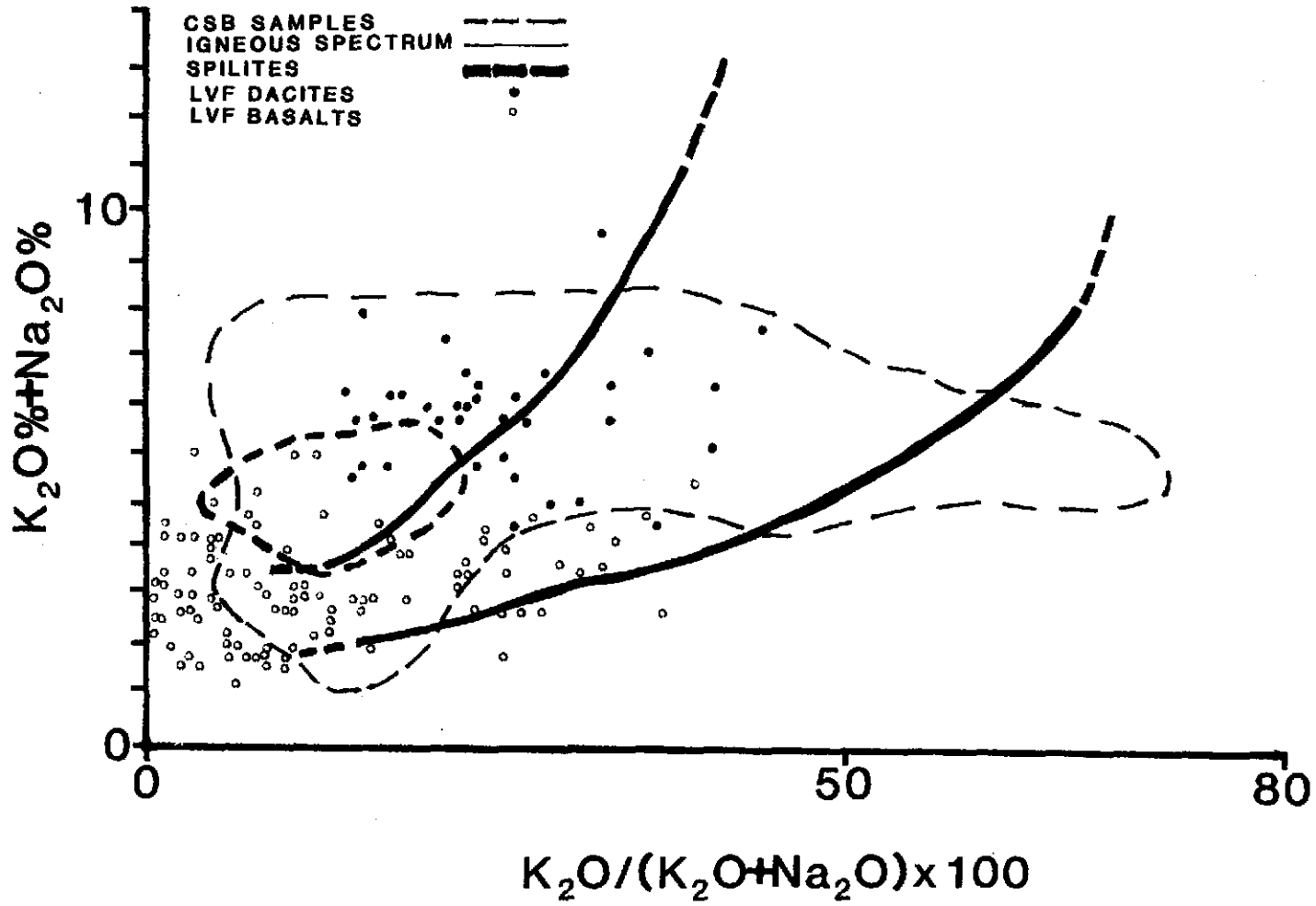
CSB SAMPLES
IGNEOUS SPECTRUM
SPILITES
LVF DACITES
LVF BASALTS
10
0
0
50
80
K2O%+Na2O%
K2O/(K2O+Na2O)x100

are a convenient means of showing how the Vermilion rocks compare with Tertiary unaltered igneous rocks. Fig. 3 shows the logs of the ratios of Al_2O_3/K_2O and SiO_2/K_2O plotted against each other. The two parallel lines in each LMPR plot are the recommended igneous spectrum of Beswick and Soucie (1978). The additional fields are for Tertiary igneous rocks as listed in the figure caption. The boundaries recommended by Beswick and Soucie do not encompass all significant igneous variation for the suites displayed; however, there is not much divergence. Spilitization does not move a rock's Si, Al or K values very far from the main sequence.

The Vermilion rocks fall into the spectrum for Tertiary igneous rocks, with only a little scatter. The same is even true for the sedimentary rocks. The Vermilion igneous rocks fall in the same region as spilites and keratophyres on this plot. The Vermilion basalts are extremely low in K_2O, almost off the edge of the diagram.

Correspondence of rock chemistries to the region of normal igneous variation as suggested by Beswick and Soucie for this plot has been used by some workers to screen rocks with altered chemistries from those with unaltered chemistries (e.g., Condie and Shadel, 1984). As this plot shows, spilitic rocks do not depart from the range of normal variation any more than unaltered igneous rocks. The similarity of spilites to unaltered rocks could be due to the influence of a mineral containing K, Al, and Si, with Al and Si in equal proportions. Changes in the amount of that mineral present would move a rock's composition along a line 45 degrees from horizontal, parallel to the range of normal igneous variation on fig. 3. A common mineral in the Vermilion rocks is

Fig. 3 -- Log mole proportion ratio plot of SiO_2/K_2O vs. Al_2O_3/K_2O (Beswick and Soucie, 1978) showing the Vermilion analyses. The parallel lines define the range of normal igneous variation recommended by Beswick and Soucie. Spilite-keratophyre analyses are of rocks from the Lesser Antilles (Gunn and Roobol, 1976; Donnelly et al., 1971). Island arc analyses from PNG (Jakes and Smith, 1970; MacKenzie and Chappell, 1972); Tonga (Ewart, et al., 1973); worldwide occurrences of Tertiary and Recent dacites (Ewart, et al., 1979); the Lesser Antilles (Brown, et al., 1978); Fiji (Gill, 1970); typical Pacific island arc values (White, et al., 1977); the Marianas (Dixon, et al., 1979); and Sardinia (Coulon, et al., 1978).

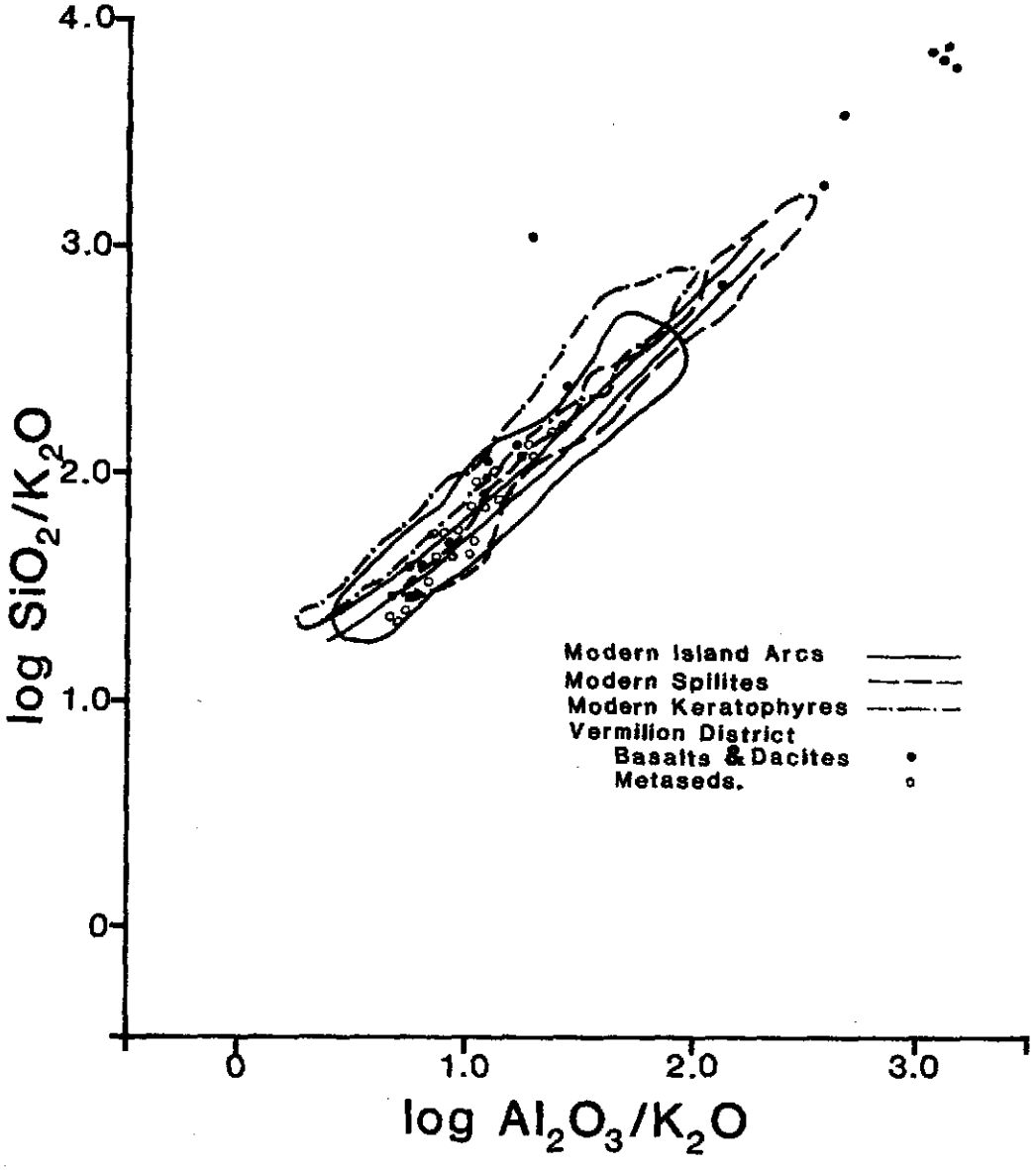
4.0
3.0
2.0
1.0
0
log SiO_2/K_2O
0
1.0
2.0
3.0
log Al_2O_3/K_2O
Modern Island Arcs
Modern Spilites
Modern Keratophyres
Vermilion District
Basalts & Dacites
Metaseds.

Fig. 4 -- Log mole proportion ratio plot of CaO/K_2O vs. SiO_2/K_2O, (Beswick and Soucie, 1978), showing the Vermilion analyses. The parallel lines define the range of normal igneous variation recommended by Beswick and Soucie. Sources for analyses of Lesser Antilles altered rocks and modern-day island arc suites and sources for sample points plotted on the diagram are found in the caption to figure 3.

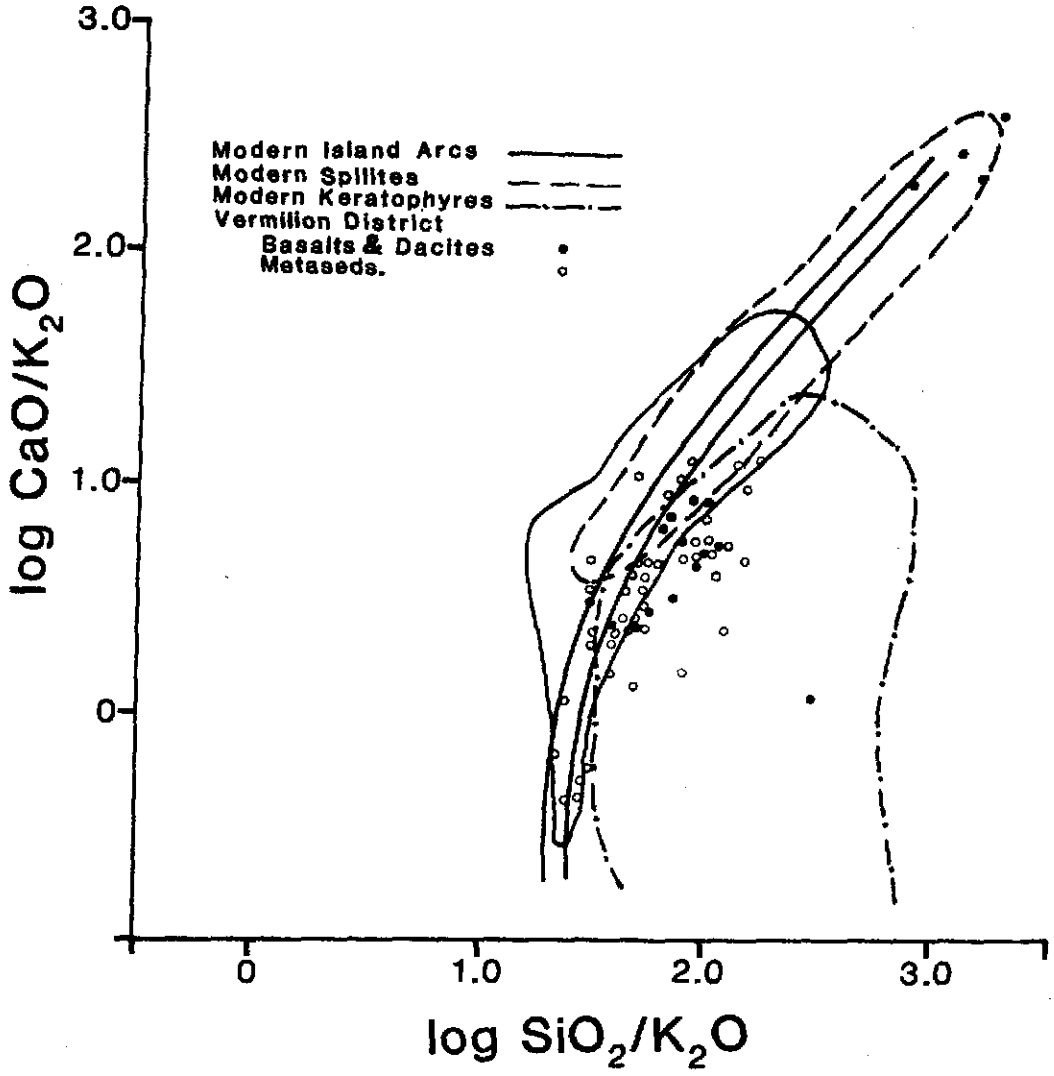
Modern Island Arcs
Modern Spilites
Modern Keratophyres
Vermilion District
Basalts & Dacites
Metaseds.
3.0
2.0
1.0
0
log CaO/K2O
0
1.0
2.0
3.0
log SiO2/K2O

Fig. 5 -- Log mole proportion ratio plot of CaO/K_2O vs. Fm/K_2O, where Fm = (Fe_2O_3Tot + MgO + MnO) (Beswick and Soucie, 1978), showing the Vermilion analyses. The parallel lines define the range of normal igneous variation recommended by Beswick and Soucie. Sources for analyses of Lesser Antilles altered rocks and modern-day island arc suites and sources for sample points plotted on the diagram are found in the caption to figure 3.

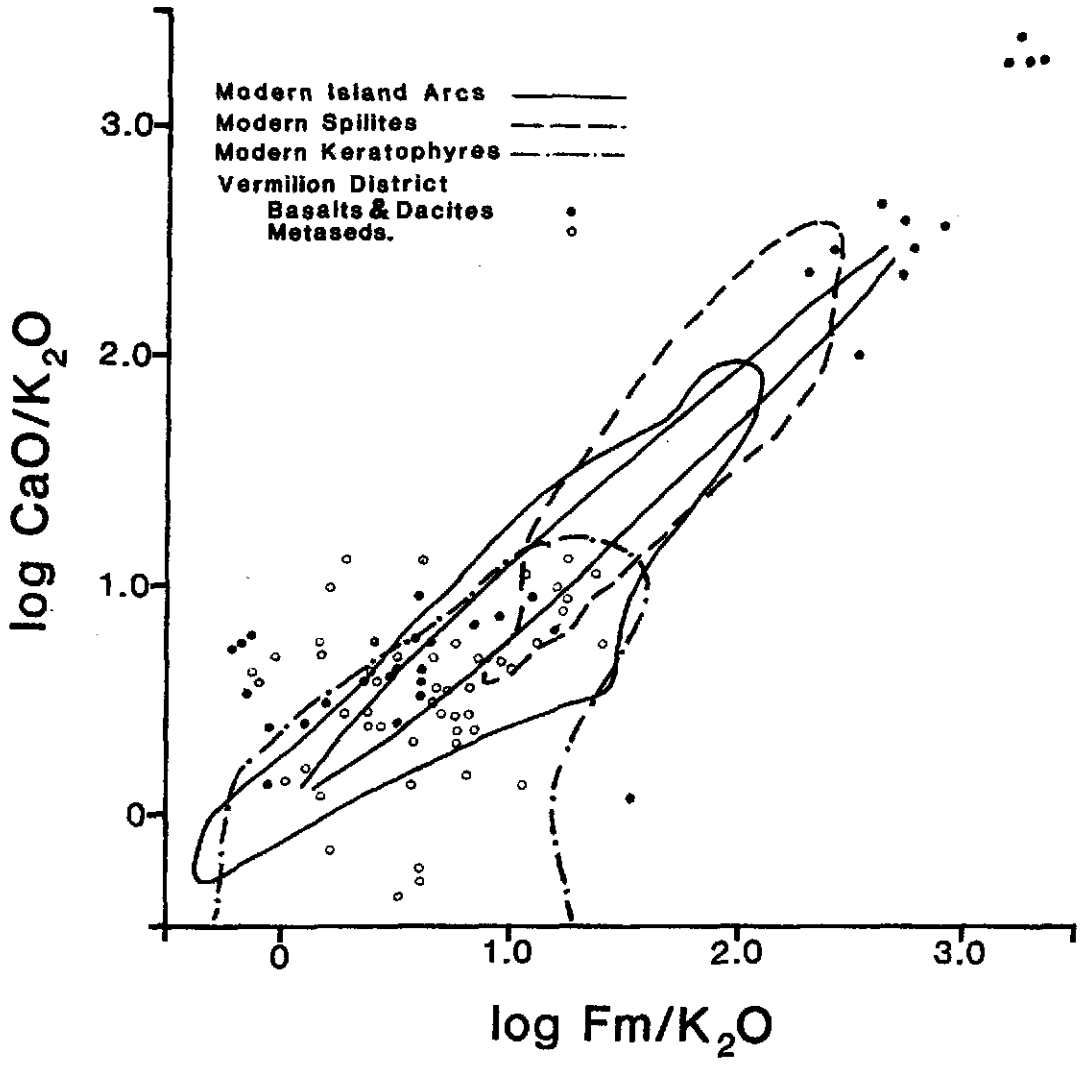
Modern Island Arcs
Modern Spilites
Modern Keratophyres
Vermilion District
Basalts & Dacites
Metaseds.
3.0
2.0
1.0
0
log CaO/K2O
0
1.0
2.0
3.0
log Fm/K2O

muscovite, which also contains Al and Si in equal proportions. Given the other indications of K_2O mobility in the Vermilion rocks, the influence of a potassium aluminosilicate mineral such as sericite is considered likely. Even those rocks which are extremely sericitized, namely the SFV65 series, plot near the normal igneous region, demonstrating that sericitization cannot be ruled out using this plot.

Fig. 4 compares CaO/K_2O and SiO_2/K_2O ratios. The Tertiary and Recent dacites included in the island-arc field on fig. 4 plot outside the region of normal igneous variation defined by Beswick and Soucie, indicating that some widening of the boundaries of the "normal" region is needed. The Vermilion dacites (and sedimentary rocks) plot in the low-CaO (or high SiO_2) region on this diagram, as do keratophyres. Addition of SiO_2 cannot explain the chemistries of these samples, because they fall within the normal igneous region in fig. 3. Therefore CaO leaching is the preferred explanation. The CSB rocks (not shown) exhibit this same trend toward low-CaO compositions, to a greater degree than the Vermilion samples. The CSB rocks are interpreted to be spilites (Whitney, et al., 1978).

Fig. 5 compares CaO/K_2O and Fm/K_2O ratios (where Fm = $Fe_2O_3T+MgO+MnO$). A plot of CaO/Na_2O vs. Fm/Na_2O is similar. The Vermilion dacites (and many sedimentary rocks) diverge from the region of normal igneous variation on this diagram, while Tertiary dacites do not. Low FeO^*/MgO ratios are characteristic of the Vermilion dacites and sedimentary rocks relative to modern igneous rocks. This may be a primary feature of the dacites, inherited by those sedimentary rocks which plot along with them. Supporting evidence for the hypothesis that

the FeO^*/MgO ratios are original was given in the petrography section, where it was suggested that most of the Vermilion rocks had undergone only Type I alteration as defined by Gelinas, et al. (1982). Gelinas, et al. found that the Type I Archean basalts they studied retained their original FeO^*/MgO and Fe_2O_3/FeO ratios. The rocks of the CSB do not have the same low Fm contents as the Vermilion dacites.

There is also a group of Vermilion metasedimentary rocks which diverge from the igneous trend toward the low-Ca (or high-Fm) region of fig. 4, indicating either Ca leaching or Fm addition. K_2O mobilization cannot be the cause of this divergence, since changes in K_2O content move the plotted points along a vector at 45 degrees to the x and y axes. CaO leaching is a preferable explanation for two reasons. First, the Vermilion rocks show CaO leaching on fig. 4. Secondly, the alteration trends expected in seafloor environments are a loss of Mg and a gain of Fe (Gelinas, et al., 1982), which would tend to cancel out on this plot. The low-CaO samples appear in the same region on this plot as do the keratophyres from the Lesser Antilles, indicating that keratophyrization could have produced the low calcium contents in the Vermilion samples. The CSB rocks show more pronounced "keratophyric" affinities than the Vermilion rocks on this plot.

Calculations Using the Grescens Equation

The Grescens equation for metasomatism (Grescens, 1967) was applied to averaged chemical analyses of subgroups of the Vermilion samples in order to ascertain 1) whether any of the mineralogical or chemical differences (e.g., calcite content or CaO content) observed in the Vermilion rocks may be relatable to any recognized open-system

alteration processes; and 2) whether open-system chemical exchange is necessary to explain differences in chemistry or mineralogy among the Vermilion samples.

The Grescens equation compares altered and unaltered samples and calculates the gains and losses of chemical components necessary to convert one to the other. Samples which are known to have been at one time identical in composition are required the calculation. In cases where no pair of altered/unaltered samples existed, mean analyses of groups of altered and unaltered samples were used (as in cases 5 and 6, below). The difference in chemistry between the groups can be examined by the Grescens method. Alteration which has affected both groups will not affect the calculations.

Selection of Samples and Treatment of the Data

All of the Vermilion samples have undergone some alteration, but they can be subdivided into groups possessing greater or lesser degrees of alteration on the basis of a variety of petrographic or geochemical criteria. Comparison of analyses which are group averages may reflect differences between the groups that are caused by normal chemical variation due to igneous or sedimentary processes. Such primary differences cannot be isolated from secondary differences due to alteration processes if the igneous-sedimentary variation is large. The means for all of the pairs discussed below were tested for significant differences at the alpha=0.95 confidence level. No significant difference was found, meaning that the means for the "altered" and "less altered" groups in each pair cannot be distinguished statistically. However, because the petrographic differences between the groups in most

pairs are demonstrable by petrography (and geochemistry in one case), it is believed that some chemical differences due to alteration do exist between the groups in most pairs. The change in concentrations for the major elements are the type that would be expected from open-system exchange with seawater. They are less consistent with igneous or sedimentary differentiation, which may mean that averaging has canceled out some of the variation due to sedimentary-igneous processes, leaving some expression of systematic differences related to secondary processes. Small numbers will be affected more than large numbers by primary variability in the samples. Some extreme values on the graphs result from large percentage changes in very small numbers. Especially affected are MnO, P_2O_5, or trace elements present in abundances close to zero ppm such as Y. Hence, MnO, P_2O_5, and Y values cannot generally be trusted to represent actual gains or losses on these diagrams. TiO_2 is also sometimes affected by this "small-number" problem, as are K_2O and Rb in basalts. The other elements do not exhibit such extreme divergences from F_v=1.0.

The sample data were grouped into seven "altered" and "less altered" subgroups depending on varying criteria:

1) "High-Cc" & "Low-Cc" non-basalt samples were grouped on the basis of thin section and XRD evaluation of calcite content, with no reference to their analyzed chemistry. Failure to observe calcite in thin section was taken as sufficient evidence to group a sample in the Low-Cc group; 10% calcite by visual estimate was the cutoff point for the high-Cc group. The absence of calcite on an XRD chart was not taken as sufficient evidence of low calcite content, since the XRD method is insensitive to small changes in

calcite content. XRD charts were used to supplement thin section data for many samples.

2) "High-Cc" & "Low-Cc" basalts were grouped on the basis of hand sample condition (presence or absence of shearing) and on chemistry: samples with high CaO and shearing were "High-Cc"; samples with little or no shearing and lower CaO were "Low-Cc".

3) "High-Ca" & "Low-Ca" sedimentary rock samples were selected solely on the basis of calcium content, 3.0% being the break.

4) "High-An" & "Low-An" samples: Only one low-An sample selected for petrographic study was chemically analyzed: TF204-2. Nine samples selected for petrographic study and chemical analysis had relatively high anorthite contents (greater than 10% An). Two samples without chemical analyses contained albitic feldspar in thin section (SFV199-1 and ST59-1), and in all three albitized sections the feldspars are extremely clouded and mica flakes are visible. This tends to confirm the grouping as indicative of a real metasomatic change, accompanied by sericitization of plagioclase and hydration of the rock, with possible addition of K_2O.

5) The dacite porphyry samples were arbitrarily divided into "normal"-K_2O, "high"-K_2O, and "Low"-K_2O subgroups using the subdivisions suggested by Gill (1981; see fig. 18). The "high"-K_2O subgroup was run as a pair with the "normal"-K_2O subgroup.

6) The single "low"-K_2O sample was run as a pair with the "normal"-K_2O group. The "low"-K_2O sample, ENES80-1, is anomalous

in its chemistry and its appearance in hand specimen (see later discussion).

7) One sample, SHEU82-1, from an andesitic dike in the Upper member of the Ely Greenstone, was separated into veined and less-veined piles, and each pile analyzed separately. The vein minerals were quartz with minor pyrite.

Specific gravities were measured on first-pass rock powders using a pycnometer to measure the volume of the rock samples by determining the volume of water displaced by the rock. This measurement as well as the weighing of the rock powder was carried out on a Mettler S5 Analytical Balance. The method differed by only 1% from the method of weighing a rock sample in air and water, and is therefore considered quite accurate.

Application of the Grescens Equation

The Grescens equation is as follows:

$$X_i = 100(F_v(g^B/g^A)C_i^B - C_i^A)$$

where

F_v = the volume change on reaction: the "volume factor".
(>1 for a positive change of volume, and
<1 for a negative change).

g^B, g^A = the specific gravities of rocks B and A.

$C_i^{B,A}$ = the weight fraction of chemical component i in rocks B and A in grams.

X_i = the net transfer of component i during reaction, expressed as weight per cent.

The averaged chemical analyses for the groups supplied C_i^B and C_i^A for the Grescens equation, and the sample specific gravities were also averaged for the groups to yield g^B and g^A.

The averaged chemical analyses for the groups supplied C_i^B and C_i^A for the Grescens equation, and the sample specific gravities were also averaged for the groups to yield g^B and g^A. A series of independent equations results, one for each chemical component, yielding X_i for $i = 1,\ldots,n$ where n is the number of components. The F_V is an indication of the degree to which the system was open to exchange of chemical components; large changes in volume factor imply large changes in composition. The direction of the changes (i.e., whether gains or losses) can be compared for the samples and for seafloor altered rocks, as a test of whether the chemical changes accompanying changes in mineralogy could be explained by seafloor alteration.

The volume factor, F_V, representing the change in volume due to alteration, cannot be determined uniquely for a volume change between two groups of samples. Grescens (1967) suggested that one may select the optimum volume factor out of the spectrum of possible volume factors by plotting gains and losses for all components against a range of volume factors. Such a composition-volume diagram has been plotted in fig. 6A for the High-Cc and Low-Cc non-basalt groups.

If it is assumed that for any given alteration process some components will be approximately immobile, then these components will all have gain-loss lines that cross the zero gain-loss line in a cluster. A more precise and convenient way of determining the location of these clusters, since the area of interest in such a C-V diagram is

Fig. 6 -- C-V diagram and C-V graph for the High-Cc and Low-Cc groups (after Grescens, 1967). The major and minor elements were treated as oxides for the calculations but are labeled as elements on the figure because of space considerations. A -- Composition-volume diagram for the High-Cc & Low-Cc groups. B -- C-V graph for the High-Cc & Low-Cc groups.

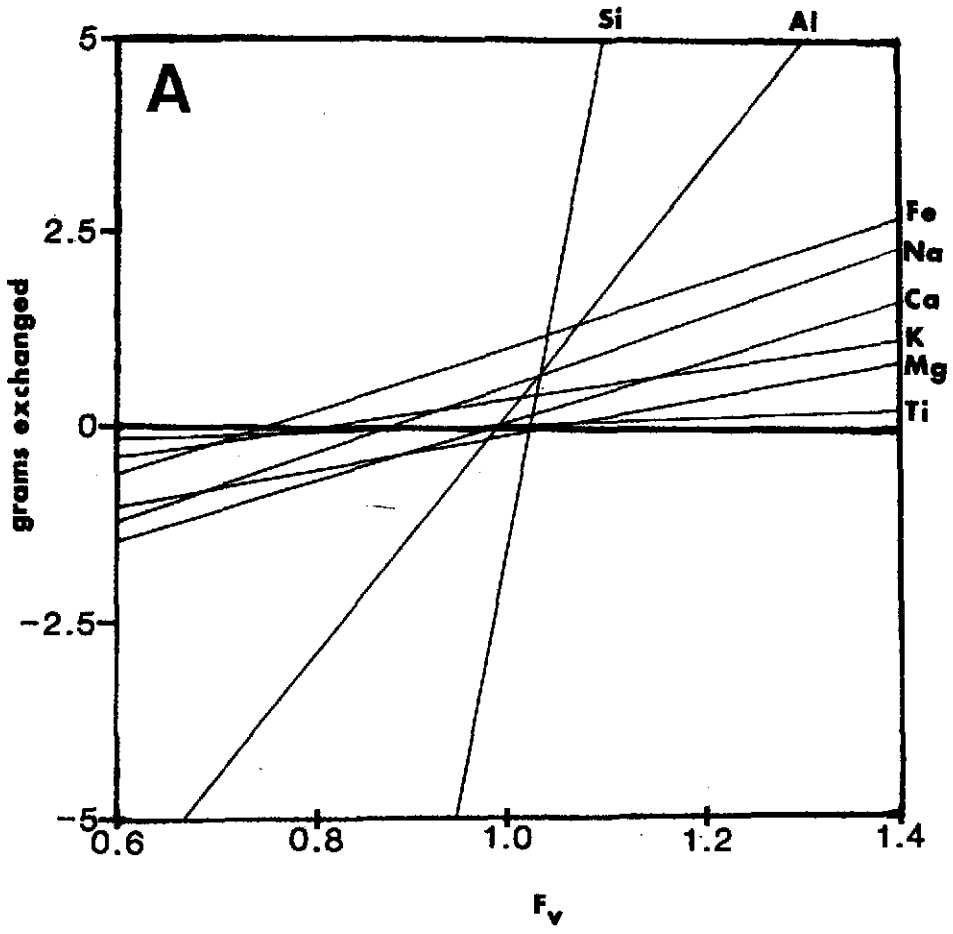
A
Si
Al
Fe
Na
Ca
K
Mg
Ti
grams exchanged
5
2.5
0
−2.5
−5
0.6
0.8
1.0
1.2
1.4
F_v

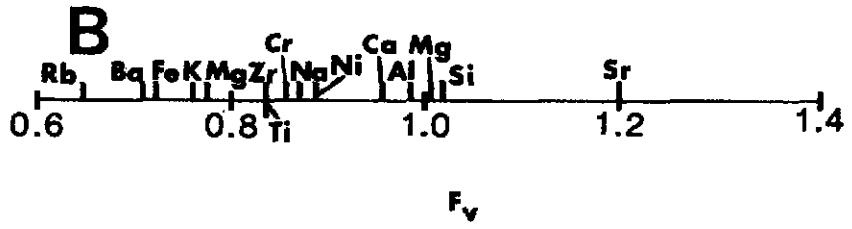
B
Rb
Ba
Fe
K
Mg
Zr
Cr
Na
Ni
Ca
Al
Mg
Si
Sr
0.6
0.8
Ti
1.0
1.2
1.4
F_v

the zero line, is to set $X_i = 0$ for the series of equations and calculate F_{vi}, the volume factor at which the line for components i=1,...,n cross the zero gain-loss line. This avoids graphical interpolation of the crossover points on a C-V plot. The example of fig. 6A is replotted in fig. 6B. The clustering for these components is readily apparent. The components which plot away from the cluster toward low F_v values should be those which were gained during the alteration process, and those with crossover values greater than that of the cluster should be those which were lost during the alteration process. Components for which the crossover points plot at a large distance from the main cluster are more likely to have been affected by some actual geological process in which components were lost and gained, rather than being affected by random fluctuations in the averaged data.

Results of the Grescens Calculations

1) High-Cc and Low-Cc non-basalts: A volume factor of approximately 1.0 is probably a good value for this group, since Al_2O_3, SiO_2, MgO, and to a lesser extent CaO, cluster here. Evidences of volume increase, such as deformation in thin section, are absent from members of this group. If anything, calcite seems to have simply replaced plagioclase isomorphously. This tends to strengthen the case for $F_v = 1.0$.

As can be seen in Fig. 6B, Ti, Fe, Ba, Rb, K, Zr, Cr, Na, Ni, and to a lesser extent Ca were gained by the High-Cc group, while Sr was lost. Ti, Zr, and Y are not immobile if this is a true grouping. Strong et al., (1979) found the same to be true in a comparison of silicified and less-silicified basalts from Newfoundland. An increase in calcite mineralization in the Vermilion basalts did not dramatically

Fig. 7 -- Composition-Volume graphs for all other pairs of groups, after Grescens (1967). A: High-Cc & Low-Cc basalts. B: High-Ca & Low-Ca metasedimentary rocks. C: High-An & Low-An rocks. D: High-K and Normal-K dacites. E: Low-K and Normal-K dacites. F: Veined and Less-veined separates.

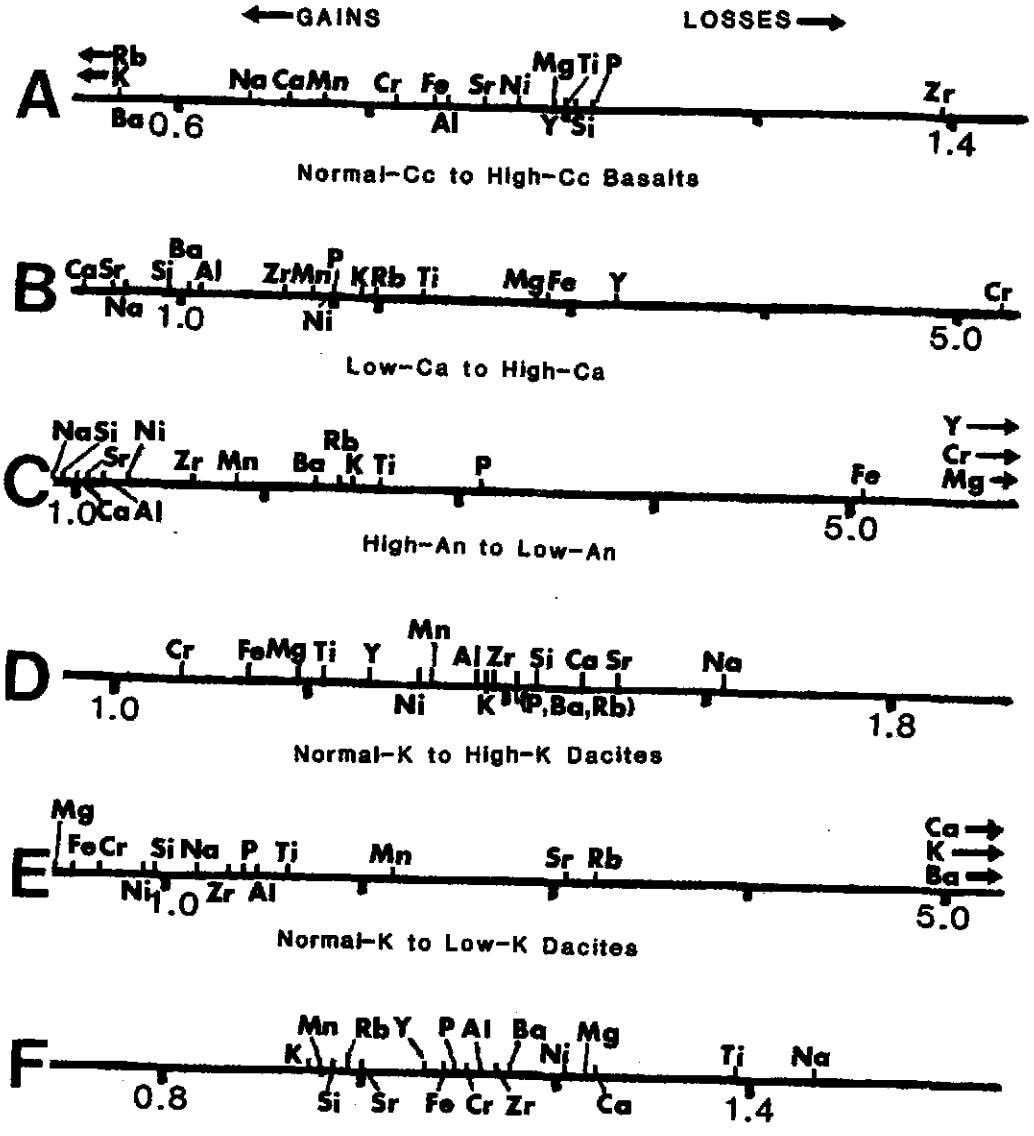
GAINS
LOSSES
A
Rb
K
Na Ca Mn Cr Fe Sr Ni Mg Ti P
Zr
Ba 0.6
Al
Y Si
1.4
Normal-Cc to High-Cc Basalts
B
Ca Sr Si Ba Al Zr Mn P K Rb Ti Mg Fe Y
Cr
Na 1.0
Ni
5.0
Low-Ca to High-Ca
C
Na Si Ni Sr Zr Mn Rb Ba K Ti P Fe
Y
Cr
Mg
1.0 Ca Al
5.0
High-An to Low-An
D
Cr Fe Mg Ti Y Mn Al Zr Si Ca Sr Na
1.0
Ni
K
(P, Ba, Rb)
1.8
Normal-K to High-K Dacites
E
Mg Fe Cr Si Na P Ti Mn Sr Rb
Ca
K
Ba
Ni 1.0 Zr Al
5.0
Normal-K to Low-K Dacites
F
Mn Rb Y P Al Ba Mg
K
Ni
Ti Na
0.8
Si Sr Fe Cr Zr Ca
1.4
Veined to Less-Veined

F_v

affect Ca or Mg, but rather added K, Fe, and Na, if the assumption of F_v = 1.0 is correct.

The relative positions of K_2O, Fe_2O_3, Na_2O, CaO, and MgO agree with the gains and losses of these components observed in seafloor basalts. For the relative positions to reflect absolute gains and losses as observed in seafloor basalts, the true F_v would have to lie somewhere in the range from 0.7 to 1.0, suggesting a net decrease in volume during alteration. Considering the hydration and carbonization accompanying calcification, this does not seem reasonable. Isomorphous replacement of mineral grains by calcite indicates little net volume change. Therefore, a volume factor close to 1.0 is preferable.

2) High-Cc and Low-Cc basalts: As seen on fig. 7A, there is again a clustering around F_v = 1.0. The Rb and K_2O values are probably not valid, since only one basalt had K_2O and Rb contents above detection limits, and this sample chanced to be in the High-Cc group.

A loss of Zr is indicated by the diagram, and is not due to "small-number" effects. Alkalis were gained by the altered basalts, as well as Fe and Al. Mg, Si, and Ti remained approximately immobile. So again the relative gains and losses of elements correspond to that found in modern seafloor basalts, with the greatest increases being for K, Na, Ca, Fe, and Al, in that order.

3) High-Ca and Low-Ca sedimentary rocks (fig. 7B): SiO_2 and Al_2O_3 cluster close together, near F_v = 1.0, suggesting that again this may be a reasonable volume factor. The fact that the best clustering is around F_v = 1.8, and the fact that the relative gains and losses of the

elements do not follow the sequence found in seafloor weathering suggest that the grouping by CaO content may not be valid. CaO content changes during igneous and sedimentary differentiation, and this effect may be obscuring any chemical variations due to alteration.

4) High-An & Low-An samples (fig. 7C): TF204-2, the low-An sample, is higher in Na_2O and lower in all other components except SiO_2 than the high-An samples. The choice of volume factor is unclear for this pair. An F_V of 1.0 is probably the best choice for volume factor, given that SiO_2 and Al_2O_3 plot close to $F_V = 1.0$. A volume increase, represented by a F_V of 1.25 or even 1.5 would also give reasonable results, since then some mobility of Na and Ca would be indicated.

If a volume factor near 1.0 is selected, then Na was slightly gained during albitization and sericitization, while Mg, Fe, Ti, K, Rb, Ba, and Zr were lost and Si, Sr, Ca, and Al remained relatively constant. If a volume factor near 1.3 is selected, then Na, Si, Ca, Sr and Al were gained while the same elements were lost as for the case of $F_V = 1.0$.

For any volume factor chosen, either Ti, or Al and Si were mobile, since these elements plot far apart. Alternatively, Ti may have been influenced by "small number" effects.

5) "High"-K_2O and "Normal"-K_2O dacites (fig. 7D): The best clustering of crossover values is clearly around $F_V = 1.4$. This is a high value relative to the other pairs of groups considered here. Relative to an F_V of 1.4, the elements Al, Si, and Ti were neither gained nor lost. Na, Rb, Sr, Ca, and Ba were lost by the high-K_2O samples. The elements Mg, Fe, Zr, and possibly K and MnO were gained.

The gain/loss profile for the high-K_2O and normal-K_2O pairing is similar to the profile which would result from normal igneous differentiation. The volume factor is unusually high. Sericitization is no more pronounced in sample TEL69-1 (the only "normal"-K_2O sample which was examined petrographically) than in ST50-2 (the only "high-K" sample that was examined petrographically). Therefore, the grouping of the samples into high and normal K_2O groups may reflect nothing more than normal igneous variation.

6) "Low"-K_2O and "Normal"-K_2O dacites (fig. 7E): ENES80-1 is from a dike intruded into iron formation. It is a road cut sample which displays pink plagioclase feldspar in hand specimen, probably indicating at least some Fe metasomatism. No post-crystallization volume change is evident in outcrop where the dike intrudes country rock, but dilation due to intrusion of the dike certainly occurred. A F_V of around 1.0 again seems reasonable.

Such a volume factor indicates that Si and Fe were substantially gained by the dike during metasomatic interaction with wall rocks, while Ca, K, Ba, Rb, Sr, and even Ti and Al were lost (Fig. 7E). This is consistent with chemical exchanges which might be expected between a dacitic magma and iron formation.

7) The veined and less-veined separates of SHEU82-1 (fig. 7F): This pair of samples certainly represents a true metasomatic process, that of quartz veining. There was probably some expansion of country rock to accomodate veining, and so the clustering about $F_V = 1.1$ may be appropriate. In that case, Si, K, Rb, Sr, and possibly Mn were gained by the rock as a result of veining, while Ti, Mg, and Ca were lost and

Al, Fe, Ba, and Zr remained relatively constant.

Summary of Results of the Grescens Calculations

Albitization and calcite mineralization are interpreted to be partly the result of open-system processes, because they have resulted in some chemical transfer. The pattern of exchange of components resembles that of seafloor alteration. A very limited amount of alteration is indicated by the fact that the F_v's are near 1.0 in most cases. Greenschist facies metamorphism does not result in the same pattern (Pearce, 1975).

It is interesting to note the pronounced correlation between K_2O and Rb, and also between CaO and Sr in these diagrams. Rb values always cluster with K_2O values, except in the case of metasomatism due to dike-wall rock interaction (case 6). CaO and Sr mobilities are similar for all cases except 6 and 7. Epidote is probably the host mineral for Ca and Sr (Ludden, et al., 1982), causing them to be mobilized coherently. Plagioclase may also have contributed to their coherent mobility, since crystal-liquid partition coefficients for Ca, Ba, and Sr are all similar (Korringa and Noble, 1971).

Summary and Conclusions

In conclusion, the processes which affected the Vermilion rocks were spilitization and keratophyrization caused by limited chemical exchange between hot rock and seawater, during extrusion and burial. Open-system chemical exchange was not a major influence on geochemistry, as evidenced by the fact that the volume factors suggested by the Grescens calculations are close to 1.0. The effects of spilitization are evident

in the behaviors of the components K_2O, MgO, Fe_2O_3T, CaO, and Na_2O, whose relative distributions are as expected for seafloor weathering. CaO has been selectively leached from many of the sedimentary rocks, leaving them peraluminous. SiO_2 and Al_2O_3 were little affected by open-system processes. The mafic elements (Fe, Mg, Ti, Ni, and Cr) show consistent linear trends and may not have been significantly remobilized. For alteration at low fluid/rock ratios such as appears to be the general case for the Vermilion District, the ratios of FeO^*/MgO and Fe_2O_3/FeO are believed to be relatively unchanged (Gelinas, et al., 1982). Fe-Ti oxides and chlorite could have provided mineral hosts for these elements during alteration. Ba, Sr, and Rb have been mobilized in this suite, while Zr and Y appear to have been less mobile, along with Cr and Ni. Rb follows K_2O, while Sr tends to follow CaO.

GEOCHEMISTRY OF IGNEOUS ROCKS OF THE VERMILION DISTRICT

General Geochemical Classification of the Rocks

Assumptions

The application of any classification system designed for use with Cenozoic rocks to Precambrian rocks assumes two and sometimes three things. First, it assumes that the diagrams take into account the entire range of chemistries present in the modern rock types being classified. Second, it assumes that the rocks have not undergone secondary alteration to a degree which has masked the original chemical patterns for those elements being considered by the individual plots. Third, for those diagrams designed to discriminate igneous rocks of different tectonic environments, it assumes that "modern" tectonic and igneous processes operated in the Precambrian. The first assumption is generally warranted, though by no means is it true in all cases for published discriminant diagrams, as will be shown below. The third assumption can be taken as a working hypothesis and in part tested by the performance of the classification schemes used. The same is true to a certain extent regarding the second assumption. There are also discriminant diagrams which attempt to use "immobile" elements (that is, elements unaffected by low-grade metasomatic processes) to avoid the problem of secondary alteration. These diagrams will be applied to the Vermilion rocks.

Geochemical Plots

Analyses of the igneous rocks (dacite porphyry, andesite, and basalt) from the Lake Vermilion Formation (LVF) and Knife Lake Group (KLG) are plotted in Fig. 9 (Irvine and Baragar, 1971). The scatter evident in this diagram relative to modern rock suite analyses (e.g., Jakes and White, 1972) is a result of secondary processes (see last section).

Despite this scatter, there is a calc-alkalic trend evident in the suite, similar to the trend found in island arcs (Jakes and White, 1972). Only a few LVF and Lower Ely basalts plot within the calc-alkaline field. Most plot in the tholeiite field, in contrast to the results of Schulz (1977), who found that his two LVF samples and most of his Lower Ely samples plotted in the calc-alkaline region of the AFM. Schulz's (1977) data for the Upper and Lower Members of the Ely Greenstone plot within the circled fields in Fig. 9. A komatiitic trend is evident in the Newton Lake data, while the Ely basalts are mainly tholeiitic with a few calc-alkaline samples belonging to the Lower Ely member.

The gap in the igneous rock compositions is evident on fig. 9; the scarcity of andesitic compositions is probably not due to sampling bias. The bimodality of the suite extends to trace elements (for example, Ti and Cr). Bimodal suites are present in Archean regions as well as Phanerozoic regions, and are characteristic of certain tectonic environments.

The alkalis and Ca are commonly mobile in altered Precambrian rocks, as they are in the Vermilion District, and the AFM diagram can

Fig. 8 -- Jensen Cation Plot (Jensen, 1976) showing the Vermilion igneous rock analyses. The plot is based on 8 LVVF dacites, 14 Upper Ely dacites, 4 Lower Ely dacites, 6 Vermilion rhyodacites, and 10 LVF basalts.

Fig. 9 -- AFM diagram (Irvine and Baragar, 1971), showing the Vermilion igneous rock analyses. The plot is based on 8 LVVF dacites, 14 Upper Ely dacites, 4 Lower Ely dacites, 6 Vermilion rhyodacites, and 10 LVF basalts.

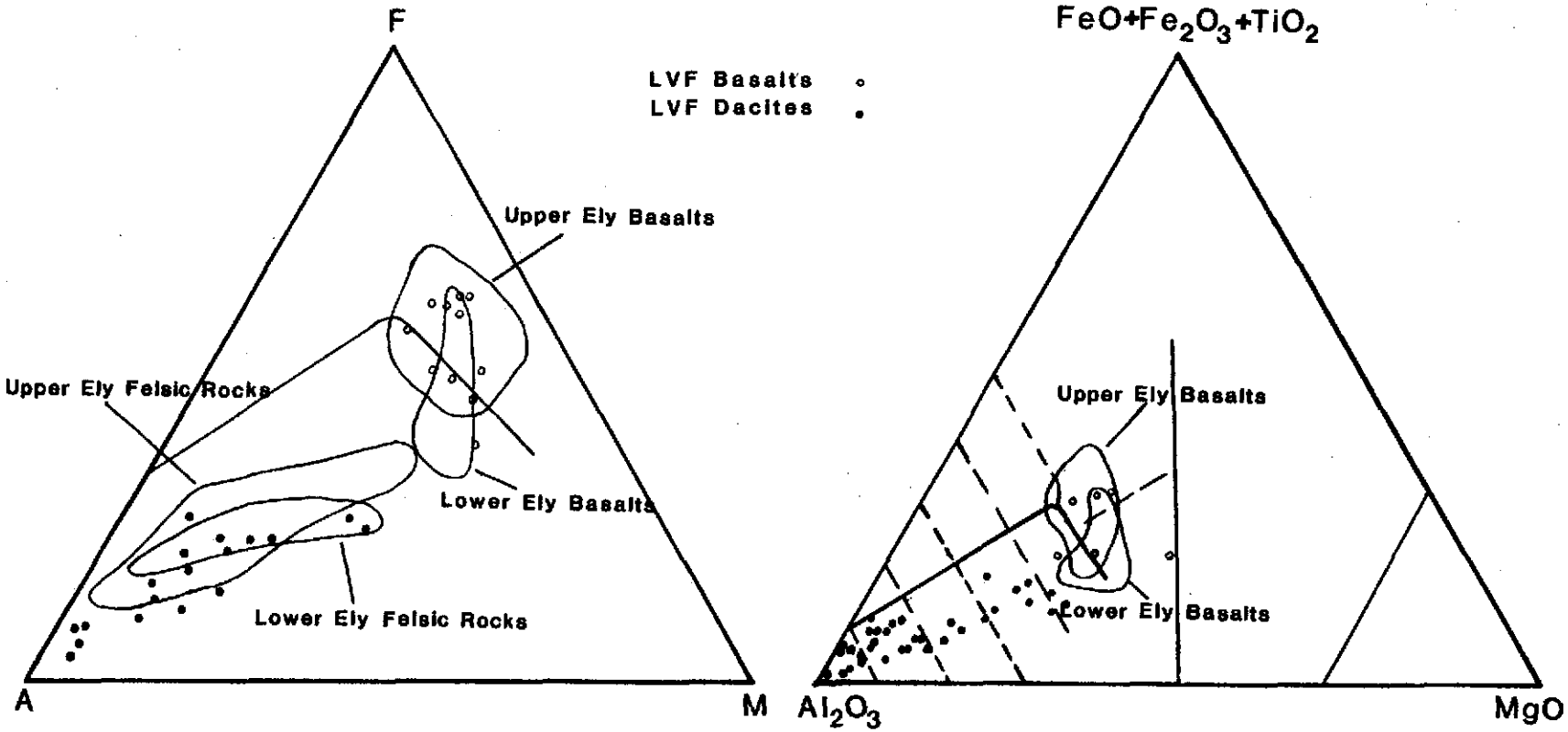
F
A
M
LVF Basalts
LVF Dacites
Upper Ely Basalts
Upper Ely Felsic Rocks
Lower Ely Basalts
Lower Ely Felsic Rocks
FeO+Fe2O3+TiO2
Al2O3
MgO
Upper Ely Basalts
Lower Ely Basalts

misclassify some samples. Jensen (1976) proposed a classification diagram which would avoid the problem of alkali and Ca mobility. His method was to use elements which were considered less mobile, but which still varied systematically during igneous differentiation processes (Al, Fe, Ti, and Mg). He used cation proportions of the elements instead of weight percentages. The advantages of the plot are that 1) it classifies a broad range of igneous rocks; 2) it assigns more specific rock names than the AFM (e.g., andesite); and 3) three distinct magmatic trends (calc-alkalic, tholeiitic, and komatiitic) are distinguishable.

The LVF and KLG igneous rock analyses are shown plotted on the Jensen Cation Plot in Fig. 8. The groupings of the rocks are no different from those on the AFM, except that they are tighter. The calc-alkalic trend of the suite, similar to an island-arc trend, is again very clear.

The LVF basalts and the Upper and Lower Ely basalts of Schulz (1977) are subdivided on the plot into high-Fe and high-Mg tholeiites. The two LVF analyses by Schulz (1977) plotted as calc-alkaline basalts on the Jensen Cation Plot and on the AFM. Half of the LVF analyses from this study plot as tholeiite basalts.

There are no known LVF andesites. The samples from this study which are andesites are from the Soudan Iron Formation and Upper Ely members of the Ely Greenstone. Sample ENES80-1 is a metasomatically altered dacite porphyry dike and its classification on the plot is not reliable. Analyses from older literature tend to be classified as andesites on the Jensen Cation Plot. Their high H_2O and CO_2 contents indicate that they

Fig. 10 -- SiO_2 vs. Zr/TiO_2 diagram (Winchester and Floyd, 1977) showing the Vermilion analyses. Analyses from Lesser Antilles (Brown, et al., 1977), Pacific island arcs (Gill, 1970; Dixon and Batiza, 1979; Jakes and White, 1972), and Tonga and Mt. Misery (Winchester and Floyd, 1977; Baker, 1968) have been plotted to establish an island arc trend for the diagram.

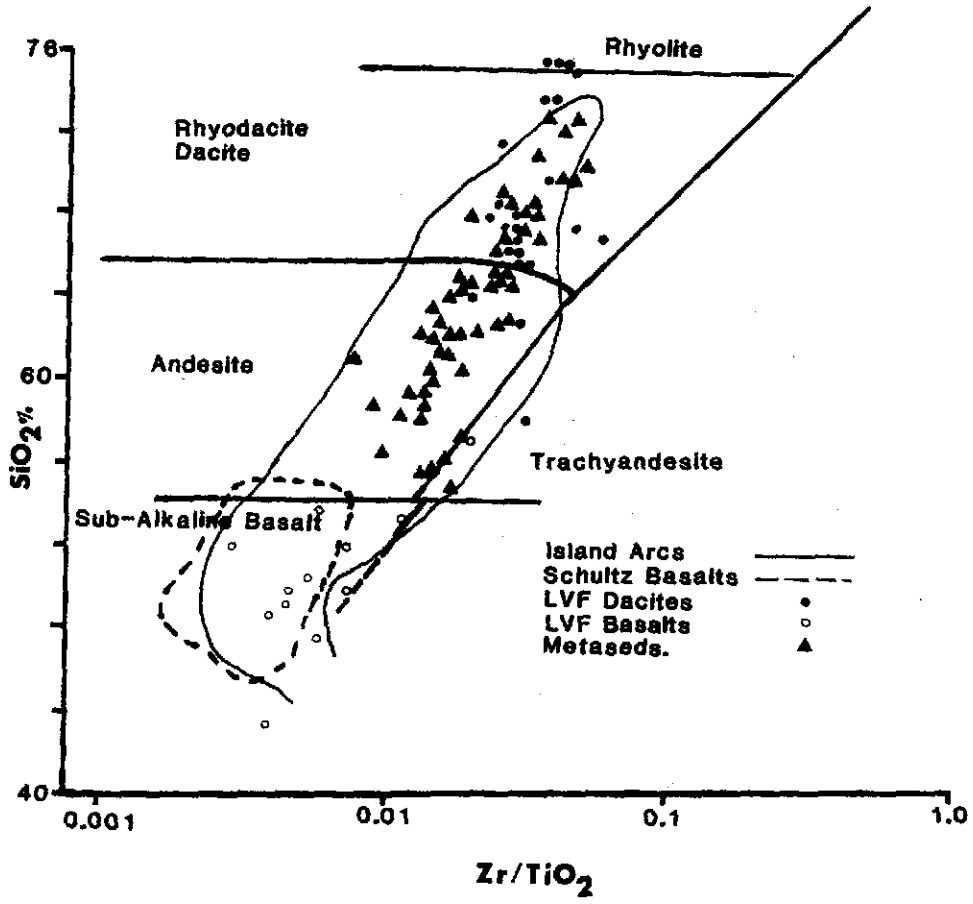
Rhyolite
Rhyodacite
Dacite
Andesite
Trachyandesite
Sub-Alkaline Basalt
Island Arcs
Schultz Basalts
LVF Dacites
LVF Basalts
Metaseds.
76
60
40
SiO2%
0.001
0.01
0.1
1.0
Zr/TiO2

may be altered samples.

Winchester and Floyd (1977) proposed using a plot of SiO_2 versus Zr/TiO_2 to classify a wide range of igneous rocks. Their plot is applied to the LVF data in Fig. 10. The igneous rock types as defined by petrography and major element chemistry correlate very well on this plot. All the basalts are classified as sub-alkaline basalts, since this plot does not distinguish tholeiitic from calc-alkaline rocks. Only one sandstone, TFV197-2, classifies as a basalt. It is possibly a mafic tuff. Sandstones and slates which grouped with the basalts on the AFM and Jensen plots are andesites on the SiO_2 vs. Zr/TiO_2 plot. In large measure, their positions on the plot are reflections of their SiO_2 contents.

The geochemical classification of the rocks presented here agrees with the classification by earlier workers using petrographic characteristics. The three chemical plots used here agree broadly on the assignment of igneous rock types to the samples. Therefore the chemistries of the rocks are probably not greatly altered from their original condition.

Discrimination of Tectonic Environments

Basalts of the Vermilion District

Classification by immobile elements

As an aid to the identification of tectonic settings for altered rock suites, a number of plots have been proposed for basalts using elements which are believed to be relatively unaffected by secondary

processes such as weathering, diagenesis, and low-grade metamorphism. Workers have concentrated on plots for basalts since this rock type is well studied and is found in a number of different tectonic environments.

The elements found to be relatively immobile during secondary alteration processes are Ti, Zr, Y, Nb, and to a lesser extent Sr, Ni, and Cr. The first workers to propose using immobile elements for basalt classification were Pearce and Cann (1973), who proposed two ternary and two binary diagrams involving the elements Zr, Ti, Y, and Sr to discriminate among four different tectonic environments for basalts. These diagrams and others have given rather consistent results for a number of different Cenozoic and older rock suites (Davies, et al., 1979; Wood et al., 1976; Stern, 1981). In applying these discriminant diagrams to altered Precambrian rock suites, the same requirements apply as were listed in the last section for geochemical plots. These are 1) that the diagrams take into account the entire range of igneous variation present in the modern rock types being classified; 2) that the elements considered by the plot are still present in essentially their original abundances; 3) for diagrams intended to discriminate among various tectonic environments of formation of the rocks, the assumption is made that modern tectonic and igneous processes operated in the Archean.

For discriminant diagrams relying on trace elements, the first assumption becomes more important than it was for the major elements; that is, it is somewhat more difficult to establish a restricted range of trace element abundances or ratios which will represent the complete

range possible in igneous rock suites globally. Two objections to the use of the Ti-Zr-Sr, Ti-Sr and Ti-Zr plots of Pearce and Cann (1973) have been made. In some cases, the plots have given results which conflict with other geological evidence. One such example is that of the Newfoundland ophiolite and island arc suites (Strong, 1977). Points on the plots from Pearce and Cann were scattered but predominantly clustered in regions of the plots representing exactly the opposite tectonic environments expected from petrologic and volcanologic evidence. It should be noted, however, that the plots were not constructed using any samples from ophiolite sequences. It is possible that ophiolites cannot be discriminated on these diagrams. In another case, Pearce and Cann's diagrams, as well as some others using Ti, Zr, Y, and Nb, did not indicate a unique tectonic environment, but indicated all possible tectonic environments, for continental basalts which were clearly from a single tectonic setting (Morrison, 1978). This was interpreted by Morrison to mean that the primary igneous variation of these rift lavas was larger than that accounted for in the diagrams. However, Holm (1982) has demonstrated that the Ti-Y-Zr diagram cannot discriminate continental tholeiites. The diagram was not defined using sufficient data. The problem that Morrison discovered is probably related to this limitation of Pearce and Cann's (1973) diagrams.

The second assumption, that the elements used on a plot have not been affected by secondary processes is particularly important. Some objections to the use of Sr as an "immobile" element have been voiced (Smith and Smith, 1976). Hellman et al., (1977) have shown that at the Cliefden outcrop in New South Wales, Australia, the trace elements Zr, Ti, Y, Sr, and the REE exhibit coherent behavior rather than immobile

Fig. 11 -- Ba vs. FeO^*/MgO diagram (Miyashiro and Shido, 1975) showing the LVF and Upper Ely basalt analyses. Data for 7 Upper Ely basalts from Jahn (1972), 2 Upper Ely basalts from Arth and Hanson (1975), 2 Upper Ely basalts from this study, 6 LVF basalts from this study.

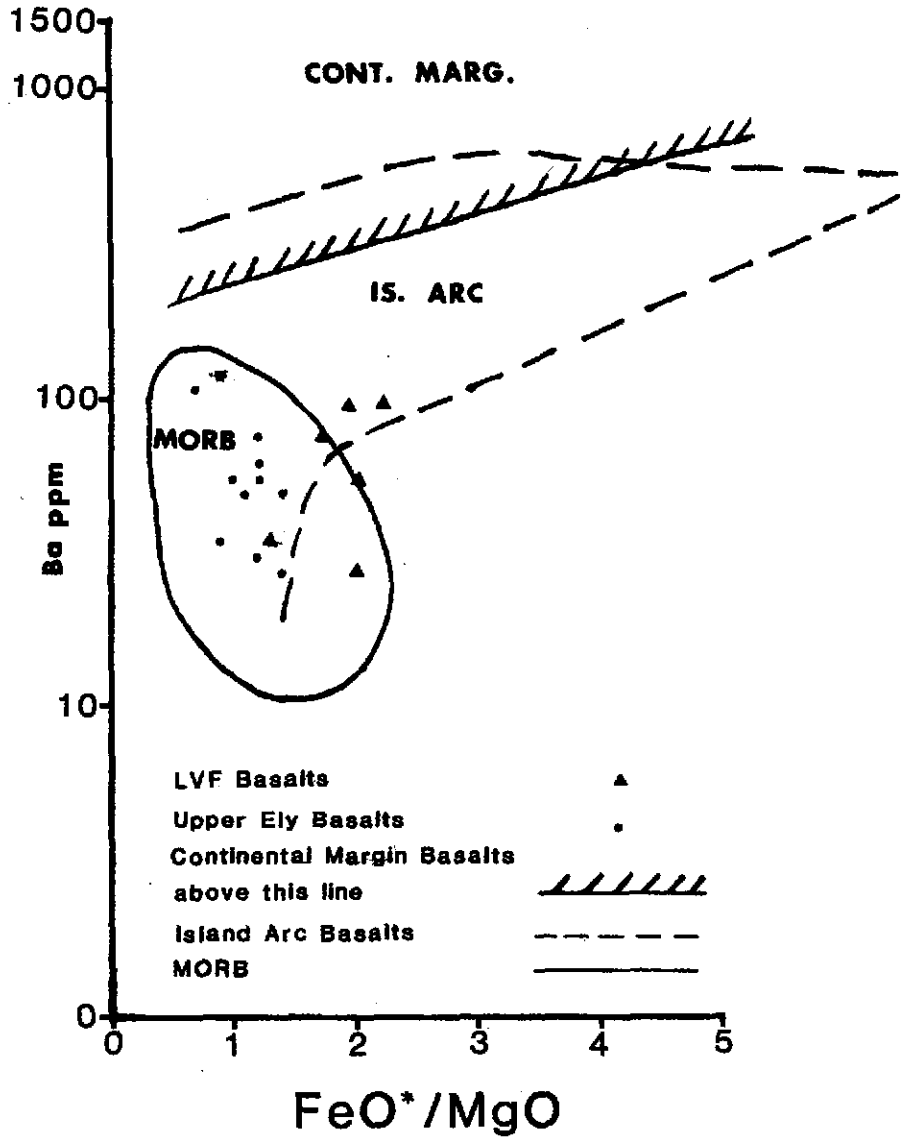
1500
1000
100
10
0
Ba ppm
CONT. MARG.
IS. ARC
MORB
0
1
2
3
4
5
FeO*/MgO
LVF Basalts
Upper Ely Basalts
Continental Margin Basalts
above this line
Island Arc Basalts
MORB

behavior; that is, they were remobilized in geochemically similar fashion and therefore retained constant ratios. Hellman et al. (1979) have demonstrated the coherent mobility of Zr, Ti, Y, and P in a number of metamorphosed terranes. In many cases the alteration produced patterns mimicking those expected by primary igneous variation. The cases described by Hellman et al. (1979) were cases of extreme alteration under clearly open-system conditions, with visibly veined and epidotized rocks. The Vermilion samples generally were only slightly affected by open-system exchange, and do not commonly display such obvious alteration features.

In summary, while there is some doubt as to the universal utility of these discriminant diagrams, their utility in discriminating among non-alkalic, noncontinental basalts has not been questioned. A battery of diagrams intelligently interpreted in the light of other geologic evidence can still be informative and useful, if they yield consistent results.

Classification Diagrams Using Ba, Ni, and Cr

Miyashiro and Shido (1975) proposed a set of plots using Ba, Ni, and Cr plotted against FeO^*/MgO to discriminate between basalts of island-arc and ocean-floor environments. The basalt analyses for the Vermilion District have been plotted on their diagrams in Figures 11, 12, and 13.

Representative modern island arc basalt data taken from Jakes and White (1972, idealized Pacific island arc values), Gill (1970, from Viti Levu, Fiji), and Brown, et al., (1977, Lesser Antilles) were plotted as a test of the Ba vs. FeO^*/MgO diagram. The results are not shown on

Fig. 12 -- Cr vs. FeO^*/MgO diagram (Miyashiro and Shido, 1975), showing the LVF, Upper Ely, and Newton Lake basalt analyses. No points overlap on the diagram; all data are from this study.

Fig. 13 -- Ni vs. FeO^*/MgO diagram (Miyashiro and Shido, 1975), showing the LVF, Upper Ely, and Newton Lake basalt analyses. No points overlap on the diagram; alll data are from this study.

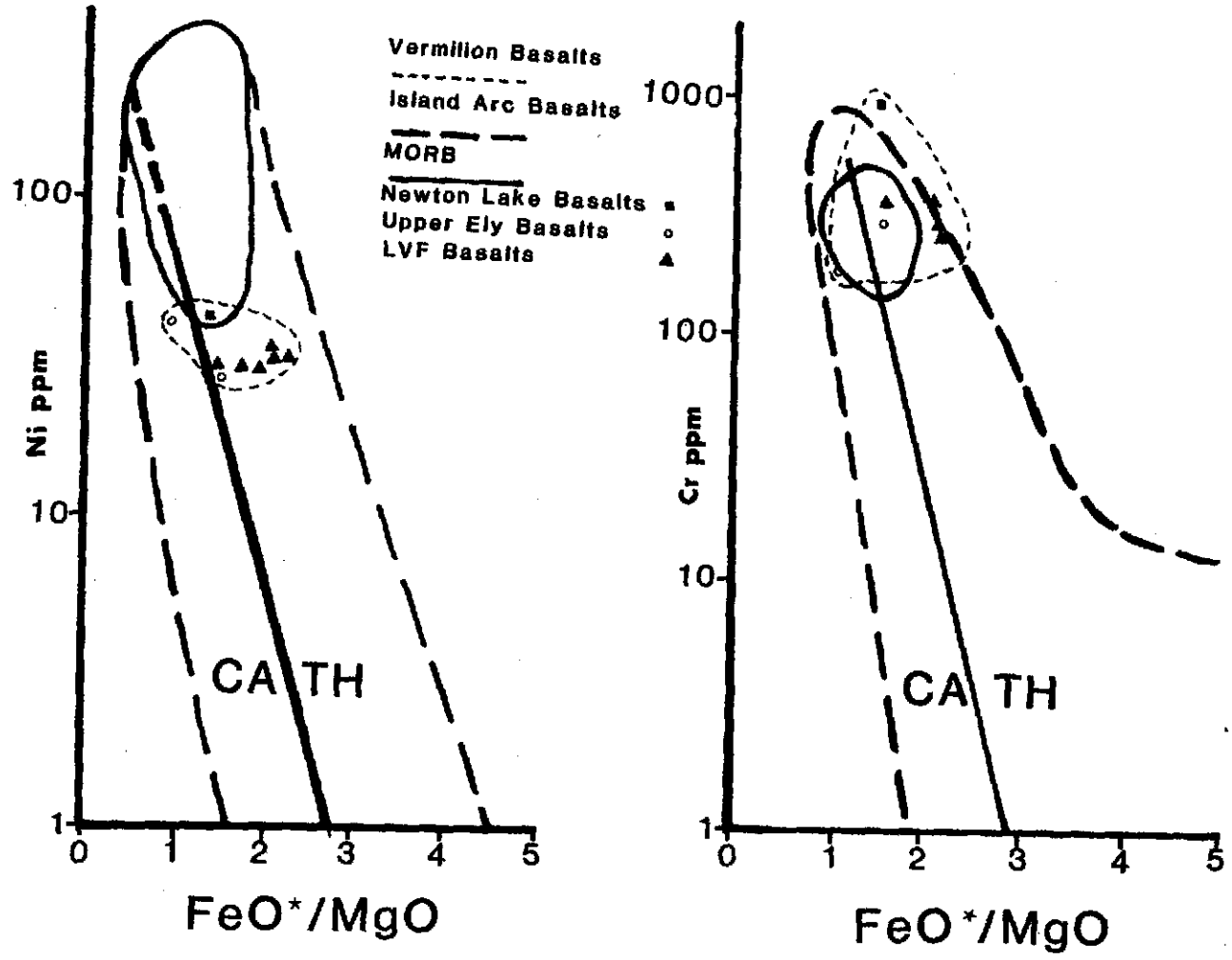
Vermilion Basalts
Island Arc Basalts
MORB
Newton Lake Basalts
Upper Ely Basalts
LVF Basalts
100
10
1
Ni ppm
CA TH
0 1 2 3 4 5
FeO*/MgO
1000
100
10
1
Cr ppm
CA TH
0 1 2 3 4 5
FeO*/MgO

fig. 11. The data for present-day island arcs verge on the abyssal tholeiite field but do not plot within it. The Upper Ely member basalts were interpreted as ocean-floor basalts by Schulz (1977), and this plot supports his suggestion. Schulz considered the few Lower Ely analyses and the two LVF analyses available to him to be calc-alkaline basalts. No Ba analyses exist for the Lower Ely member. Ba values for the LVF basalts cluster in the MORB-IAB overlap region of the diagram, and could be island-arc basalts. This diagram shows that the Upper Ely and LVF basalts have lower Ba abundances than most modern-day island-arc basalts.

The samples from this study are plotted on the other two diagrams from Miyashiro and Shido (1975) in figs. 12 and 13. Two Upper Ely and one Newton Lake basalt were analyzed as part of this study. The Vermilion samples plot within the island-arc basalt regions of the Cr vs. FeO^*/MgO and Ni vs. FeO/MgO plots (12 and 13, respectively), and dominantly on the tholeiitic (high-iron) side.

Ni values for the Upper Ely and Newton Lake basalts from this study, similar to the LVF values, plot in the island arc basalt field. The Newton Lake sample has been strongly affected by alteration and its Ni content may also have been changed. Ni values for the two Upper Ely samples are consistent with other trace element clues concerning the basalt type of these samples. Cr values for all three of these samples are high, and typical of MORB's rather than island arc basalts. Some of the Cr values may be inflated as an artifact of the analytical procedure (see Appendix A), and Ni results are more reliable than Cr results.

Classification Diagrams Using Zr, Ti, Y, and Sr

The ternary diagrams of Pearce and Cann (1973) are shown in figs. 14 and 15 for the Vermilion basalts. If these elements are truly immobile or only slightly mobile during secondary alteration processes, then the resultant primary igneous variations shown on these plots reveal a mixture of chemistries representative of several modern tectonic environments. The Lesser Antilles samples plot as CAB and LKT on the Ti-Zr-Sr diagram and as CAB on the Zr-Ti-Y diagram. Many samples plot in the overlap & OFB region. This implies that the Ti-Zr-Sr diagram does not always discriminate uniquely, and that island arc suites can plot in both fields. On the Ti-Zr-Y diagram many samples from the Lesser Antilles suite plot in the overlap region, but enough samples plot in the CAB region to identify this suite as a CAB suite.

On fig. 16, the Lesser Antilles data plots dominantly in the CAB region, with some samples classified as LKTs. One sample from Viti Levu, Fiji also plots as calc-alkaline. Data from two basalt flows from Shasta volcano (Mertzmann, pers. comm., 1984) plot partly as CAB and partly as LKT. The trends of the test suites plotted here are consistent with the volcanic arc trend of constant Ti with increasing Zr (Garcia, 1978). From the data presented here, it appears that island arcs are transitional to this trend, depending on their stage of evolution; young arcs have basalts whose Ti-Zr values cluster in the LKT region while more mature volcanic arc basalts have Ti-Zr values clustering in the CAB region of the diagram.

Schulz (1977) suggested that the "transitional" chemical character of the Lower Ely basalts relative to basalts from modern tectonic

Fig. 14 -- Ti/100-Zr-YX3 plot (Pearce and Cann, 1973) used to classify the LVF, Upper Ely, Newton Lake, and Lower Ely basalts. Data for 1 LVF basalt, 3 Lower Ely basalts, 4 Upper Ely basalts, and 26 Newton Lake basalts from Schulz (1977);all others (incl. 1 Newton Lake basalt) are from this study.

Fig. 15 -- Ti/100-Zr-Sr/2 plot (Pearce and Cann, 1973) used to classify the LVF, Upper Ely, Newton Lake, and Lower Ely basalts. Data for 1 LVF basalt, 3 Lower Ely basalts, 4 Upper Ely basalts, and 26 Newton Lake basalts from Schulz (1977);all others (incl. 1 Newton Lake basalt) are from this study.

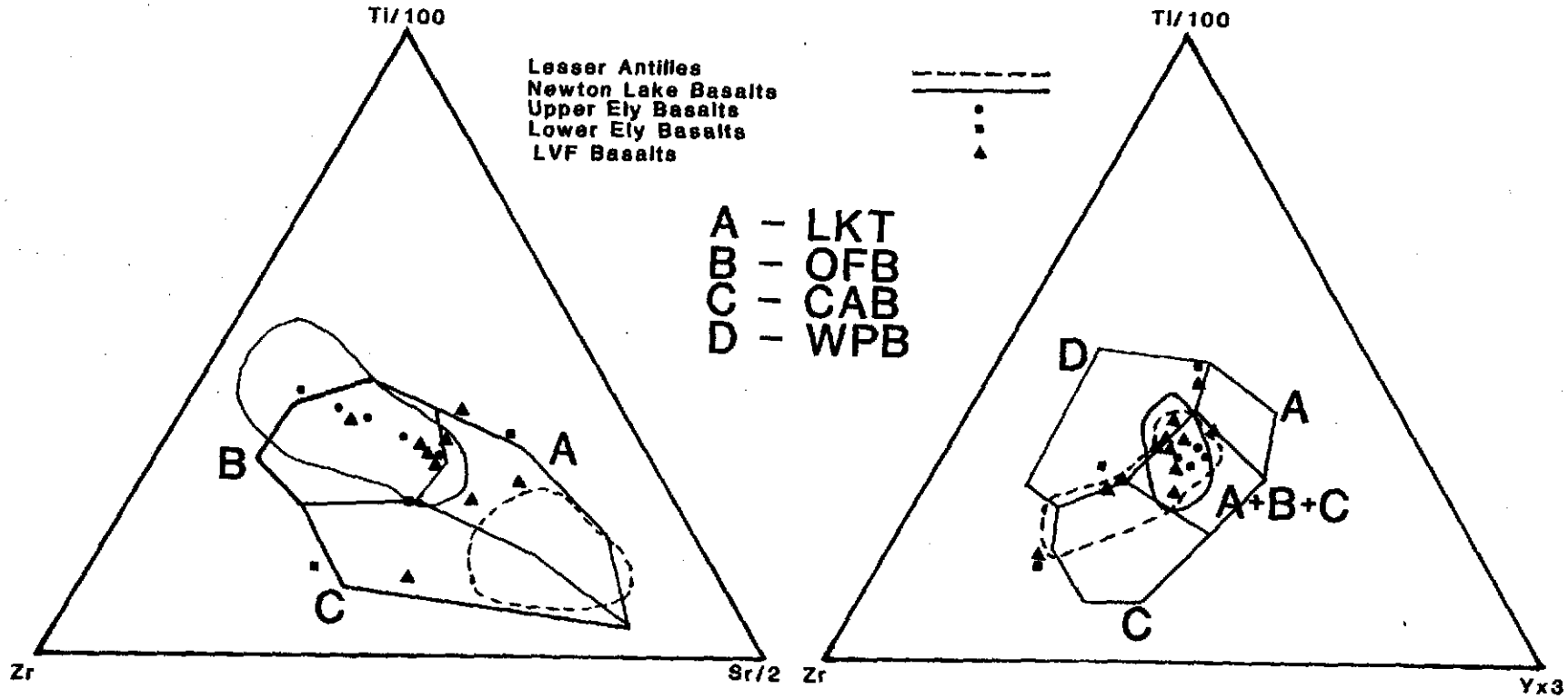
Ti/100
Zr
Sr/2
B
A
C
Lesser Antilles
Newton Lake Basalts
Upper Ely Basalts
Lower Ely Basalts
LVF Basalts
A – LKT
B – OFB
C – CAB
D – WPB
Ti/100
Zr
Yx3
D
A
A+B+C
C

environments may be a reflection of different tectonic and igneous processes operative in the Archean versus the present time. The Lesser Antilles data presented here, as well as data from other Cenozoic suites plot dominantly in one or another region on these discrimination plots, but are still "transitional" to other regions. Hence, these diagrams do not provide any evidence of processes or conditions in the Archean that were fundamentally different from those operating now.

On fig. 15, the LVF-Lower Ely samples display similar trends, from OFB to LKT. The Upper Ely samples classify as OFB, as do the Newton Lake rocks. All the basalts cluster in the OFB region, with a few Lower Ely and LVF samples in the LKT and even CAB regions. This diagram is difficult to interpret for the LVF and Lower Ely, and mobility of Sr may account for the scatter. It serves to show that the LVF and Lower Ely basalts possess similar ranges of values for Ti, Zr, and Sr.

On fig. 14, much the same pattern for the Vermilion basalts is evident as on fig. 15. Very low Y contents for the basalts may explain why the analyses verge on the WPB field. The Upper Ely basalts plot as OFBs, as do the Newton Lake basalts. The LVF and Lower Ely basalts scatter through all the fields, but cluster in the OFB/overlap region.

On fig. 16, the Upper Ely basalts resemble OFTs and display a trend of increasing Ti with increasing Zr, typical of OFBs (Garcia, 1978). Garcia (1978) showed that region D of fig. 16 includes high-TiO_2 members of the OFB suite as well as WPBs. The LVF and Lower Ely samples plot as LKTs to CABs, following the volcanic arc trend of Garcia (1978). The calc-alkaline basalts (GL16-1 and TMV146-1) may represent minor LVF-Lower Ely calc-alkaline basaltic volcanism which took place in the

Fig. 16 -- Ti-Zr diagram (Pearce and Cann, 1973) used to classify the LVF, Upper Ely, Newton Lake, and Lower Ely basalts. Data for 1 LVF basalt, 3 Lower Ely basalts, 4 Upper Ely basalts, and 26 Newton Lake basalts from Schulz (1977);all others (incl. 1 Newton Lake basalt) are from this study.

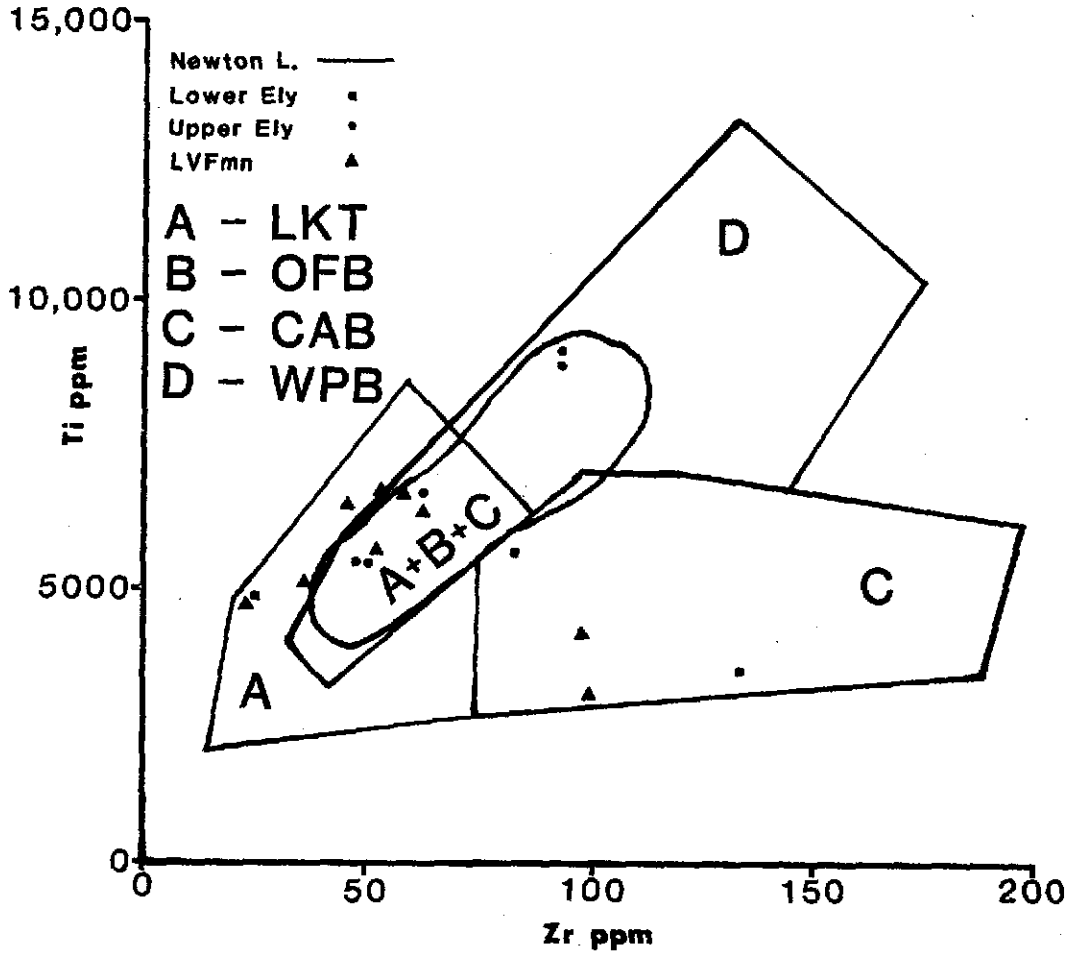
15,000
10,000
5000
0
Ti ppm
Newton L.
Lower Ely
Upper Ely
LVFmn
A – LKT
B – OFB
C – CAB
D – WPB
A+B+C
A
C
D
0
50
100
150
200
Zr ppm

Vermilion District even though the dominant type was IAT. No assessment of relative stratigraphic position for the LKT and CAB samples is possible.

The Lesser Antilles data plot from MORB to IAB on a Zr/Y vs. Zr diagram (fig. 17; Pearce and Norry, 1979). No anomalous samples such as are found in the Vermilion District data are found in the Lesser Antilles data, which are averages of many analyses. The alkalic members of the Lesser Antilles suite plot into the WPB region of the diagram. The diagram appears to classify island arc rocks correctly. The Upper Ely basalts plot dominantly in the region for OFB. The fact that some Newton Lake, Lower Ely, and LVF basalts have higher Zr/Y ratios than the basalts used to define the plot is a reflection of the low Y in the Vermilion basalts. The LVF basalts plot dominantly in the IAB region. TMV146-1 and GL16-1, which plotted as calcalkaline basalts before, now plot off the diagram, indicating very low Y in these basalts.

Other Trace Element Comparisons

The Upper Ely and Newton Lake Ba, Sr, and Zr abundances are lower than those of IATs and resemble OFT values. As Schulz (1977) pointed out, the Ely and Newton Lake basalts have low Y (9.5 to 37 ppm) and low Al compared to modern basalt suites. The same is true for the Upper Ely samples analyzed in this study (table 5). Low Y values are typical of Archean calc-alkaline rocks (Lambert and Holland, 1974). K/Rb ratios and Rb abundances are the same as calc-alkaline or continental margin abundances, but the K and Rb contents of these rocks are probably not original.

Fig. 17 -- Zr/Y - Zr diagram (Pearce and Norry, 1979) used to classify the Vermilion basalt samples. Data for 1 LVF basalt, 3 Lower Ely basalts, 4 Upper Ely basalts, and 26 Newton Lake basalts from Schulz (1977);all others (incl. 1 Newton Lake basalt) are from this study.

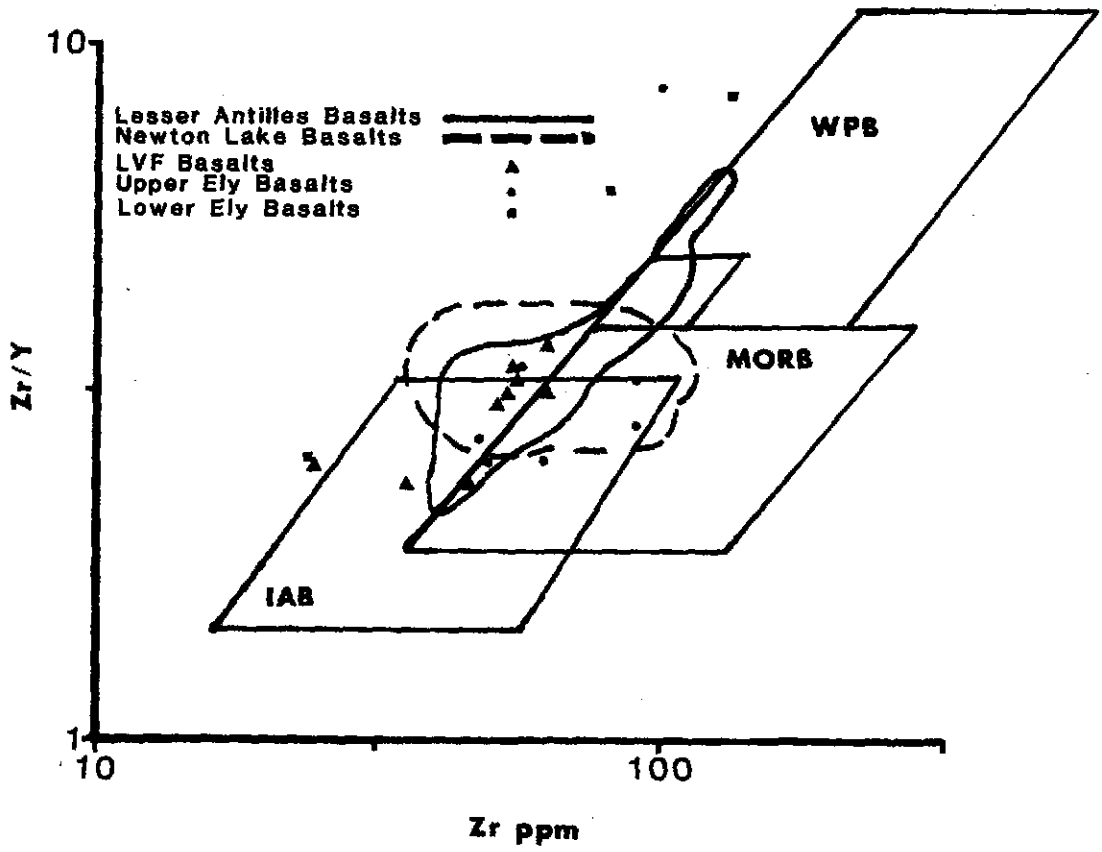
10
1
10
100
Zr/Y
Zr ppm
Lesser Antilles Basalts
Newton Lake Basalts
LVF Basalts
Upper Ely Basalts
Lower Ely Basalts
WPB
MORB
IAB

Table 5

Comparative Basalt Geochemistries[1]

	IAT	OFT	CAB	LVF	Lower Ely	Upper Ely	N. Lake
SiO_2%	45-70 53.0	47-62 49.0	53-70 59.0	41-54 50.5	48-59 54.2	51-54 52.5	46-61 52.1
Al_2O_3%	14-19	14-19	16-19	12-16	14-17	11-17	12-20
Rb ppm	3-10 5	0.2-0.5 ---	6-45 10	0.15-39 8.8	6-15 11.73	0.4-59 14.6	14-81 9.2
Sr ppm	100-220 200	70-150 ---	236-397 330	79-450 157.3	134-176 154.0	52-253 135.0	21-337 118.9
Ba ppm	50-150	6-30	86-336	30-411	---	6-507	29-188
K/Rb	--- 1000	--- 1000	367-617 340	186-213 203.9	248-365 313.7	103-1290 352.8	232-767 387.8
Ni ppm	0-30 ---	30-200 ---	--- 25	28-35 30.8	--- ---	27-40 33.0	--- 42.0[2]
Cr ppm	0-150 ---	100-500 ---	--- 40	213-736 368.0	--- ---	198-300 249.0	--- 1085.0[2]
TiO_2%	0.3-1.2 ---	1.0-2.5 ---	0.5-1.2 ---	0.7-1.1 0.99	0.6-1.5 0.87	0.5-1.6 1.00	0.5-1.9 1.05
Zr ppm	--- 70	--- ---	--- 100	36-98 58.8	24-134 80.7	48-100 72.0	25-111 71.0
Y ppm	--- ---	--- ---	--- 20	11-20 16.7	10-16 13.2	12-33 21.8	10-37 21.6

[1]Second number is mean or preferred value.
[2]Single sample only, from this study.
Sources: Jakes and Gill, 1970; Jakes and White, 1972; Garcia, 1978; Chow, et al., 1980; Arth and Hanson, 1975; Schulz, 1977; Jahn, 1972; this study.

The Lake Vermilion Formation basalts resemble IATs in their Ba, Sr, and Ni contents. The Cr contents can be very high, but may be inflated. Cr values are in the OFT range, if they are real; however, they do not match the Ni abundances. Zr is slightly low for IATs. The LVF basalts, like the rest of the Vermilion basalts, have low Y.

Summary

Schulz's (1977, 1980) conclusion that the Upper Ely member basalts are ocean-floor tholeiites is supported by their location on the discriminant diagrams used in this study, and by their Sr, Ba, and Zr contents. The LVF basalts may be called LKTs on the basis of their Ni abundances, FeO^*/MgO ratios, and their trends on Ti-Y-Zr-Sr diagrams. The LVF basalt trend resembles the Lower Ely trend in that some specimens plot as LKT-OFB and CAB on the Ti-Zr-Y plots, reinforcing the conclusion of Schulz (1977) that the Lower Ely basalts resemble the LVF basalts, and probably had a similar history and mode of origin. Schulz (1977) concluded that the LVF and Lower Ely basalts were calc-alkaline in nature, based on their location on an AFM and a Jensen Cation Plot. The data of this study indicates that the LVF is dominantly LKT in nature, trending toward calc-alkaline chemistries. That LKT volcanism is predominant in younger arcs and becomes progressively more and more calc-alkaline in mature volcanic arcs is indicated by Garcia's (1978) Ti-Zr trends as well as the trends for the Shasta and Lesser Antilles suites on a Ti-Zr diagram. The Lower Ely is probably dominantly LKT by analogy to the LVF, as originally suggested by Jahn et al. (1974) and Arth and Hanson (1975). Ni abundances in the LVF basalts are too low for modern MORB, but fit Ni abundances for island arc basalts. Cr abundances are in the normal range for either island arc basalts or MORBs. The Ti and Zr values for the LVF basalts are low compared to average Tertiary LKT basalts; the Upper Ely and Newton Lake samples are likewise lower in Ti and Zr than modern OFBs; this is further evidence of an impoverishment in HFS elements other than Y.

Dacites of the Vermilion District

Dacites have not been the subject of as much intense study as basalts, and trace element classification diagrams such as were used in the section on basalts have not been prepared for dacites. This section will discuss characteristics of the Vermilion dacites and compare their chemistry to what is known about Tertiary dacites from different tectonic environments.

On a K_2O-SiO_2 plot (boundaries after Gill, 1981), the Vermilion dacites show considerable scatter (see fig. 18), but the bulk of the samples are in the calc-alkaline (C-A) and low-K regions. The high-K samples may have been affected by alteration (see chapter 3).

Weight per cent Al_2O_3 in the Vermilion dacites is low relative to modern calc-alkaline dacites, and has a wide range. MgO values do not depart significantly from values for Tertiary suites except that they are a little high. Fe_2O_3T is low relative to dacites from modern island arcs, even to those of the calc-alkaline series.

The dacites are lower in TiO_2 than modern dacites in suites considered by Pearce and Norry (1979, figs. 17 and 20) and lower than typical values for dacites from orogenic regions (Table 6). Most modern calc-alkaline island arc dacites are higher in TiO_2 than the Vermilion dacites (Ewart, 1979). Dacites of the island-arc tholeiite series are even higher in TiO_2 (Jakes and White, 1972), as are those of oceanic plagiogranites (Coleman and Donato, 1979). The Vermilion dacites resemble calc-alkaline island arc rocks rather than dacites of the island arc tholeiite series or ocean floor plagiogranites in their Rb,

Fig. 18 -- Scatter diagram of K_2O vs. SiO_2 showing the Vermilion igneous rock analyses. Reference lines for rock types follow Gill (1981). Each point represents an individual analysis on this plot; all data are from this study.

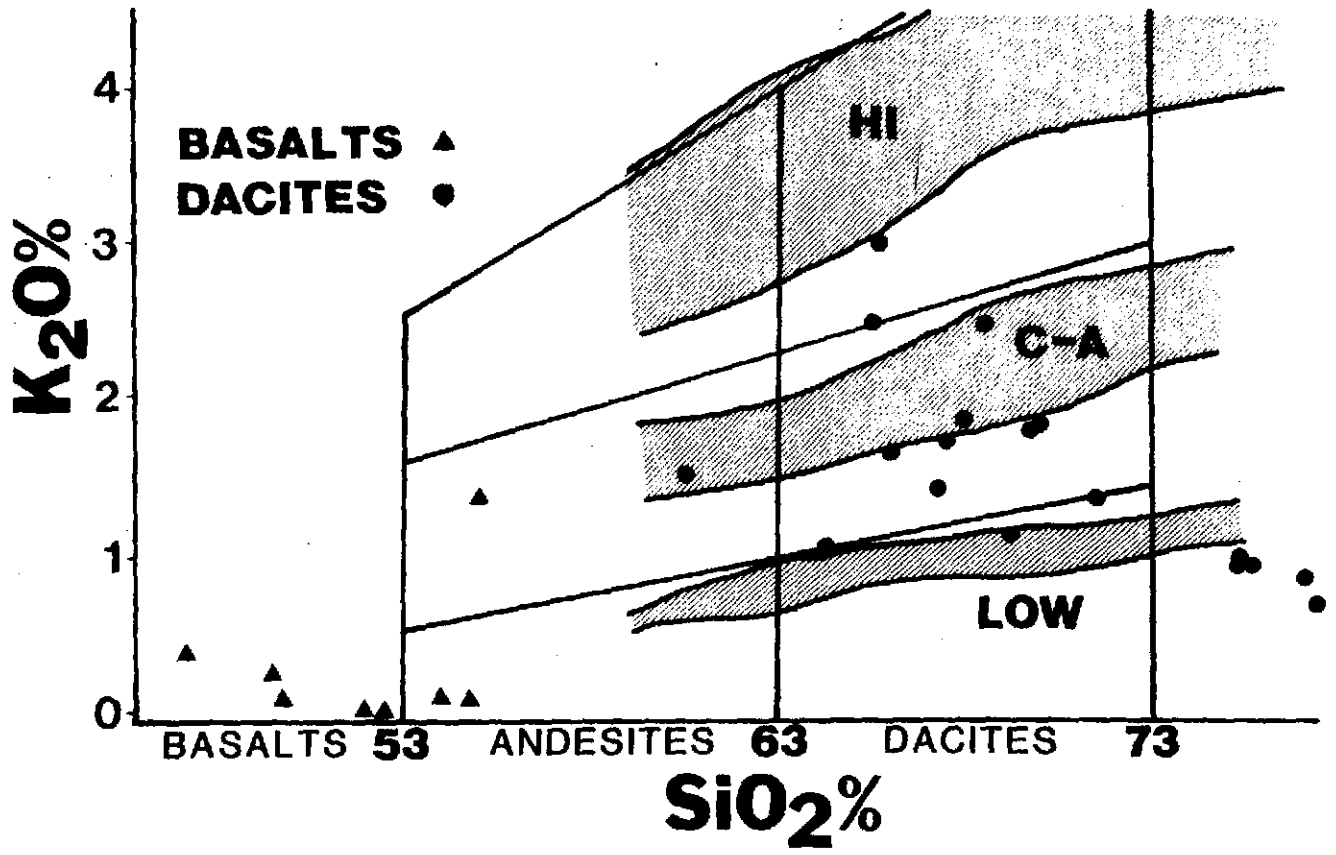
BASALTS
DACITES
HI
C-A
LOW
4
3
2
1
0
K2O%
BASALTS
53
ANDESITES
63
DACITES
73
SiO2%

Table 6
Comparative Dacite Geochemistries[1]

	IAT series	Calcalkaline series	Continental margin series	Vermilion Dacites
SiO_2	---	---	---	58-73
	63.0	63.0	63.0	66.9
Al_2O_3	---	16-19	16-17	12-20
Rb ppm	---	10-45	98-143	14-81
	15	---	112	44.7
Sr ppm	---	330-460	533-1082	164-690
	90	---	799	495.8
Ba ppm	---	270-520	783-1730	46-762
	175	---	1270	519.3
K/Rb	---	---	---	108-289
	870	380	---	218.7
Ni ppm	---	5-18	19-49	6-33
	1	---	34	13.7
Cr ppm	---	13-56	11-95	5-142
	4	---	60	55.0
TiO_2%	0.5-1.5	0.5-1.2	0.69-0.89	0.16-0.76
	---	---	0.81	0.33
Zr ppm	---	---	100-331	61-184
	125	100	209	88.8
Y ppm	---	---	8-25	2-13
	23	20	20	6.05

[1]Second number is mean, or preferred value at SiO_2=63 wt.%. Sources: Jakes and Gill, 1970; Jakes and White, 1972; Garcia, 1978; Ewart, 1979; Arth and Hanson, 1975; Schulz, 1977; Jahn, 1972; this study.

Sr, and Ba contents.

K/Rb values for the Vermilion dacites cluster in the calc-alkaline

range for average Cenozoic dacites from all over the world (Ewart, 1979), rather than in the low-K or high-K ranges. Sr/Ba ratios range from 0.66-3.58, and have probably been disturbed by metasomatism, because no single Cenozoic dacite suite has such high maximum values or such a wide range.

LeFevre et al. (1974) showed that island arc lavas have K_2O, Rb, and Ba concentrations that are generally somewhat lower than are found in continental margin calc-alkaline suites. Data from Ewart (1979, see table 6) reflect the same distinction. While the values for K, Rb, Sr, and Ba verge on values for continental margin suites, they are low compared to mean values for continental-margin dacites, and are within the range for island arc dacites. Elevated Rb, Sr, and Ba contents are typical of spilites and keratophyres (see chapter 3).

Ni abundances in the dacites are similar to either the island-arc tholeiite or calc-alkaline series (see table 6), but their Cr abundances range too high for calc-alkaline rocks. As with the basalts, some of the Cr may be an analytical artifact. Y and Zr values for the Vermilion dacites are low relative to Tertiary dacites.

Geochemical Constraints on Magma Genesis

Abundances of Fe and the HFS Elements

The low Fe and HFS element contents of the dacites could be explained by fractionation of magnetite, amphibole, or ilmenite, or by partial melting leaving a residuum composed of these minerals. Ilmenite is commoner in dacites than in andesites, but it is rarer than magnetite by far, due to low activity of TiO_2 and low fugacity of O_2 (Gill, 1981).

Magnetite phenocrysts are common in the dacites. Amphibole phenocrysts are also known from the Vermilion district.

The Ti, Zr, and Y contents of these dacites and the Vermilion rocks in general are lower than values for modern igneous rocks of the same magma types. Low contents of TiO_2 in Archean rocks have been noticed by other workers. Mueller (1970) noted a negative correlation between TiO_2 abundance and K-Ar age for Precambrian mafic rocks of the Beartooth Mountains. Archean rocks are typically lower in TiO_2 than Proterozoic rocks from the Canadian Shield (Fahrig and Eade, 1968). The low contents of Fe, Ti, Zr, and Y in the Vermilion rocks are probably primary.

Ti-Zr-Y Systematics

Pearce and Norry (1979) have compared Y-Zr and Ti-Zr variations among a number of modern igneous rock suites from island arcs, continental margins, and intraplate settings. They have proposed petrogenetic models to account for the observed Ti-Zr-Y variations. Figs. 19 and 20 show the Vermilion suite analyses plotted on their Y-Zr and Ti-Zr diagrams. Fractionation vectors for the major rock-forming minerals are shown on the diagrams. A fractionation vector is the vector along which the trend for the suite will move when the mineral represented by that vector is crystallizing from the melt, or when it is present in the residuum from partial melting. Garnet, it should be noted, has partition coefficients for Ti-Zr-Y almost identical to those of amphibole, and garnet's fractionation vector is therefore almost identical to amphibole's. The "hairpin" turns in the trends from basic to acidic rocks are similar to the trends for the island-arc and

Fig. 19 -- Y-Zr plot (Pearce and Norry, 1979) showing the Vermilion igneous rock analyses. The trend arrow drawn on the diagram is for increasing SiO_2. Fractionation vectors calculated by Pearce and Norry for the important rock-forming minerals are shown in the inset. Garnet's fractionation vector is almost identical with amphibole's. Plot based on 1 LVF basalt, 3 Lower Ely basalts, 5 Upper Ely basalts, and 26 Newton Lake basalts from Schulz (1977); 7 LVF basalts, 2 Upper Ely basalts, 1 Newton Lake basalt, 6 LVF dacites, 3 Soudan dacites, 2 Lower Ely dacites, and 5 Upper Ely dacites from this thesis.

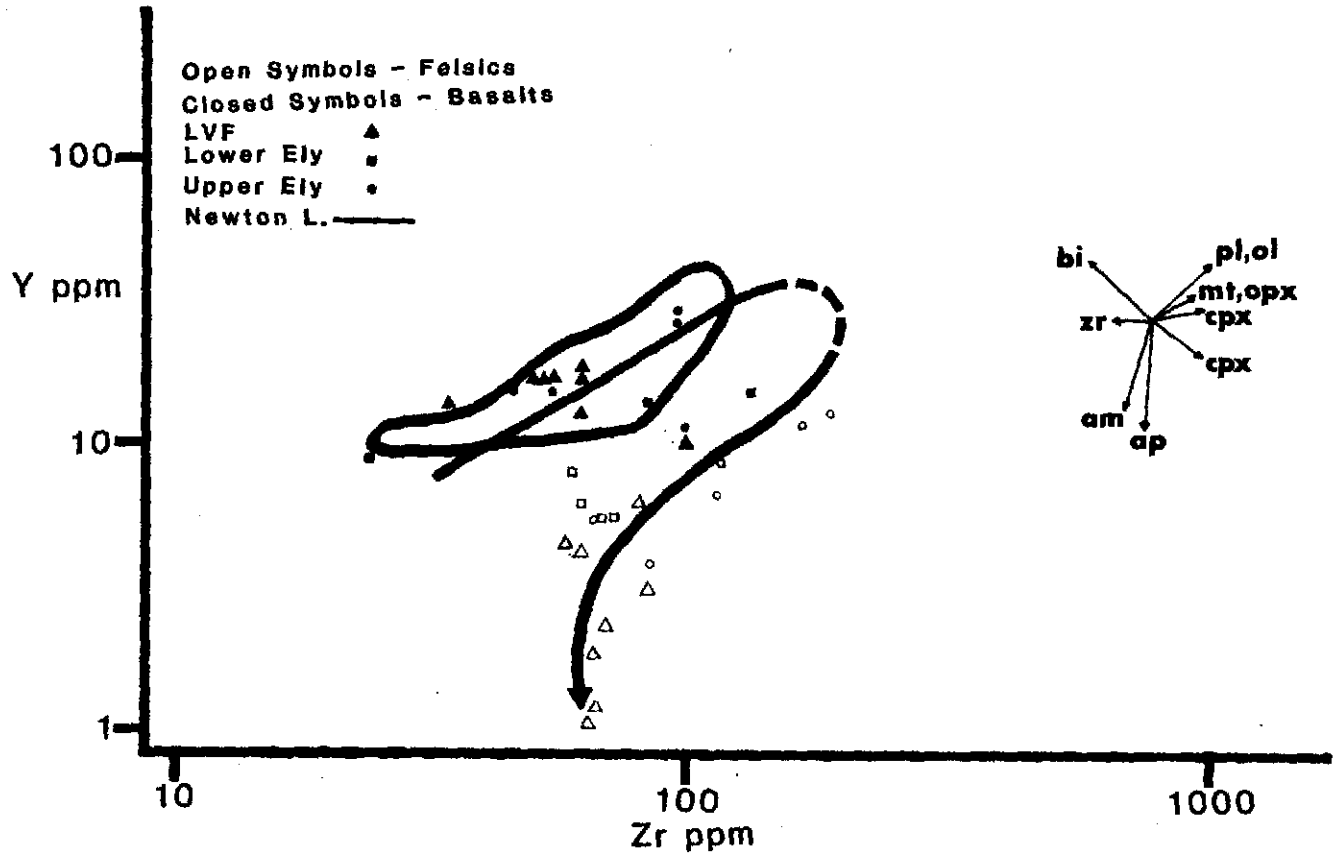
Open Symbols - Felsics
Closed Symbols - Basalts
LVF
Lower Ely
Upper Ely
Newton L.
100
10
1
Y ppm
10
100
1000
Zr ppm
bi
pl,ol
mt,opx
cpx
zr
cpx
am
ap

continental-margin suites investigated by Pearce and Norry. The genetic histories of the Vermilion rocks and these modern suites may therefore also be similar.

Trends on figs. 19 and 20 will be almost identical whether they arise from partial melting or fractional crystallization. Pearce and Norry used their Ti-Zr-Y diagrams to examine fractional crystallization models for modern orogenic suites, because Zr variations in the modern suites were best explained by simple fractional crystallization.

Arth and Hanson (1975) have demonstrated that the REE, major and selected trace element characteristics of the Vermilion rocks can be explained by varying degrees of partial melting alone. A summary of their model was given in the Introduction (Table 2). Pearce and Norry (1979) noted that Cr varies little during partial melting but increases rapidly during fractional crystallization, as expressed by increasing Zr. The range in Zr values in the Vermilion basalts is too narrow to perceive any Zr-Cr trend, but the dacites display a wide range in Zr values: In the dacites Cr is high and constant with increasing Zr, commensurate with a partial melting origin for the Vermilion igneous rocks. Partial melting is therefore the preferred mechanism for the origin of the rocks, and although fractional crystallization could also explain the trends seen on the Ti-Zr-Y diagrams, mechanisms involving fractional crystallization will generally be omitted from further consideration.

The basalts display a roughly linear trend on the Y-Zr diagram, with a slope of 0.8. Rock suites from all volcanoes studied by Pearce and Norry exhibit similar trends. Such a trend corresponds to partial

Fig. 20 -- Ti-Zr plot (Pearce and Norry, 1979) showing the Vermilion igneous rock analyses. The trend arrow drawn on the diagram is for increasing SiO_2. Fractionation vectors calculated by Pearce and Norry for the important rock-forming minerals are shown in the inset. Garnet's fractionation vector is almost identical with amphibole's. Plot based on 1 LVF basalt, 3 Lower Ely basalts, 5 Upper Ely basalts, and 26 Newton Lake basalts from Schulz (1977); 7 LVF basalts, 2 Upper Ely basalts, 1 Newton Lake basalt, 6 LVF dacites, 3 Soudan dacites, 2 Lower Ely dacites, and 5 Upper Ely dacites from this thesis.

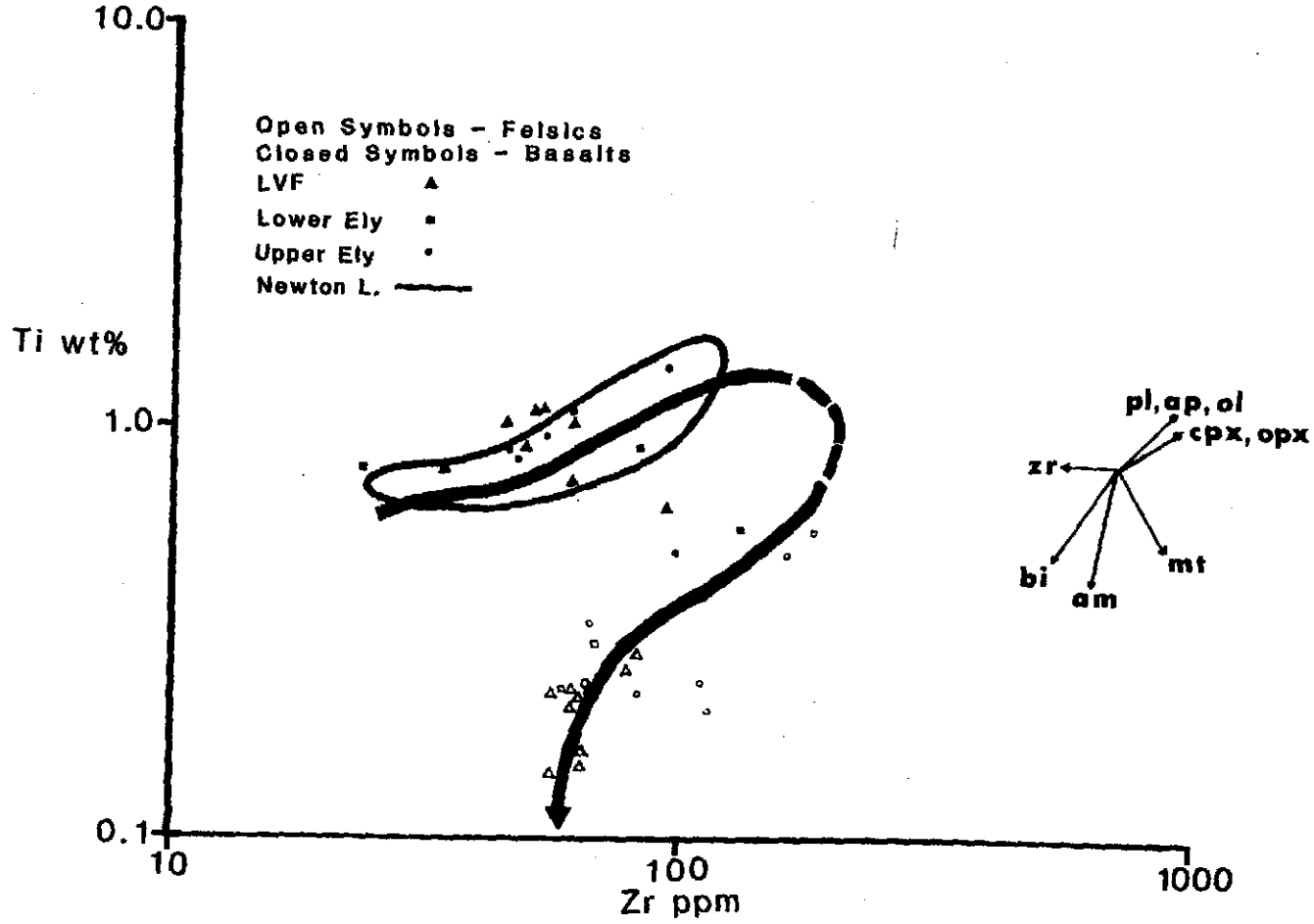
10.0
1.0
0.1
Ti wt%
Open Symbols – Felsics
Closed Symbols – Basalts
LVF
Lower Ely
Upper Ely
Newton L.
10
100
1000
Zr ppm
pl, ap, ol
cpx, opx
zr
bi
am
mt

melting with olivine - plagioclase - clinopyroxene ± magnetite ± orthopyroxene in the residuum. These are phases one would expect in a residuum derived from mantle peridotite (Arth and Hanson, 1975).

Some basalts plot along almost the same trend as the dacites because they have lower Y than the other basalts. The presence of magnetite, garnet, or amphibole in equilibrium with these liquids during partial melting would have depleted them in Y. Alternatively, they could be related to the high-Y basalts by fractionation involving clinopyroxene, magnetite or amphibole.

The patterns for the basalts on the Ti-Zr plot (fig. 20) are very similar to those on the Y-Zr plot (fig. 19). The slope is 1.0. This is commensurate with the same residual minerals as were listed above for the Y-Zr plot, because the same fractionation vectors apply on the Y-Zr and Ti-Zr plots for each mineral considered.

The change in direction of the Y-Zr and Ti-Zr trends on figs. 19 and 20 indicates a change in the mineral assemblage present in the residuum left after partial melting. Arth and Hanson (1975) showed that the Vermilion tonalites and dacites could be derived from the Vermilion basalts after conversion of the latter to eclogite or amphibolite at depth. The trend for the dacites has a slope of -1.5 on both the Y-Zr and Ti-Zr diagrams. The trend for the dacites as shown by the arrows is for increasing SiO_2. Because the fractionation vectors for amphibole, garnet, biotite, and possibly zircon would move the compositions of successive melts in the direction of decreasing Ti or Y with decreasing Zr, the dacite trend implies partial melting with the above-mentioned minerals in the residuum. Amphibole phenocrysts are found in many of

the dacite samples (Green, 1970; Sims, 1972b), and so amphibole was at least often a liquidus phase; detrital biotite grains are found in the Vermilion graywackes, presumably derived from tuffaceous source material (Ojakangas, 1972). It is difficult to test for the presence of biotite in the source region for the dacites without using Ba or K (Arth and Hanson, 1975), which have been remobilized by secondary processes in the Vermilion rocks.

Y trends

Constant or decreasing Y contents are typical of continental margin suites in modern environments (Gill, 1981, p. 130), but there are a few ensimatic volcanic suites which display these variations, notably volcanoes in the Japan Sea (Masuda, et al., 1975) and on Dominica, in the Lesser Antilles (Brown, et al., 1977). Values of 20-25 ppm are considered standard for orogenic andesites (Gill, 1981), and dacites are similar (Jakes and White, 1972). The Vermilion samples have constant or decreasing Y with increasing SiO_2 or CaO.

Figure 21 shows the Vermilion samples plotted on a CaO-Y diagram (Lambert and Holland, 1974). Also plotted is the "reference" calc-alkaline trend of Lambert and Holland (1974). The Vermilion samples have a very constant and low abundance of yttrium relative to the modern trend and show a decrease in Y with a decrease in Ca. This is characteristic of the "J-type" trend of Lambert and Holland (1974), indicating hornblende or calcic garnet fractionation. Whether the basalts and dacites are taken as part of a single trend or not, the dacites do show the influence of amphibole or garnet. This again is commensurate with Arth and Hanson's (1975) model for the genesis of the

Fig. 21 -- CaO-Y diagram (Lambert and Holland, 1974), showing the Vermilion analyses. The "standard" trend for calc-alkaline suites is shown, as well as the suites with a "J"-type ("hornblendic") trend discussed by Lambert and Holland.

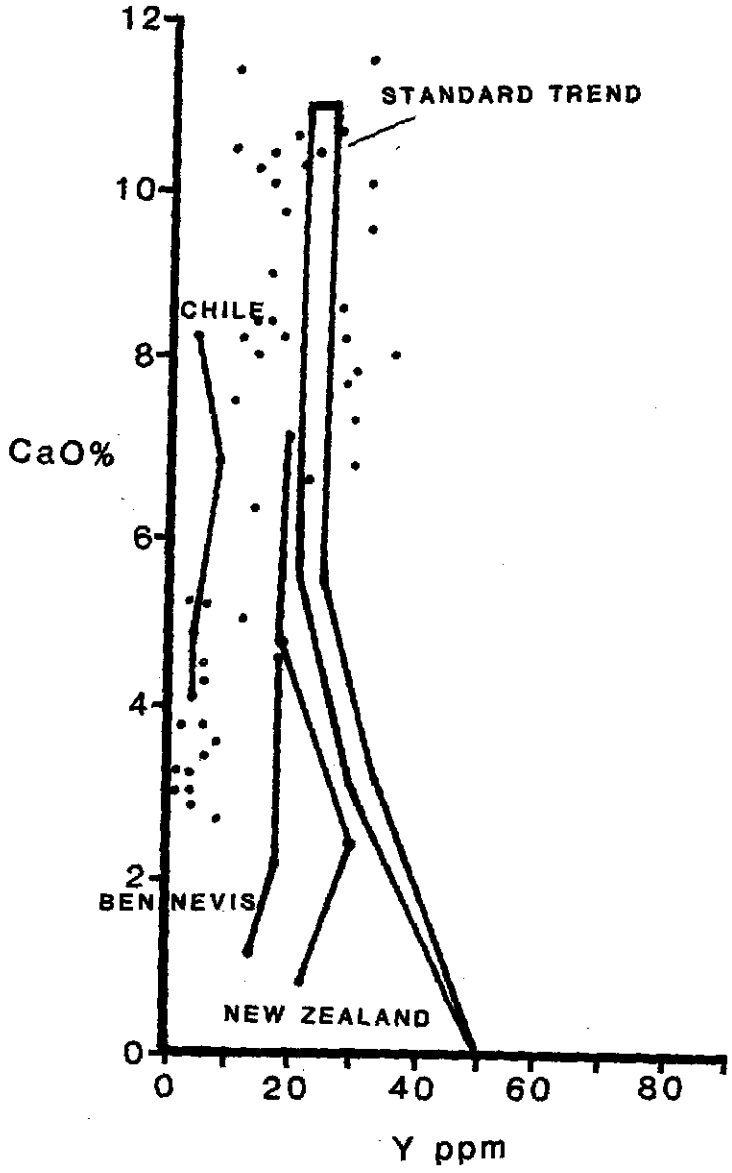
12
10
8
6
4
2
0
CaO%
STANDARD TREND
CHILE
BEN NEVIS
NEW ZEALAND
0
20
40
60
80
Y ppm

dacites.

Comparisons to Suites with Similar Ti-Zr-Y Systematics

There are some modern suites which show a "hairpin" turn in Y-Zr and Ti-Zr trends similar to the Vermilion samples. To the extent that recent suites with analogous Ti-Zr-Y trends are found, they demonstrate that the processes that formed the Vermilion District are still operating today. The modern suites listed by Pearce and Norry (1979) which display the "hairpin" turn (called "Andean-type" by Pearce and Norry) are the Andes (Chile and Ecuador (Pearce, unpubl.; Francis and Thorpe, unpubl.), Tonga (Ewart, et al., 1973), Mt. Ararat (Lambert, et al., 1974), and Papua New Guinea (Jakes and Smith, 1970; MacKenzie and Chappell, 1972). These Andean-type suites are island arc or continental-margin suites, all the products of convergent plate volcanism. The Papua New Guinea (PNG) region is a tectonically anomalous one. There may have been subduction occurring there in the past, but no active seismic zone exists beneath New Guinea today (MacKenzie and Chappell, 1972).

The basaltic members from each of the suites mentioned above are interpreted by the authors listed above as the results of partial melting of eclogite or mantle peridotite; in the case of the Tongan rocks this is accompanied by minor olivine fractionation. For each of the suites, partial melting is succeeded by fractionation involving clinopyroxene + orthopyroxene + plagioclase $\pm$ magnetite $\pm$ ilmenite $\pm$ and olivine. Fractionation of amphibole is considered important for the low-Y series from Ararat (Lambert, et al., 1974).

Table 7 summarizes the important chemical comparisons between the

Table 7
Chemical Comparisons of the Vermilion and "Andean-type" Rocks

	Vermilion	Tonga	Ararat low-Y	PNG
K, Rb, Sr, Ba	avg	low	low	high
Fe_2O_3Tot wt. %	0.97-6.11 2.76	7.10-7.50 7.37	2.6-4.1 3.1	3.9-9.7 6.55
TiO_2 wt. %	0.16-0.76 0.33	0.47-0.73 0.58	0.44-0.63 0.47	0.26-0.71 0.62
Al_2O_3 wt. %	12 - 20 15.0	12 - 15 14.0	15 - 15.8 ----	14 - 19 16.8

Sources: Tonga (Fonualei only): Ewart, et al., 1973; Ararat: Lambert et al., 1974; Lambert and Holland, 1974; Papua: Jakes and Smith, 1970; MacKenzie and Chappell, 1972; Vermilion: Arth and Hanson, 1975; Schulz 1977; MGS unpub. data; this study.

"Andean-type" suites and the Vermilion rocks. Both the Ararat low-Y series and the Tonga rocks are depleted in K, Rb, Ba, and Sr relative to most calc-alkaline rocks; the Vermilion andesites and dacites are enriched in these elements. The PNG rocks are high in K, Rb, Sr, and Ba. They also display low and variable Al contents as do the Vermilion rocks, and have low TiO_2 at similar SiO_2 values. Differences include lower K_2O and higher SiO_2 in the Vermilion dacites. The PNG andesites are the most similar to the Vermilion dacites of all the "Andean-type" andesite-dacite suites considered by Pearce and Norry (1979).

Amphibolite xenoliths found in some PNG samples indicate that amphibolite may be a logical choice of source rock for the suite. MacKenzie and Chappell (1972) suggest three models for the genesis of these high-K rocks, of which partial melting of amphibolite is one; they

favor the partial melting of a subducting slab which was enriched in radioactive elements and Rb, Sr, and Ba.

The continental-margin suites of the Andes also display the Ti-Y-Zr systematics of the Vermilion rocks, and have the same low Y abundances -- actually, lower for the basalts. Another similarity of the Vermilion rocks to these suites is in their CaO-Y variations. The Vermilion samples are similar to the Chilean suite discussed by Siegers, et al. (1969), and Lambert and Holland (1974, see fig. 21). Low Y abundances are also found in the low-Y suite from Ararat (Lambert, et al., 1974). The Andean continental-margin rocks could be considered further as an analog.

Summary

High and constant Cr values with increasing Zr values in the Vermilion dacitic rocks is evidence of a partial melting rather than fractional crystallization origin for the suite. Ti-Zr-Y variations in the basalts of the Vermilion District support the hypothesis of partial melting with an olivine-clinopyroxene-orthopyroxene residuum, such as mantle peridotite. Analogies to suites with similar Ti-Zr-Y variations support this hypothesis also: basalts from these suites are thought to be derivative from partial melts of mantle peridotites. Amphibole may have been present in the residuum for the low-Y basalts. The Ti-Zr-Y variations in the dacites support the theory of derivation by partial melting of amphibolite or eclogite, because amphibole or garnet present in equilibrium with the liquid can produce the Ti-Y depletion pattern evident in the Vermilion rocks. For the same reason, biotite is implicated in the residuum for the dacites.

Rocks from convergent plate margins (either island arc or continental margin suites) provide the best analogs for the Vermilion igneous rocks. The basic members of all the suites discussed here were interpreted as products of partial melting of mantle peridotite, as are the Vermilion basalts (Arth and Hanson, 1975). The silicic members of the PNG suite may be products of partial melting of amphibolite derived from basalt, as the Vermilion rocks are thought to be (Arth and Hanson, 1972). The major processes and characteristics of the Vermilion rocks are duplicated in convergent-plate settings today.

GEOCHEMISTRY OF SEDIMENTARY ROCKS OF THE VERMILION DISTRICT

General Relationships

Figure 23 shows the sedimentary rock data for the LVF and KLG with the fields for LVF dacite and basalt. The compositional field for the biotitic graywackes is also shown. Individual analyses of non-biotitic samples from the chloritic facies of the graywacke member and the volcanic sandstones and tuffs from the felsic volcaniclastic (FV) member of the LVF are plotted as dots and triangles. These non-biotitic samples will be discussed as a group, and will be referred to as graywacke-tuffs, since both rock types are included in this group. The graywacke-tuffs (solid dots) and slates (triangles) of the LVF scatter across the entire compositional range of the igneous rocks of the district. Intermediate compositions are not as common as dacitic or "basaltic" compositions. The slates tend to be andesitic or basaltic; a few graywacke-tuffs are, also. Most graywacke-tuffs are dacitic in composition, including every sample from the "volcanic sandstone" unit (formerly informally designated the feldspathic quartzite member by Morey, et al., 1970).

Figure 22 shows the sedimentary rock analyses from the LVF plotted on a Jensen plot, along with the fields for the igneous rock analyses from the LVF. The division between the graywacke-tuffs and slates is even sharper on this diagram. Slates have basaltic or andesitic compositions, along with a few of the graywacke-tuffs, while the majority of the graywacke-tuffs have rhyodacitic or dacitic

Fig. 22 -- Jensen Cation Plot (Jensen, 1976) showing the Vermilion sedimentary rock analyses. The composition fields for the Vermilion igneous rocks are also shown. The plot is based on 7 LVF slate analyses and 2 KLG analyses from this thesis, 23 KLG slate analyses published by Rogers, et al. (1972), 17 LVF graywacke-tuff analyses from this thesis, and 7 KLG graywacke-tuff analyses published by Rogers, et al. (1972).

Fig. 23 -- AFM diagram (Irvine and Baragar, 1971) showing the Vermilion sedimentary rock analyses. The composition fields for the Vermilion igneous rocks are also shown. The plot is based on 7 LVF slate analyses and 2 KLG analyses from this thesis, 23 KLG slate analyses published by Rogers, et al. (1972), 17 LVF graywacke-tuff analyses from this thesis, and 7 KLG graywacke-tuff analyses published by Rogers, et al. (1972).

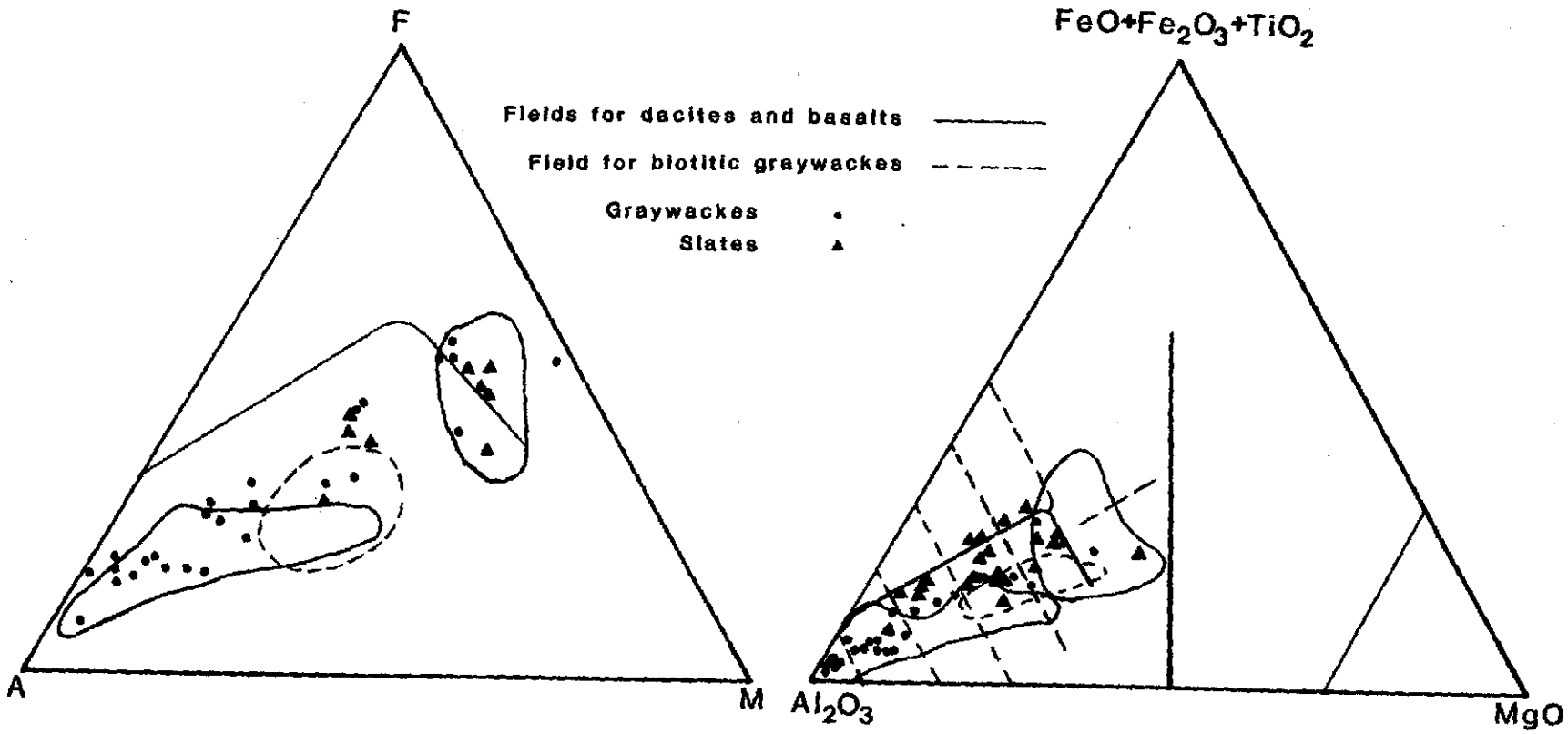
F
A
M
Fields for dacites and basalts
Field for biotitic graywackes
Graywackes
Slates
FeO+Fe2O3+TiO2
Al2O3
MgO

compositions. The slates tend to have higher Fe_2O_3T + TiO_2 than the graywacke-tuffs, while the graywacke-tuffs have compositions almost identical to the dacites.

Table 8

Comparative Archean and Phanerozoic Graywacke Chemistries
(Number of samples in parentheses)

	LVF FV grayws (16)	LVF Bio grayws (17)	Grout (1933) (1)	Arth & Hanson (1)	Archean grayws[1] (12)	Phanerozoic graywackes[1] (61)	Rensselaer graywackes[2] (119)
Wt. %:							
SiO_2	64.10	62.54	62.40	63.20	64.67	66.75	70.59
Al_2O_3	17.92	15.82	15.20	15.10	13.41	13.54	12.59
Fe_2O_3T	4.61	5.81	5.69	5.72	6.27	5.53	4.97
MgO	2.68	4.49	3.52	3.42	3.23	2.15	1.51
CaO	3.69	4.37	4.59	2.76	3.04	2.54	1.61
Na_2O	4.28	3.67	2.68	3.51	2.99	2.93	2.76
K_2O	2.16	2.40	2.57	2.09	2.02	1.99	2.19
TiO_2	0.41	0.60	0.50	0.50	0.57	0.63	0.64
P_2O_5	0.08	0.22	----	0.11	0.14	0.16	----
MnO	0.06	0.08	----	0.07	0.13	0.12	0.08
ppm:							
Ni	16.2	17.7	----	----	----	----	8.0
Cr	112.1	153.3	----	----	----	----	44.0
Zr	83.5	103.0	----	----	----	----	413.0
Rb	64.5	64.9	----	58.4	----	----	-----
Sr	369.8	540.8	----	457.0	----	----	110.0
Ba	423.6	561.7	----	566.0	----	----	400.0
K/Rb	210.5	235.3	----	296.0	----	----	------
Rb/Sr	0.21	0.13	----	0.128	----	----	------
Sr/Ba	1.08	1.05	----	0.807	----	----	3.63

[1]Pettijohn, 1963, Table D.
[2]Cambrian graywackes, Ondrick and Griffith, 1969, Table I.

The biotitic graywacke analyses cluster near the middle of the calc-alkaline trend, probably because of analytical problems due to the presence of mica in these samples. The biotitic graywackes are intermediate in composition between the dacites and basalts of the

district, as are the FV member graywackes. The seven samples of the chloritic graywacke facies rocks (see Appendix C) are not significantly different in composition from the biotitic graywackes. The suggestion in the section on petrography that the chloritic graywacke samples were biotitic graywackes that have undergone retrograde metamorphism is supported by the compositional similarity of the two types.

Comparisons to Other Graywackes

Ojakangas (1972a) found the Vermilion graywackes to be low in SiO_2, Na_2O, Fe_2O_3T, and high in other oxides compared to other Archean graywackes and to modern graywackes, on the basis of one analysis from Grout (1933). Table 8 shows the analysis from Grout compared to the mean for LVF graywacke-tuffs and the graywacke used in the petrogenetic model of Arth and Hanson (1972, 1975), which was from the KLG. The mean for graywackes from the biotitic graywacke member are shown in a separate column, since, as explained in Appendix A, these analyses may be less trustworthy. The graywacke-tuffs better resemble other Archean graywackes than does the analysis from Grout (1933). The depletion in Fe_2O_3 relative to both modern and Archean graywackes (Ojakangas, 1972a) is supported by the data of this study; also supported are a depletion in TiO_2 and an enrichment in Al_2O_3. The dacites of the district are also lower in iron and titanium, and higher in aluminum, than comparable igneous rocks from other areas, so the graywacke-tuffs' chemistries were probably inherited from their source rocks.

Comparisons to the Dacites of the Vermilion District

The FeO^*/MgO ratios of sedimentary rocks of the district are in many

cases slightly higher than those of the dacites. This can be seen on figures 22 and 23. On fig. 22 it can be seen that the sedimentary rocks, especially the slates, plot closer to the Fe_2O_3 + TiO_2 apex than the field for the dacites. The iron contents of the sedimentary and dacitic rocks have the same range, with sedimentary rocks tending toward higher iron contents. This may be a reflection of some diagenetic process in which Mg was leached to seawater and Fe precipitated from seawater, as has been observed in seafloor basalts. Preferential weathering of Mg-rich minerals in transport could accomplish the same result, but is considered unlikely for three reasons: first, the graywackes have been shown to be sedimentologically immature, and certainly the tuffs are also; second, highly Mg-rich phases such as Mg-pyroxene or olivine are not found in the Vermilion dacites, nor are they common in modern dacite suites (Ewart, 1979); third, many slates and graywacke-tuffs have higher mafic element contents than the dacites, indicating the presence of mafic components (see discussion below).

Graywacke-Tuff Provenance

Mafic Components in the LVF Graywacke-Tuffs

As shown in figures 22 and 23, the slates are mainly intermediate in major element composition between basalt and dacite, while the graywacke-tuffs are dominantly dacitic in major element composition. The non-biotitic sedimentary rocks can be subdivided on the basis of their mafic element contents (Fe, Mg, Ti, Ni, and Cr) into "high-MAF" and "low-MAF" groups. Zr also correlates with these elements, but less consistently. The low-MAF samples have abundances of the mafic elements that are within the range of abundances found in the Vermilion dacites.

The high-MAF samples have mafic element contents intermediate between dacites and basalts or equivalent to the basalts.

All slates but one (SFV65-6A) are in the high-MAF group. Similar Fe and Mg enrichments of slates over associated graywackes have been noted in the Canadian Shield (Bell and Jolly, 1975). Elevated Ni and Cr relative to associated graywackes and to modern shales is common in Archean slates, notably in the Fig Tree Group (McLennan, et al., 1983b; Condie, et al., 1970), the Pilbara slates (McLennan, et al., 1983a), and metapelites from the Dharwar Craton of India (Naqvi, et al., 1983). The conclusion by each of these authors was that enrichments in the elements Fe, Mg, Ni, and Cr indicated probable hidden mafic components, derived from labile mafic minerals which weathered into clays and were incorporated into the slates.

Seven graywacke-tuffs also classify into the high-MAF group (TFV197-2, ST79-1, SFV46-1, SFV65-6B, SFV155-1, SXF206-2, and SXF211-1). The graywacke-tuffs listed above plot within the field for LVF basalts shown in figs. 22 and 23. The biotitic graywacke member of the LVF outcrops to the west and south of the FV, and a couple of the biotitic graywacke analyses are also high in Ni and Cr (see table 16, Appendix C). Samples TFV197-2 and ST79-1 contain large amounts of epidote and are high in calcite. TFV197-2 is iron stained to a rusty brown in hand specimen. Both samples appear highly recrystallized in thin section and may have been chemically altered. The five other graywacke-tuffs with basaltic MAF contents were not examined petrographically but may also have been highly altered. The CaO contents of these samples are about half of that in basalts of the LVF, making it seem unlikely that they

are mafic tuffs.

A few graywacke-tuff samples shown on figures 22 and 23 plot in the region intermediate between the LVF dacite and basalt fields. They appear to be enriched in MAF elements also. Similar mafic element enrichments in graywackes have been noted in the Gamitagami Lake Group in Lake Superior Park, Ontario, by Ayres (1983). Ayres' interpretation was that the enrichments indicated the presence of mafic components in the matrix or as rock fragments that were unrecognizable in thin section. Mafic rock fragments have been recognized in the KLG (Vinje, 1978; Ojakangas, 1972b), and it is possible they are present in some units of the LVF also. All these samples are from the eastern end of Lake Vermilion, (mainly because of deliberate omission of biotitic samples) near the northern and eastern limits of the LVF, where the Upper Ely member of the Ely Greenstone interfingers with the LVF to the east and possibly to the north. There could have been contributions of sediment from the Upper Ely member in these areas. Mafic lavas within the LVF could have contributed mafic detritus also. Another possibility is that these samples are from graywacke-tuff beds which were largely derivative from intermediate volcanic sources.

Elevated Fe, Mg, Cr, and Ni is also a feature of some Phanerozoic graywackes, which are tabulated by Ayres (1983, table 7; table 8, above). The similarity of the Phanerozoic graywackes to the Vermilion graywacke-tuffs demonstrates that the high Ni and Cr contents are not unique to the Precambrian. McLennan, et al. (1983a) were able to show that the Ni and Cr abundances in the graywackes of the Pilbara district were not fully explainable by addition of mafic components, but that

some secondary enrichment process was also called for. No secondary enrichment process is necessary to explain the Ni and Cr abundances of the Vermilion slates or graywacke-tuffs.

Plutonic Components in the LVF Graywacke-Tuffs

Jahn (1972) analyzed a composite sample of six LVF and three KLG graywackes and tuffs for K, Rb, Sr, and Ba. He concluded that a minor plutonic component, around 10%, was necessary in the Vermilion graywacke-tuffs on the basis of enriched Sr and Ba in the composite sample.

Table 9
Comparative LVF Graywacke-Tuff Chemistries

Sample	K	Rb	Sr	Ba	K/Rb	Rb/Sr	Sr/Ba
Jahn (1972)	13400	46.4	578	369	291	0.08	1.57
Volcanic SS	6630	29.3	475	515	234	0.066	1.26
FV Tuffs	13408	64.5	369	423	210	0.214	1.07
Biotitic Grayws.	14870	64.9	540	561	235	0.128	1.05

Table 9 gives the mean values for the samples of the volcanic sandstone of the FV (which outcrops west of Tower on Highway 169-1; designated Avfs and Wvfs on the Soudan and Tower quads, respectively by Sims, et al., 1980, and Ojakangas, et al., 1978), the tuffs of the rest of the FV, the biotitic graywackes of the LVF, and Jahn's graywacke composite. The TFS52 samples are from the same outcrops as some of the LVF graywacke-tuff samples which were included in Jahn's composite sample (see Appendix D). The Sr values for Jahn's sample are very high. Sample LLF39-1, a volcanic sandstone, has 569 ppm Sr, close to Jahn's

value. The Ba value of Jahn's composite is high but the mean for the volcanic sandstones is higher. Sample TFS52-1, another volcanics sandstone, has 1243 ppm Ba.

The sampling by Jahn (1972) in the LVF concentrated on the border area between the biotitic graywacke member and the volcanic sandstone unit along highway 169-1 near Tower. These latter do not have compositions representative of graywacke-tuff compositions in the LVF. Analyses of samples from this unit cluster in the dacitic region of figs. 22 and 23. The volcanic sandstone samples are enriched in Sr and Ba relative to the FV graywackes. The biotitic graywackes are also enriched in Sr and Ba relative to lower-grade graywackes of the FV, and may be artificially high due to metamorphism. The graywackes and tuffs of the present study are intermediate in Sr and Ba contents between the dacites and basalts of the LVF. The Ba content of Jahn's composite is also within the range of values for dacites analyzed in this study, but its Sr content is not. It is unclear why the composite of Jahn has such a high Sr content, but it is not typical of graywackes in the district.

Turbidite-Slate Comparisons

The clastic rocks of the FV have been mapped as tuffs. They have been discussed in the previous section along with the chloritic graywackes as graywacke-tuffs. On well-exposed outcrops (such as at Armstrong Bay, Soudan quad) they display all the bedding features characteristic of the graywackes of the graywacke member (as at Pike Bay dam -- Ojakangas, 1972b, fig. III-23A). Both sequences were probably deposited by turbidity currents (Ojakangas, 1972a,b), and could be called turbidites. One of the objectives of this study was to compare

the graywacke-tuff and slate compositions for rocks of the district to determine if they are related as turbidite-slate units from single depositional events, termed turbidite-slate pairs below, or if the slates are from longer periods of accumulation than one depositional event such as deposition from a turbidity current. In this comparison study, only samples from the FV were considered, plus some KLG samples from this study and from Rogers, et al. (1972). The biotitic graywacke analyses are not included since these analyses are suspect (see Appendix A). The graywacke-tuffs and the slates do not show systematic trends up-section, as evidenced by the plots of elemental abundances versus relative stratigraphic height given in Appendix B.

Ojakangas (1985) reviewed evidence that Archean slates generally have higher K/Na ratios than Archean graywackes, and noted that the explanation could be albitization of the graywackes, addition of K_2O to the slates, or a combination of both processes. The Vermilion data of this and previous studies show a tendency for slates as a group to be higher in K_2O/Na_2O at a given Na_2O content. Figure 24 shows the K_2O/Na_2O ratios of the Vermilion slates and graywacke-tuffs plotted against Na_2O content. Slates range to higher K_2O/Na_2O ratios at a given Na_2O content. This is true for the main body of samples and also true within the set of high-K_2O samples appearing in the upper left corner of the graph.

One stratigraphic section of graywacke-tuffs and slates, measuring approximately 3 meters, was sampled in detail to provide stratigraphic control on turbidite-slate pairs. The section chosen was on the eastern shore of Lake Vermilion, sample location SFV65 (see fig. 25, Appendix

Fig. 24 -- K_2O/Na_2O vs. Na_2O plot of the Vermilion slates and turbidites. The plot is based on 7 LVF slate analyses and 2 KLG slate analyses from this thesis, 23 KLG slate analyses published by Rogers, et al. (1972), 17 LVF graywacke-tuff analyses from this thesis, and 7 KLG graywacke-tuff analyses published by Rogers, et al. (1972).

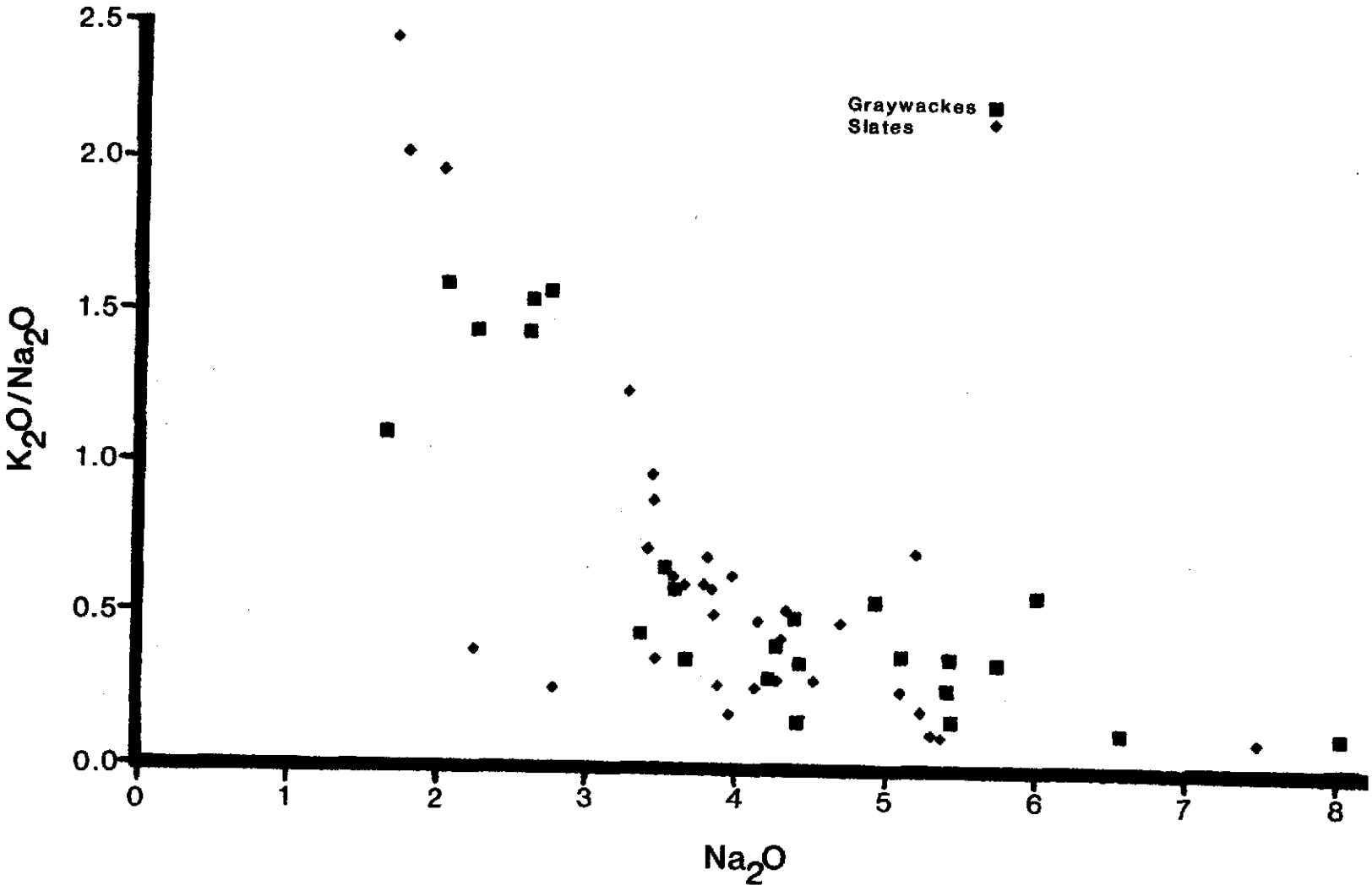
Graywackes
Slates
2.5
2.0
1.5
1.0
0.5
0.0
K_2O/Na_2O
0
1
2
3
4
5
6
7
8
Na_2O

B). This section was poorly exposed, but did contain units which could be sampled with a sledgehammer, something not possible on smoother, more completely exposed outcrops. One graded bed indicated that stratigraphic top is to the north for the section. Six stations on the outcrop were sampled from south to north. Individual stations were not always aligned along a single north-south line of section. Only samples from the last four stations were analyzed. The samples from this section are shown in Table 10, along with other samples which were high in alkalis. SFV65-5A and B are sandy and slaty parts from a single

Table 10
Comparative LVF Graywacke-Tuff-Slate Chemistries

Spl. no.	Rock Type	MAF content	K2O K2O/Na2O	CaO wt%	Y content	XRD Peak Heights Chl	Musc	Plag
---STRAT. TOP--								
SFV65-6B	TURB	Hi	Hi	Lo	Hi	---	----	----
SFV65-6A	SL	Lo	Lo	Hi	Av	1	0	24
SFV65-5B	TURB	Lo	Hi	Hi	Av	20	5	11
SFV65-5A	SL	Hi	Hi	Lo	Hi	41	10	10
SFV65-4	SL	Hi	Hi	Lo	Hi	39	8	8
SFV65-3	TURB	Lo	Hi	Hi	Av	19	4	11
--STRAT. BASE--								
SFV155-1AB	TURB	Hi	Hi	Lo	Hi	37	9	10
46-1	TURB	Hi	Hi	Lo	Hi	75	22	15
KLV3-1	SL	Hi	Av	Hi	Hi	32	6	16
181-3	SL	Hi	Lo	Lo	Av	41	13	11

sample. The same is true for SFV65-6A and B.

Samples 65-5A and 65-4 were taken about 3 meters apart along strike and could not be unequivocally correlated in outcrop. They are almost identical in major element and trace element contents, with only Sr being significantly different. The two samples are probably of the same slate bed. They are both compositionally distinct from 65-3, the underlying turbidite-conglomerate bed. The sample for 65-3 was taken from near the base of the bed, however, and may not be representative of

the entire bed. The slate is more mafic in composition than the underlying turbidite-conglomerate.

Samples 65-6B is the graywacke-tuff underlying slate 65-6A. The slate (sample SFV65-6A) plots separately from all the other slates on the Jensen Cation Plot and the AFM diagram. The sample's chemical composition resembles that of the rhyodacite clasts from Tower State Park (TFV195 and 196 series samples, see Appendix C), and has lower Al_2O_3, Fe_2O_3T, MgO, K_2O, and higher Na_2O, quartz and feldspar content (mineralogy estimated by XRD) than sample 65-5B which underlies it. It is therefore unlikely that the slate is the fine fraction which settled out from the turbidity current that deposited the underlying graywacke-tuff bed. Sample 65-6A could be a felsic ash bed from a single depositional event.

No correlation between thicknesses of slates and the graywacke-tuff beds immediately underlying them was found for any of the sections examined in this study, and no such correlations are mentioned by others who have studied the Vermilion sedimentary rocks. Therefore most of the slates probably represent extended periods of accumulation rather than parts of single depositional events by turbidity currents.

Heavily Altered Metasedimentary Rocks

All the metasedimentary rock samples listed in Table 10 evidence extreme alteration as indicated by their very high Al_2O_3, low CaO, and high MAF contents. Elevated contents of chlorite and muscovite could produce these characteristics, including high Cr and Ni (Deer, et al., 1978). Besides being high in the MAF elements, these samples are

anomalously high in Zr.

XRD chlorite, muscovite and plagioclase peaks are listed for those samples in table 10 for which XRD was run. The chlorite peak average for the low-MAF samples is 13.3. For muscovite it is 4.6. The high-MAF mean for muscovite is 9.6; for chlorite it is 44.2, indicating that chlorite and muscovite play key roles in the distribution of mafic elements and Ca. Not all the high-alkali samples are high in MAF components. The two which are low in MAFs also have the low mica contents, and more feldspar and quartz, as indicated by the XRD peak heights for these minerals. The samples with high alkali contents listed in Table 11 may be classified as poeneites, because of their extreme sericitization and because of very high contents of K, Rb, Sr, and Ba.

Although the alkali contents of the rocks in table 10 are similar, especially those from the SFV65 site on the eastern shore of Lake Vermilion, the mafic contents are variable. Table 10 compiles the high-MAF samples as well as the high-alkaline samples, the latter of which chemically resemble keratophyres and are presumably altered. Sample 65-3 is a turbidite-conglomerate, while 65-5 is a coarse-grained graywacke-tuff. Both are rocks for which low mafic contents would be expected. The consistency of mafic element content with rock type independent of location, and the correlation of alkali content with location independent of rock type (sandstone or slate), imply outcrop-scale alkali metasomatism, and relative immobility of the mafic elements.

Summary

The few chloritic graywacke samples analyzed in this study are not significantly different in composition from the biotitic graywackes. Their mineralogic differences are probably only a difference in metamorphic history. Slates of the FV have higher Fe_2O_3, MgO, TiO_2, Ni, Cr, and less consistently Zr contents FV graywacke-tuffs and chloritic graywackes of the graywacke member, probably because they are enriched in mafic components. Many graywacke-tuffs appear to contain mafic components or to be derivative from intermediate (andesitic) volcanic sources. No plutonic component, enriched in Ba and Sr, is necessary to explain the Ba and Sr abundances in the LVF graywackes and tuffs. Slates have a wider range of K_2O/Na_2O ratios than graywackes and tuffs, even graywacke-tuffs with which they are associated. Outcrop-scale metasomatism of alkali elements is implied by their variability with location; relative immobility of Fe, Mg and other mafic elements is implied by their consistency with respect to rock type, regardless of location.

TECTONIC MODELS AND CONCLUSIONS

Bimodality

Similarities between the Vermilion rocks and island arc rocks have been noted by many workers (e.g., Jahn and Murthy, 1975; Schulz, 1980). Bimodal island arc suites were largely unknown in the last decade of research on island arcs, and so the scarcity of andesites in Archean greenstone belts has been used as an objection to interpreting them as relics of ancient island arcs. The paucity of andesites is probably not a function of sampling bias in the Vermilion District. Andesites are also scarce in many greenstone belts of the Canadian Shield (Ayres, 1983), for instance in the Yellowknife district (Henderson, 1972) and the Sioux Lookout region (Turner and Walker, 1973).

Bimodal volcanic suites are present in some island arcs in all periods of post-Archean time. Bimodality is characteristic of immature island arcs today (Jakes and Gill, 1970; Mitchell and Reading, 1971). Examples of Phanerozoic bimodal arcs include the Ordovician North Carolina volcanic slate belt (Seiders, 1978; Whitney, et al., 1978); the Ordovician Tetagouche Group (Whitehead and Goodfellow, 1978); the Cambro-Ordovician rocks of central Newfoundland (Strong, 1977); parts of the Jurassic-Cretaceous northeastern Caribbean Antilles (Donnelly and Rogers, 1980); the Devonian rocks of the western Shasta district (Barker, et al., 1979; Mertzman, 1984). There are numerous Proterozoic examples, for instance the Green Mountain Formation of Wyoming (Condie

and Shadel, 1984), and the Gunnison-Salida area of Colorado (Bickford and Boardman, 1984). Conversely, greenstone belts which are not bimodal are also known, for instance the Proterozoic Grenville and the Archean Uchi, Wabigoon, and Abitibi regions (Condie and Moore, 1977; Goodwin, 1977).

This series of bimodal suites of all different ages implies some continuity through time of the geologic process(es) which formed them. Modern examples of such bimodal suites are the result of convergent plate volcanism, and it is therefore reasonable to infer that plate tectonics has been the mechanism of generation for these older suites, also. If that is so, then plate tectonics has been a major process shaping the earth's surface for at least the last 3 billion years, perhaps with a variation in some parameters such as spreading rates and crustal thickness.

Accretionary Tectonics in the Archean

Langford and Morin (1976) proposed that the Superior Province originated through the welding of island arcs onto a microcontinent. This process is now termed accretionary tectonics (as recently summarized by Nur and Ben-Avraham, 1982). Langford and Morin noted the beltlike geometry of the greenstone and gneiss subprovinces of the Superior Province, and pointed out the broad similarities to the subprovinces of the Canadian Rockies accreted terranes.

Accretionary tectonics is now accepted by most workers as a continent-building mechanism as far back as the Proterozoic (Kroner, 1981; Schermer, et al., 1984), and is hypothesized by many workers for

the Archean (Condie, 1980; Windley, 1981). The question of whether plate tectonics was operative in the Archean is still unresolved, however; many workers avoid models which invoke subduction in the Archean (Zhang, et al., 1985; Renmin, et al., 1985; Bickford, et al., 1984).

The presence of large-scale thrust nappes in Archean shield areas (Lowe, et al., 1985) and the evidence for coalescence of microcratons into larger cratons (e.g., Cordani, et al., 1985) both imply that large-scale horizontal movements (tens to thousands of km) did take place in the Archean. Rapid recycling of large amounts of crustal material are required by petrogenetic modeling in many greenstone belts (e.g., Schulz, 1980, for the Vermilion District). These considerations argue in favor of some form of plate tectonics for the Archean.

An accretionary plate-tectonic model for the Archean is favored here. The reasons for favoring such a model are largely arguments from similarity. Structural analogies between accreted terranes and the typical structural features of greenstone belts abound: viz., the dominance of strike-slip faulting; multiple deformational events; repetitive rock types with difficult or impossible stratigraphic correlation (Nokleberg, 1983; Csejtey, et al., 1982; Stone, et al., 1982). Plutonic rocks in greenstone belts are similar to rocks in accreted terranes which are interpreted to be products of partial melting in the roots of an island arc (Payne and Strong, 1979). The supracrustal rocks are similar to island arc supracrustal rocks in mineralogy and chemistry as well as in relative proportions of each rock type.

Comparisons to Young Island Arcs

Rogers, et al. (1985) have discussed criteria for the recognition of ancient ocean floor, island arc, continental margin, and continental rift environments. Evidence of subaqueous eruption (pillow basalts) and the absence of peralkaline magma types distinguish the Vermilion rocks from continental-margin suites. The greater abundance of basalts than that expected in continental-margin suites, plus the scarcity or absence of true rhyolites and andesites, is further evidence against a continental margin environment for the suite. The association of pillow basalts with volcanic rocks, particularly pyroclastic volcanic rocks, of >55% SiO_2 distinguishes the LVF rocks from suites formed in midocean ridges or small ocean basins. The presence of clinopyroxene phenocrysts in some of the Upper Ely basalts further distinguishes them from basalts formed in a midocean ridge or small ocean basin environment.

Table 11

Comparative chemistries of basalts of different tectonic environments (after Rogers, et al., 1984)

	Ocean floor	Young arcs	Lk Vermil	Lower ELy	Upper Ely
K_2O%	0.1 - 0.2	0.5	0.39	0.62	0.47
Rb ppm	2.0	5.0	8.1	11.7	14.6
Ba ppm	15.0	100.0	132.0	------	108.0
Sr ppm	100.0	200.0	192.3	154.0	135.0
TiO_2%	1.5	0.8	0.98	0.87	1.00
Zr ppm	100.0	50.0	58.6	80.7	72.0
Cr ppm	300.0	50.0	363.0	------	248.0
Ni ppm	100.0	50.0	30.7	------	33.2
FeO^*/MgO	<1.5	>1.5	1.81	1.39	1.92

Table 11 summarizes the geochemical characteristics which distinguish midocean ridge and small ocean basin environments from young ensimatic island arcs. Averages of data for all basalt analyses from the LVF,

Lower Ely, and Upper Ely are tabulated for comparison.

The Vermilion basalts from both members of the Ely Greenstone and also from the Lake Vermilion Formation are intermediate in these characteristics, but tending toward the characteristics of young island arc basalts. Flat REE patterns are characteristic of the Vermilion basalts (Arth and Hanson, 1975) and are a feature of young arc basalts as opposed to LREE depletion for ocean-floor basalts, and LREE enrichment for more mature island arcs. A linear relationship of Zr to TiO_2 is present in the Vermilion samples, and is characteristic of basalts from young arcs or ocean floor environments as opposed to mature island arcs or continental margins. Bimodal associations of dacite-keratophyres with basalts is typical of young volcanic arcs as opposed to more mature arcs, in which basalt-andesite predominates. The general predominance of epiclastic versus pyroclastic sediments in the district is also more like an immature island arc than a mature one.

The petrographic and geochemical features of the Vermilion District fit those of a young ensimatic island arc better than they do any other modern tectonic environment. In particular, analogies to two island arcs, the Carolina Slate Belt of the Appalachians (early Paleozoic), and the island of Papua New Guinea, have been mentioned in this thesis. Whitney, et al., (1978) consider the southern part of the Carolina Slate Belt to be an example of an immature island arc, for many of the same reasons just stated for the Vermilion District. A tectonic mechanism similar to that which accreted the Carolina Slate Belt to the North American craton before the closing of the proto-Atlantic is therefore also a plausible mechanism for the accretion of a Vermilion greenstone

Belt arc onto the Superior craton.

Conclusions

1) Alteration in the Vermilion District rocks was probably a combination of seafloor weathering (spilitization) and an unknown degree of burial metamorphism, with later greenschist facies metamorphism overprinted. Only limited open-system exchange of components at low fluid/rock ratios occurred. Poeneitization occurred in at least a few cases. Alkalis were the most mobile major elements, followed by Ca, Fe, and Mg. Mg and Fe contents, as well as FeO^*/MgO ratios, are likely to be original. Si, Al, and the minor elements Ti, P, and Mn were less mobile and in many cases almost immobile. Rb, Sr, and Ba were the most mobile trace elements; Rb follows K in all cases, probably stabilized in muscovite; Sr follows Ca in most cases, probably stabilized in epidote. Fe, Mg, Zr, Y, Cr, and Ni were less mobile or immobile during low-grade alteration, and can serve as fairly consistent indicators of original rock type.

2) The sedimentary rocks of the LVF do not display consistent chemostratigraphic trends for any elements analyzed as part of this study.

3) The basalts and dacites of the Vermilion District are impoverished in Ti, Zr, and Y relative to modern igneous rocks of otherwise similar composition.

The basalts of the Lake Vermilion Formation are similar to those of the Lower Ely member of the Ely Greenstone Formation.

Immobile element abundances indicate that LVF volcanism was dominantly low-K tholeiitic (LKT) in nature interspersed with minor calc-alkaline basaltic (CAB) volcanism. Lower Ely volcanism was probably similar. The Upper Ely basalts are similar to ocean floor basalts (OFBs).

The dacites of the Lake Vermilion Formation are calc-alkaline in major and trace element (Zr, Y, Ni, Cr) geochemistry, with Rb, Sr, and Ba contents verging on continental-margin values. The Rb, Sr, and Ba contents have been elevated by spilitization.

4) The basalts of the district have Zr-Ti-Y variations compatible with partial melting of mantle peridotite leaving a residuum of olivine and pyroxenes. The dacites of the district have Ti-Zr-Y variations commensurate with partial melting of amphibolite or eclogite.

5) Suites with Ti-Zr-Y systematics similar to the Vermilion samples are from convergent plate-margin settings. The rocks of the Papua New Guinea (PNG) highlands are a close analog to the Vermilion District rocks. Petrogenetic and tectonic similarities may also exist.

6) The graywacke-tuffs of the Lake Vermilion Formation have hidden mafic components not recognized in petrographic study, possibly in the matrix of the rocks. This is a similarity between the LVF and KLG graywackes. Slates of the LVF tend to be intermediate in composition between dacite and basalt, while graywacke-tuffs tend to be similar to the dacites. A few graywacke-tuffs seem to have

been derived from dominantly intermediate/andesitic detritus. No plutonic component, enriched in Ba and Sr, is necessary to explain the Ba and Sr contents of volcaniclastics of the Lake Vermilion Formation.

7) The best modern tectonic analog for the Vermilion District is that of a young, ensimatic island arc. It is suggested that plate tectonics has operated at least this far back into the Precambrian, and may have involved accretionary tectonics.

APPENDICES

APPENDIX A

ANALYTICAL METHODS

Sampling Methods

Sampling efforts were concentrated along roadcuts and railroad cuts to ensure that samples would be taken from below the weathering zone. For those areas where fresh rock was not readily available, such as along lakeshores and in wooded expanses, samples were collected from at least three inches into the exposed surface of the outcrops. An attempt was made at the outcrop to sample away from visibly weathered, veined, or sheared areas, except in the one case where the objective was to sample veined material. Larger samples were taken from rocks with larger grain size, such as conglomerates, to guarantee that the sample chemistries would be representative of the outcrops from which they came. Samples included as many beds as possible in bedded sedimentary rocks, except in cases in which selection of individual beds was an objective of sampling.

Sample Preparation

Samples selected for geochemical analysis were first broken into fist-sized pieces by sparing use of a sledgehammer, and then broken down in a hydraulic rock breaker into pieces from 1 to 3 inches in long dimension. Some rocks were sawn before being broken down. Sawed surfaces were polished with 240 grit followed by 600 grit to remove saw

marks. These samples were washed with tap water to remove as much residual grit as possible. Larger samples (500 grams minimum) were taken for coarser-grained rocks, such as conglomerate. The average sample size used for analysis was 300 grams. Care was taken to sort the pieces into a weathered and an unweathered group, by separating out those pieces which showed weathering rinds, veining or shearing. Where unveined material was rare, larger samples were taken to dilute the effect of veining.

The samples were next crushed in two passes through a chipmunk crusher with a case-hardened steel impact plate. Before the first crushing step, the expendable weathered material from the sample being processed was passed through the crusher first, as a precaution against cross-contamination of the samples. Next the less weathered material from the sample was passed through once or twice to obtain the desired particle size (approximately 1 cm). The crusher jaw region was scrubbed and rinsed with tap water and blown out after each use. A second crush step proved desirable to minimize time on the grinding steps. Again, weathered material from the sample being processed was passed through the crusher before the less-weathered material was passed through. The final particle size of the crushed material was about 4 mm.

The samples were next homogenized in a beaker and split from 300 grams down to 10 grams using a sample splitter with half-inch openings. The splitter was blown out between samples. For samples which were to be run as duplicates, the second half of the initial split was also split down to 10 grams, and run separately through the rest of the procedure.

Grinding was performed in a Spex Mixer/Mill. The samples were ground in two steps as follows:

1) The entire 10 grams of the sample was placed in a tungsten carbide vial with two tungsten carbide balls and ground for 5 minutes.

2) The 10 grams of the sample were divided into fourths and ground for five minutes in four Spex methacrylate cylinders with tungsten carbide lined nylon caps and with one tungsten carbide ball in each cylinder.

All grinding surfaces were cleaned with a test tube brush and tap water and blown dry after each step. Before using the Spex equipment for the dacite and sedimentary rock samples, numerous test runs had been performed to perfect the grinding procedure, and these were judged to have impregnated the cylinders and other equipment with Vermilion District dacitic material sufficiently to avoid serious contamination from previous projects. Before grinding the basalts, material from a hornblende syenodiorite was run through the grinding process.

The final material passed a 250 mesh screen as determined by sieving on test runs. SEM studies showed the material to be averaging 80 microns (with many pieces 100 microns in diameter).

Pressed powder pellets were used for X-ray fluorescence analysis. These were made by pressing 5 to 7 grams of sample with a few drops of distilled water as binder in a 30-ton press under vacuum at 3.5 tons for 5 minutes.

X-Ray Fluorescence Analysis

Analyses of the samples were performed on a Rigaku S/Max (end-window Rh tube type) wavelength-dispersive X-ray fluorescence spectrometer. Calculations of bulk chemistry and trace element contents were performed on a PDP-11/03 minicomputer running XRF-11 software (Criss Software, Inc.). The Criss fundamental alphas method was used for calculating major element analyses, and the Criss fundamental parameters method was used to calculate trace element contents. Eleven whole-rock standards were used for major element calibration and six were used for trace element calibration.

XRF-11 allows the user to declare only a single value for each element in the matrix of the unknowns. Since the major element contents of the basalts and dacites differ widely, basalts were run separately from all other samples for trace elements, with a basaltic matrix composition. All other samples were run with a dacitic matrix element composition.

The analyses were normalized to 100% on an anhydrous basis. Since the X-ray fluorescence method analyzes for total iron only, ferrous and ferric iron were apportioned from the analyzed total Fe_2O_3 (Fe_2O_3T) by the method of Nicholls and Whitford (1976):

$$\%Fe_2O_3 = \%Fe_2O_3T * 0.85$$

$$\%FeO = (\%Fe_2O_3T - \%Fe_2O_3) * 0.8998$$

Table 12
Major Element Precision (data from five test runs)*

	AGV-1	G-2	MicaFe	MicaMg	MRG-1
SiO_2	0.20	0.174	0.128	0.276	0.138
	60.73	71.12	35.58	40.10	40.58
Al_2O_3	0.34	0.436	0.644	0.529	0.553
	17.00	15.66	19.05	14.91	9.29
Fe_2O_3	0.131	0.138	0.191	0.363	0.228
	6.804	2.65	21.49	9.27	15.77
MgO	4.5	5.28	4.08	3.31	3.33
	1.45	0.72	3.73	18.75	11.94
CaO	0.617	0.560	1.40	20.1	0.486
	4.92	1.95	0.38	0.02	14.63
Na_2O	1.68	1.95	4.65	8.02	3.49
	4.19	4.03	0.27	0.19	0.81
K_2O	0.131	0.172	0.277	0.21	45.0
	2.88	4.50	8.63	10.21	0.01
TiO_2	0.240	0.10	0.423	0.486	0.590
	1.06	0.48	2.93	1.87	4.24
P_2O_5	0.456	0.13	0.904	31.1	1.78
	0.524	0.13	0.32	0.01	0.07
MnO	1.03	1.74	0.692	0.547	1.14
	0.10	0.03	0.37	0.27	0.17

* First number is standard deviation as % relative.
Second number is amount present, in wt. %.

Evaluation of Potential Sources of Error in Sample Preparation and Analysis

Interelement Interferences

The Ti K_B line interfered with the V K_A line, making accurate analyses for vanadium impossible. V was run anyway as a check for Cr;

Table 13
Trace Element Precision (data from five to eight test runs)*

	DTS-1	MicaFe	MicaMg	NBS-1633	STM-1
V	0.892	31.8	9.52	7.22	45.2
	15.45	408.6	87.81	187.1	0.333
Cr	2.21	6.70	4.90	2.91	104.0
	5515.0	89.98	94.82	131.35	1.80
Ni	1.63	1.54	1.17	2.03	4.06
	2620.8	23.68	102.5	88.1	4.85
Rb	0.0	0.575	0.638	1.15	0.933
	0.0	1251.7	1174.8	98.75	119.2
Sr	50.1	9.82	3.72	1.07	0.769
	0.47	3.18	22.53	1252.5	837.6
Y	0.0	1.07	0.874	0.974	2.20
	0.0	14.15	15.63	41.60	59.43
Zr	0.0	0.595	10.0	0.385	0.193
	0.0	467.4	22.93	192.2	1453.3
Ba	89.5	1.58	3.53	3.54	6.36
	7.98	217.9	4048.2	2630.5	582.9

* First number is standard deviation as % relative.
Second number is amount present, in ppm.

where V contents are high, the Cr content is probably elevated above its true value, because the V K_B line interferes with the Cr K_A line just as Ti does with V. The estimated accuracy for Cr is shown in table 17, below. Four Vermilion District samples (one basalt, one dacite porphyry, one biotite graywacke, and one slate) were scanned for other lines which could interfere with the other major and trace element lines. No others were found.

Titanium Contamination

During the course of sample preparation, it was noticed that the

tungsten carbide used in the Spex Mixer/Mill system could contain up to 15 wt% TiO_2. A test for TiO_2 contamination based on the amount of tungsten present in sample 197-2 versus a Spex tungsten carbide cap showed negligible amounts of contamination. The calculation was based on a simple proportion, assuming the Spex cap is 100% tungsten:

$$\frac{X\%\ W_{197-2}}{100\%\ W_{WC}} = \frac{100\ CPS\ W_{197-2}}{200{,}000\ CPS\ W_{WC}}$$

X = 0.2% by weight. Assuming that Ti is 20% or 1/5 of the Spex WC alloy (a larger percentage than was indicated by SEM/Probe analysis of a cap), the amount of Ti added by grinding was 0.2%/5 = 0.01% by weight. This was smaller than the analytical error for Ti.

Precision

The element-by-element precisions of the S/Max instrument on multiple runs using data reduction by Criss XRF-11 software are given in Table 12 for major elements in five whole rock standards. Table 13 is a similar presentation of data on five whole rock standards for trace elements using Criss XRF-11 software. Up to 8 repeat runs were performed on the standards over a period of one week. Standard errors were always less than 1.5% relative for major elements, and less than 2.5% relative for trace elements.

Accuracy

The XRF-11 software package has been demonstrated to give analyses of steels containing eight components to an accuracy of 1.2% relative (that

is, per cent of amount present; Criss, et al., 1978), but rocks are much more complex than steels. Extensive testing was performed to determine the accuracy of the S/Max instrument and the XRF-11 software when

Table 14

Elemental Accuracies

Major Elements		Trace Elements	
Oxide	95% Confidence Limits (in weight% absolute)	Element	95% Confidence Limits (in absolute ppm)
SiO_2	2.0	V	300
Al_2O_3	1.5	Cr	97
Fe_2O_3	0.75	Ni	53
MgO	0.75	Rb	63
CaO	0.35	Sr	115
Na_2O	0.5	Y	?
K_2O	0.5	Zr	75
TiO_2	0.5	Ba	75
P_2O_5	0.03		
MnO	0.02		

applied to whole rocks, and especially to trace elements.

The accuracy of the analyses produced by the XRF-11 software package was estimated by analyzing all 26 whole-rock standards available at the NMAL, and checking the resultant values against the recommended values published in Abbey (1980). Linear regression using SAS was performed to aid in estimation of an error envelope for the samples. Micaceous samples were found to vary significantly from recommended values. Table 14 gives the estimated accuracies for each element, excluding micaceous samples.

Grain Size Problems

The final material was of a consistency such that 90% would pass a 250 mesh screen. Grain size anayses on the SEM showed a bimodality in grain sizes that could significantly effect the XRF analyses; however, the same bimodality is present and even more pronounced in the USGS whole-rock standards used for the analyses, and so any grain size problems would affect samples and standards equally.

Biotite Effect

Samples from the biotitic graywacke member of the LVF contain large amounts of biotite. The biotitic graywacke analyses form a very homogeneous group compared with analyses of the sandstones and slates of the felsic volcaniclastic member (FV). They are dominantly of a slightly different composition from the FV rocks, which lack biotite (see figs. 9 and 8). Because it was noted that micas affected the accuracy of analyses of USGS whole-rock standards, the biotitic graywacke analyses were suspected of being invalid due to mica effects. Biotite can resist grinding and can preferentially orient during pellet pressing, presenting a surface area which is disproportionately large relative to the actual amount of biotite present in the sample. SEM examination of the surface of one pellet revealed that the grain sizes of the biotites were not larger than average for the sample, but they were preferentially oriented on the pellet surface. Microprobe analyses of thin sections of eight biotitic graywackes yielded chemistries which do not cluster but plot closer to the dacites and sediments of the FV. It was concluded that the biotitic graywacke analyses are not trustworthy. In discussions of the rocks of the LVF, these analyses

have been treated as semiquantitative.

APPENDIX B

CHEMOSTRATIGRAPHIC SECTIONS

Stratigraphy along the eastern shore of Lake Vermilion has been carefully mapped and is reasonably well known. The section tops to the north, although there are probably many local top reversals because of the two superimposed fold sets which are present in the area (Bauer, 1985). Samples from this study which were taken along the eastern shore of Lake Vermilion, and on nearby islands, were treated as a stratigraphic section and examined for stratigraphic variations in chemistry. Fig. 25 shows the locations (and therefore the approximate relative stratigraphic heights) for samples taken along the eastern end of Lake Vermilion. Sample numbers for the section are given at the right of the map in fig. 25. The plots on pages 131-141 show the results for the section along the eastern shore. A trend of increasing K_2O, SiO_2, Al_2O_3, and Rb is apparent, but insufficient samples are included in the data set to rule out random variation as the cause of this trend. The trend could also represent a change in low-grade metamorphic conditions from south to north. No other chemostratigraphic trends are observable on the plots. Covariations of certain elements, such as that of the mafic elements, or that of K_2O and Rb, are apparent on these plots.

Fig. 25 -- Sample location map for eastern part of Lake Vermilion (map from Sims, et al., 1980).

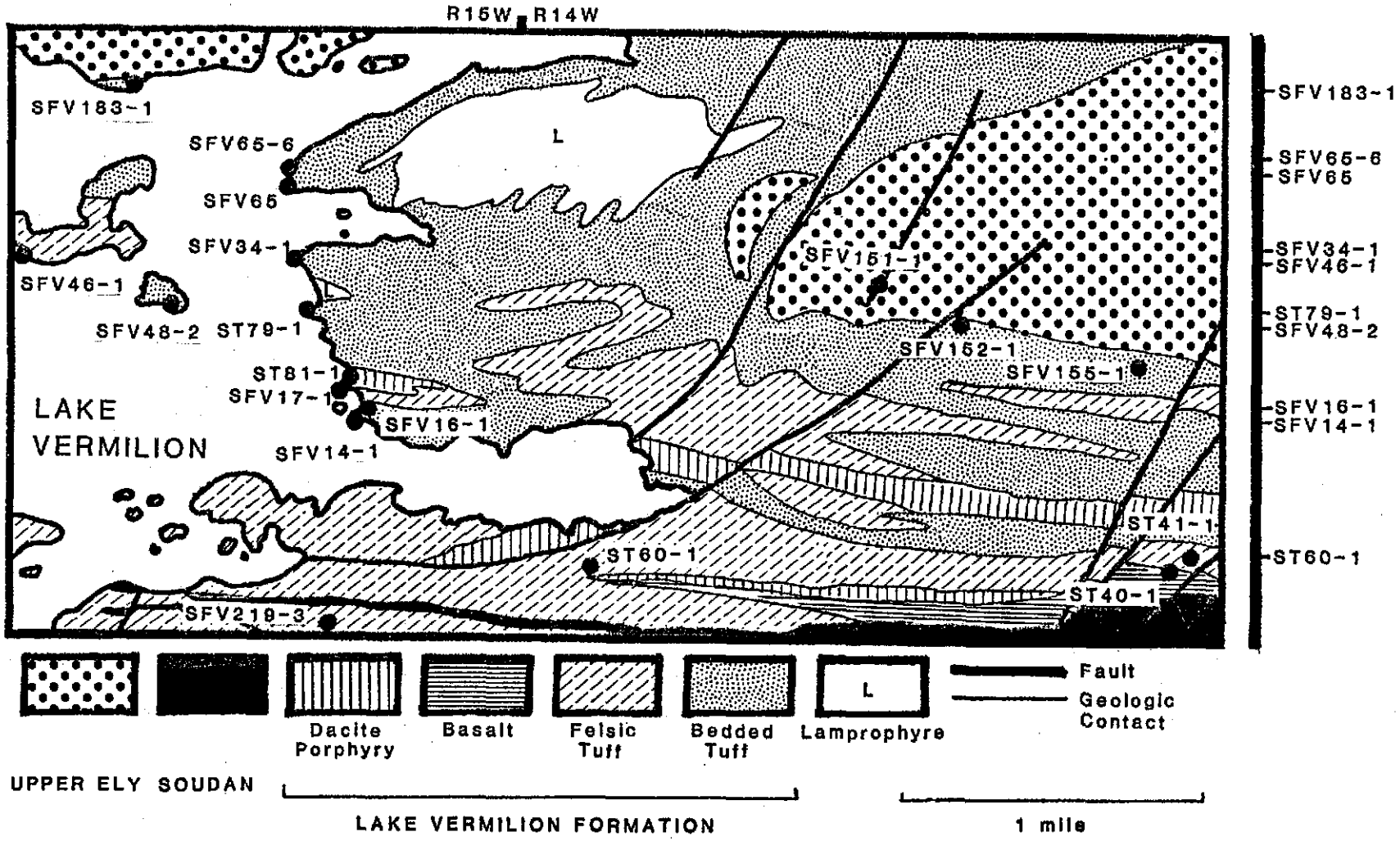
R15W
R14W
SFV183-1
SFV65-6
SFV65
SFV34-1
SFV46-1
SFV48-2
ST79-1
ST81-1
SFV17-1
SFV16-1
SFV14-1
LAKE
VERMILION
L
SFV151-1
SFV152-1
SFV155-1
ST41-1
ST60-1
ST40-1
SFV219-3
SFV183-1
SFV65-6
SFV65
SFV34-1
SFV46-1
ST79-1
SFV48-2
SFV16-1
SFV14-1
ST60-1
Dacite Porphyry
Basalt
Felsic Tuff
Bedded Tuff
L
Lamprophyre
Fault
Geologic Contact
UPPER ELY SOUDAN
LAKE VERMILION FORMATION
1 mile

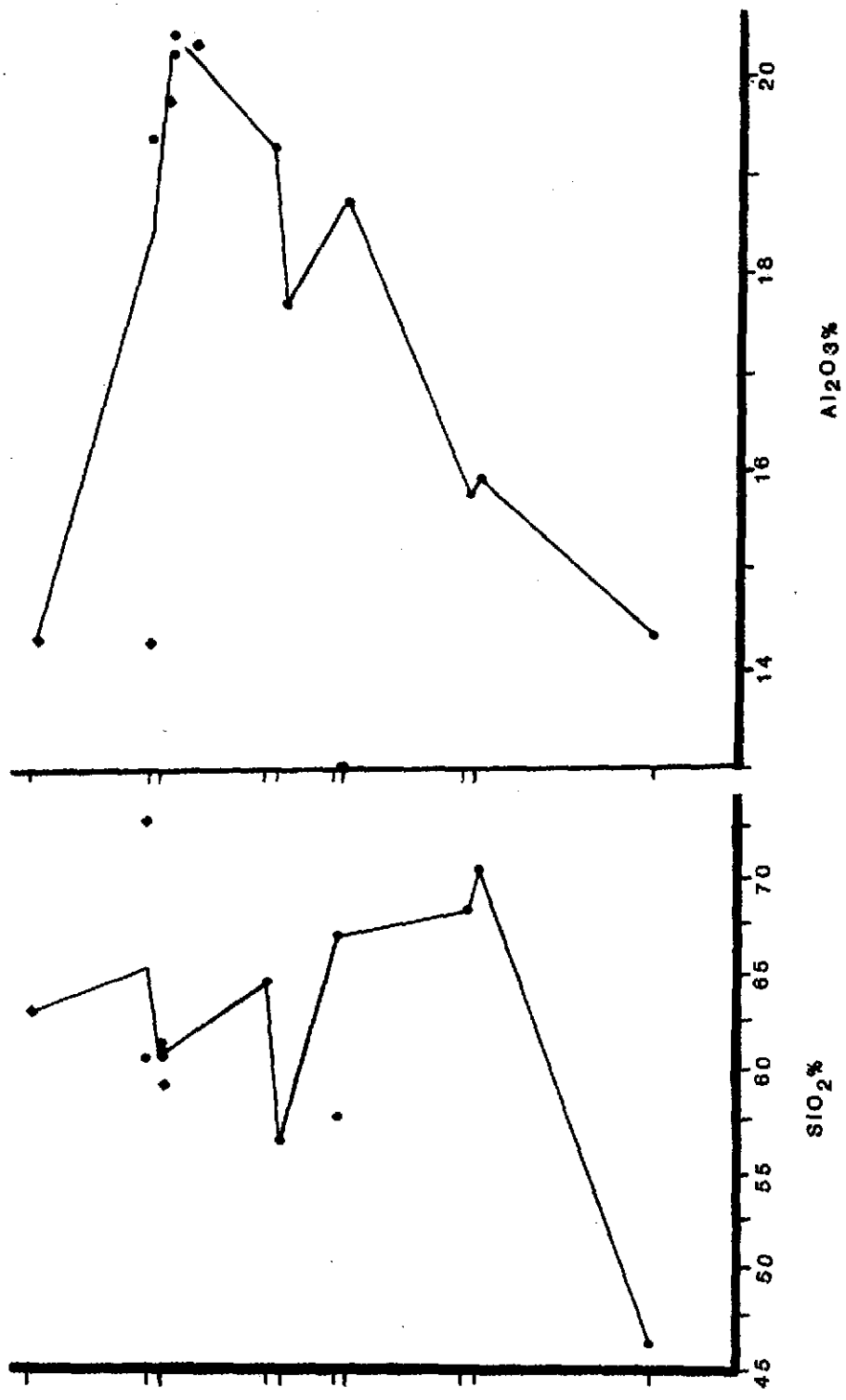
20
18
16
14
Al2O3%
70
65
60
55
50
45
SiO2%

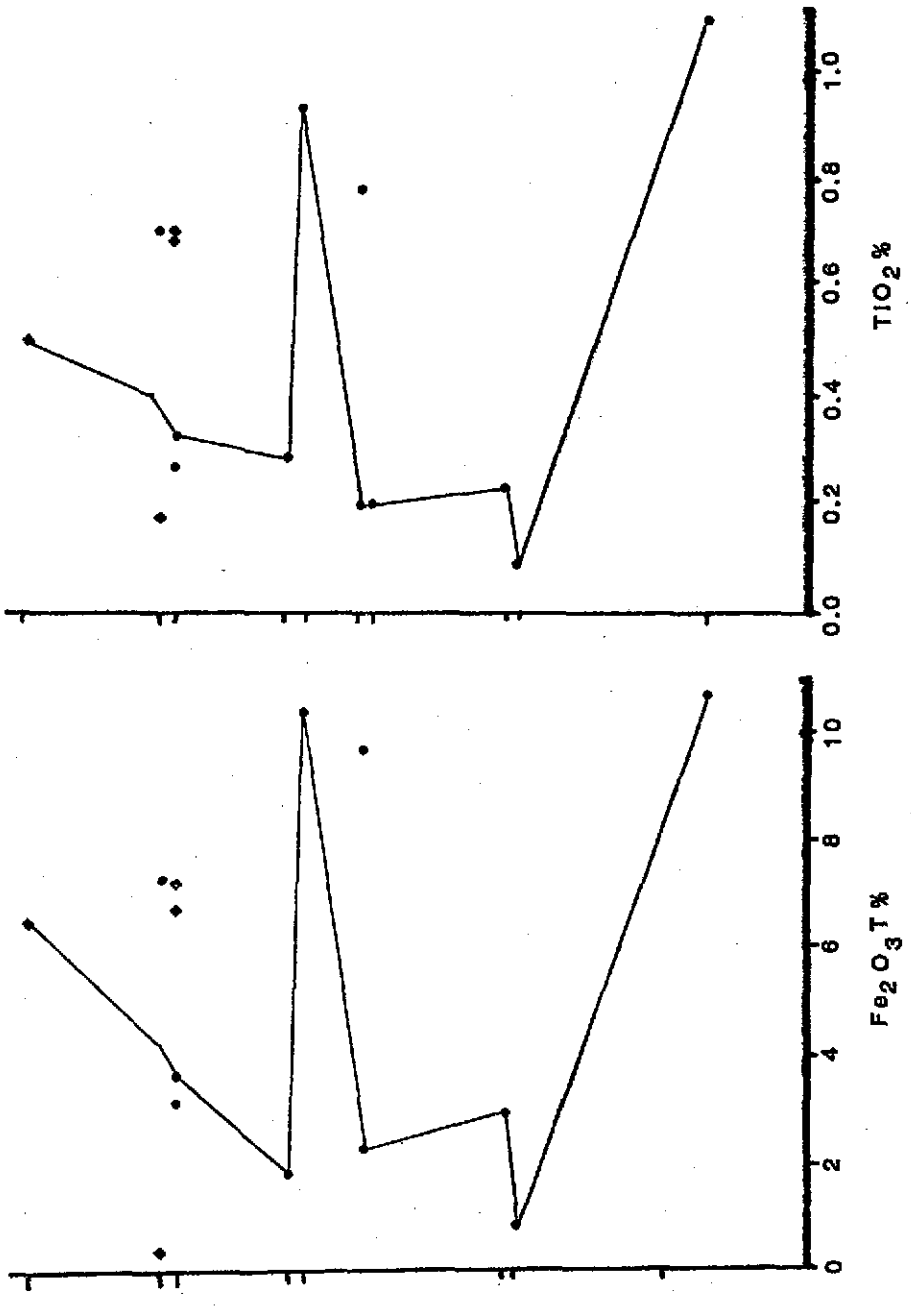
0.0
0.2
0.4
0.6
0.8
1.0
TiO_2 %
0
2
4
6
8
10
Fe_2O_3T %

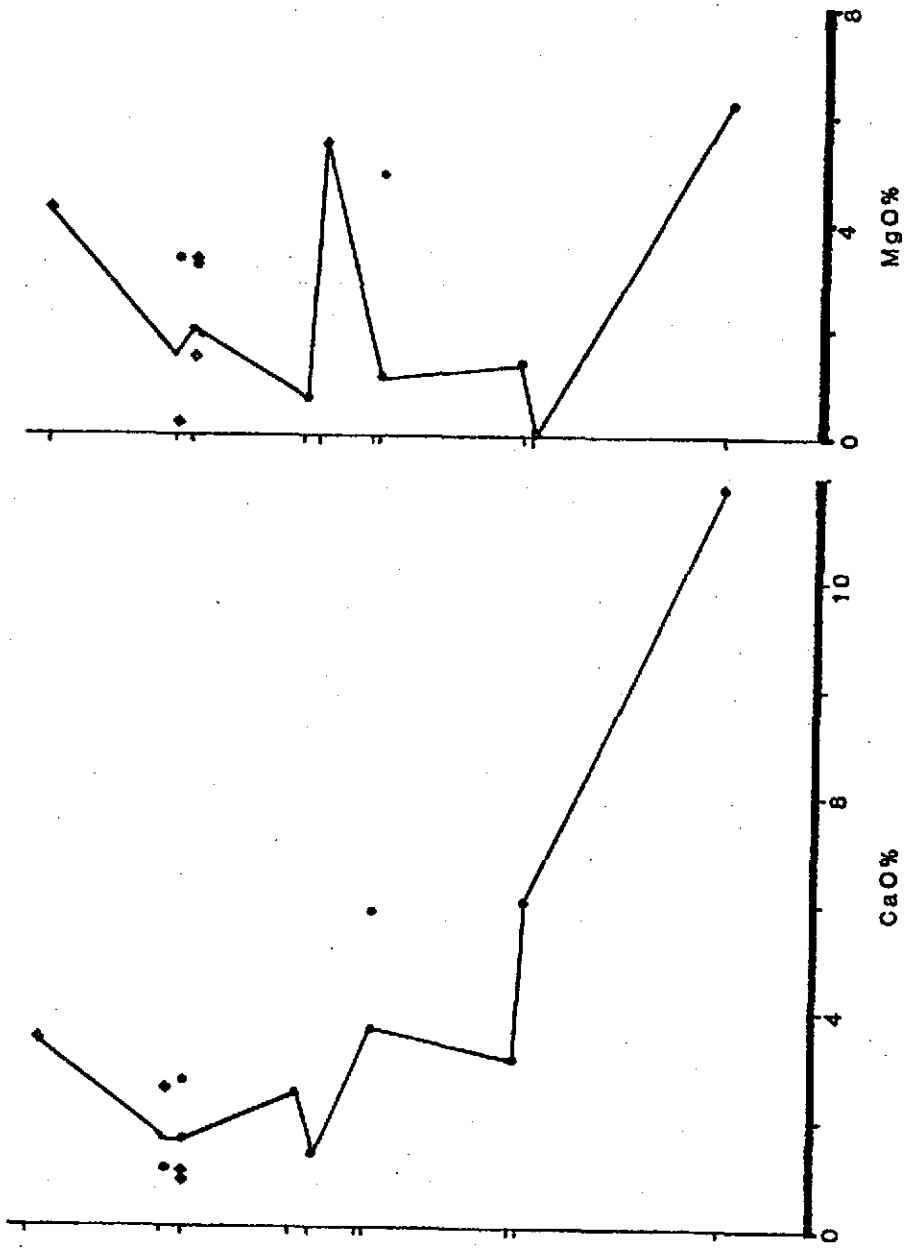
MgO%
0
4
8
CaO%
0
4
8
10

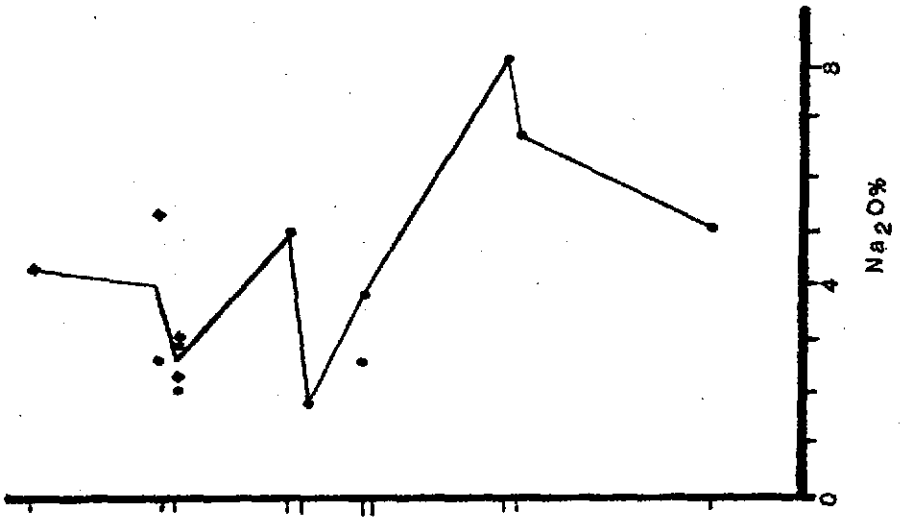
8
4
0
$Na_2O\%$

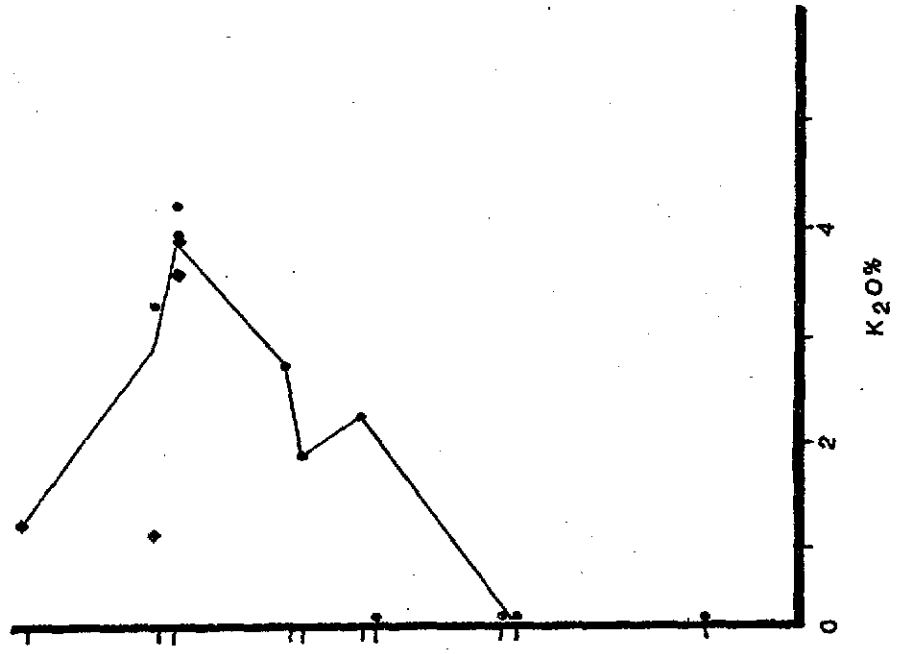
4
2
0
$K_2O\%$

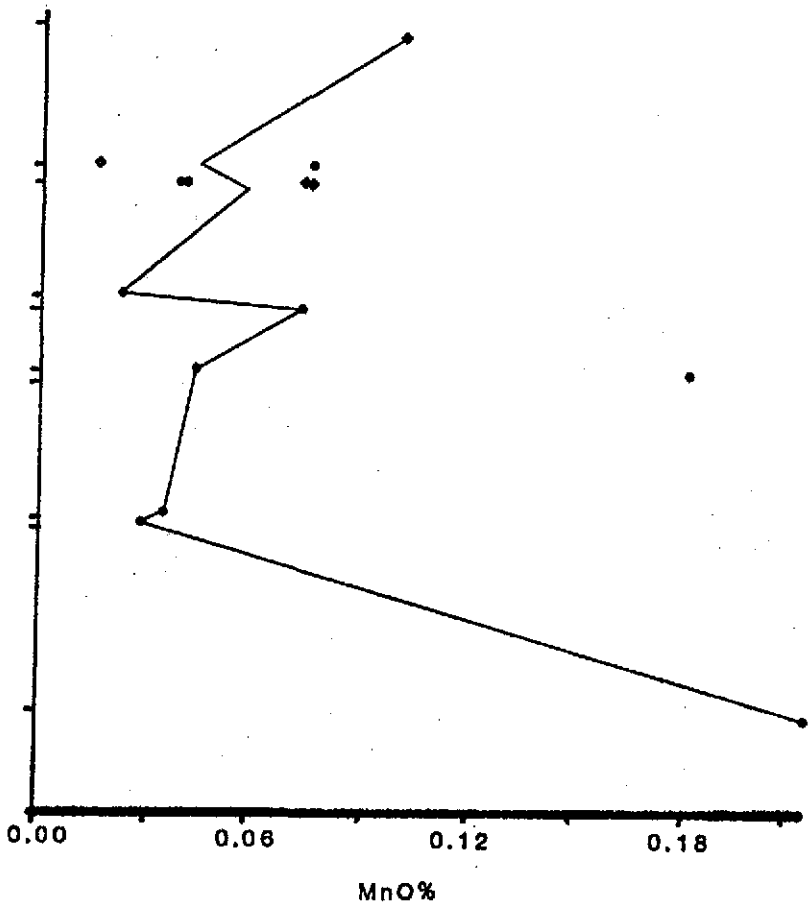
0.00
0.06
0.12
0.18
MnO%

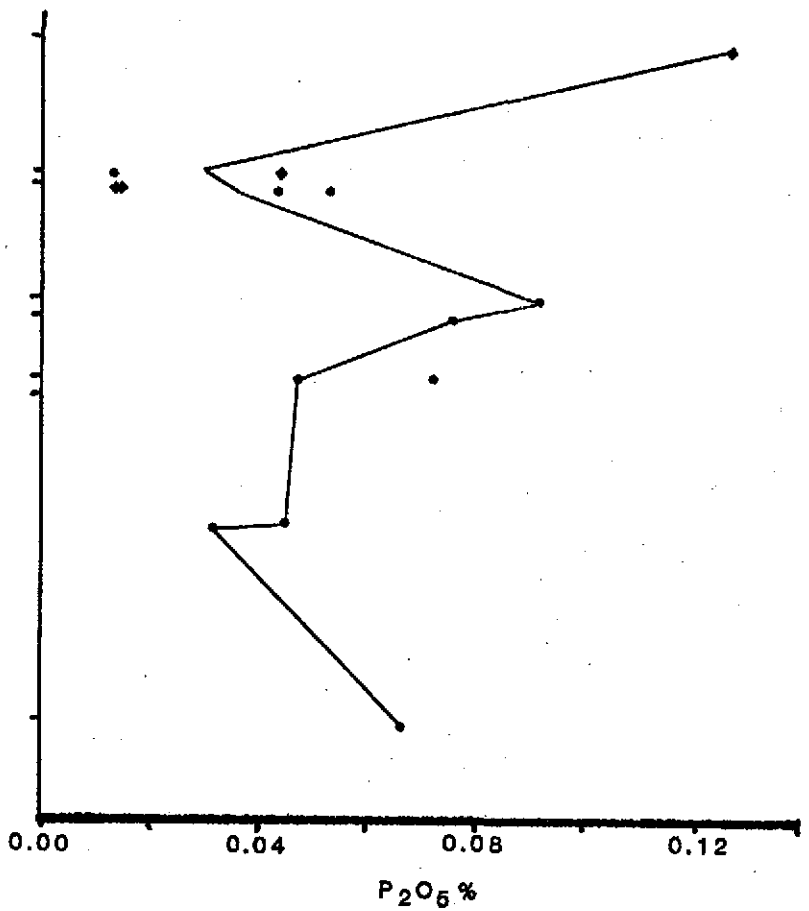
0.00
0.04
0.08
0.12
P_2O_5 %

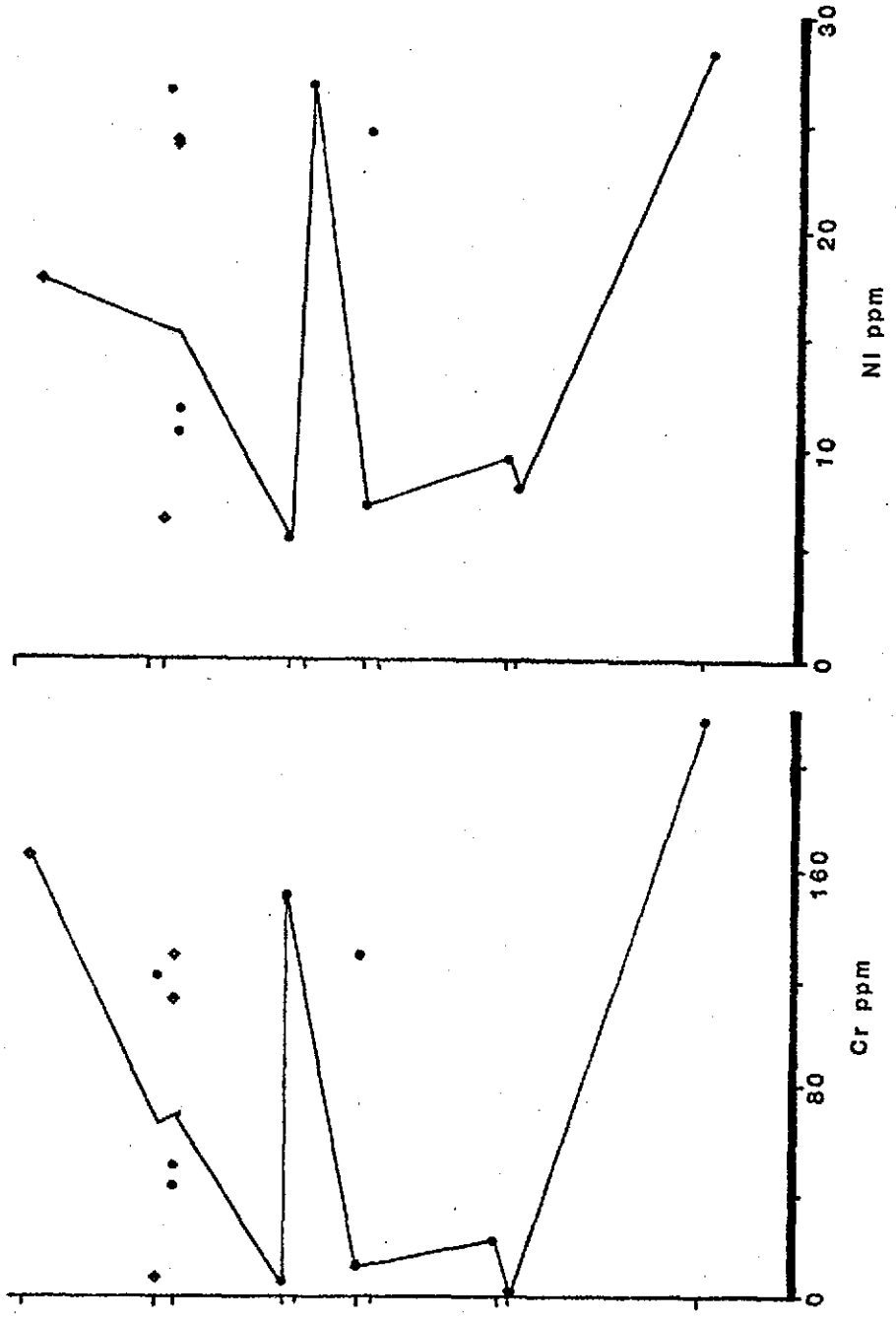
30
20
10
0
Ni ppm
160
80
0
Cr ppm

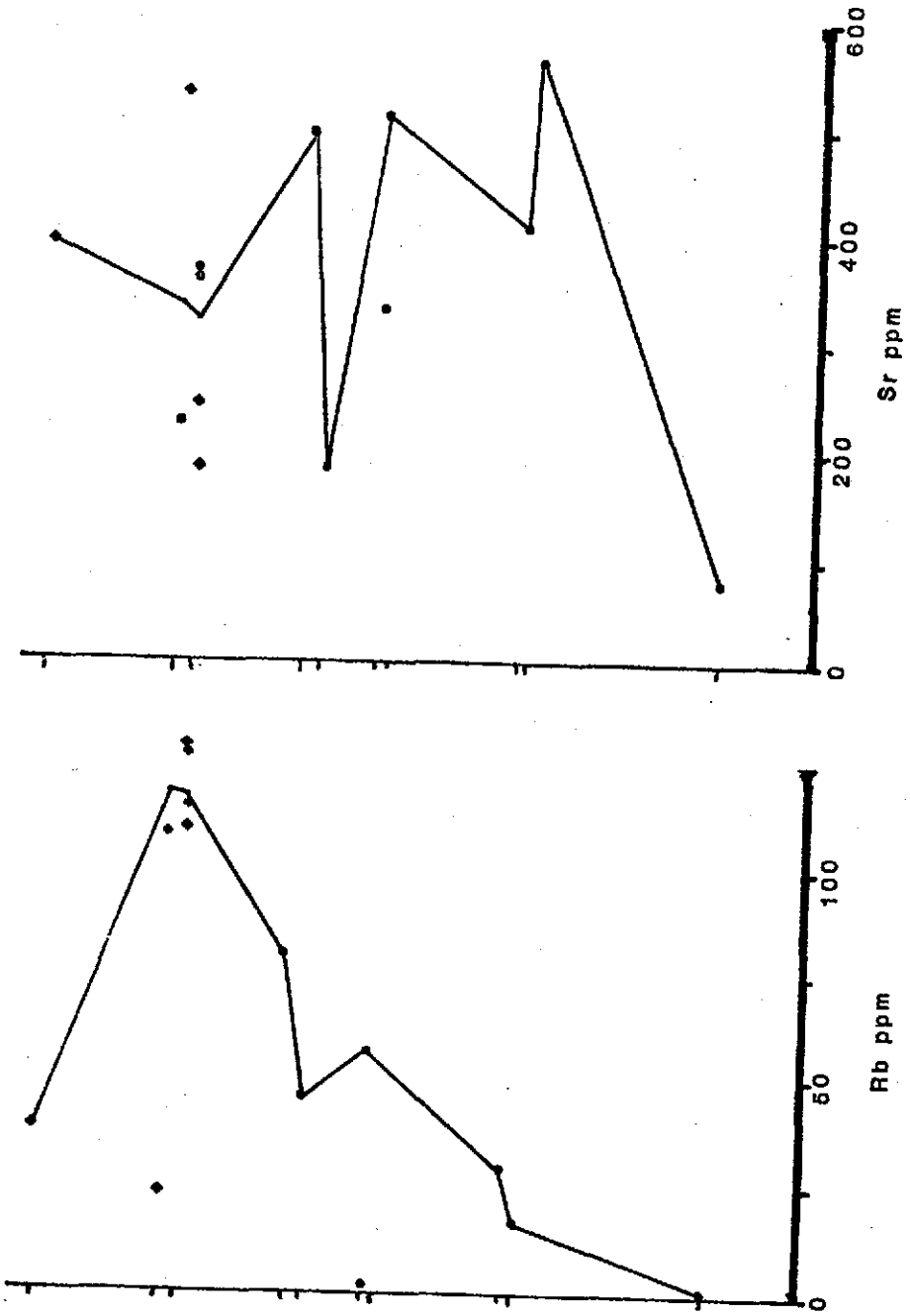
600
400
200
0
Sr ppm
100
50
0
Rb ppm

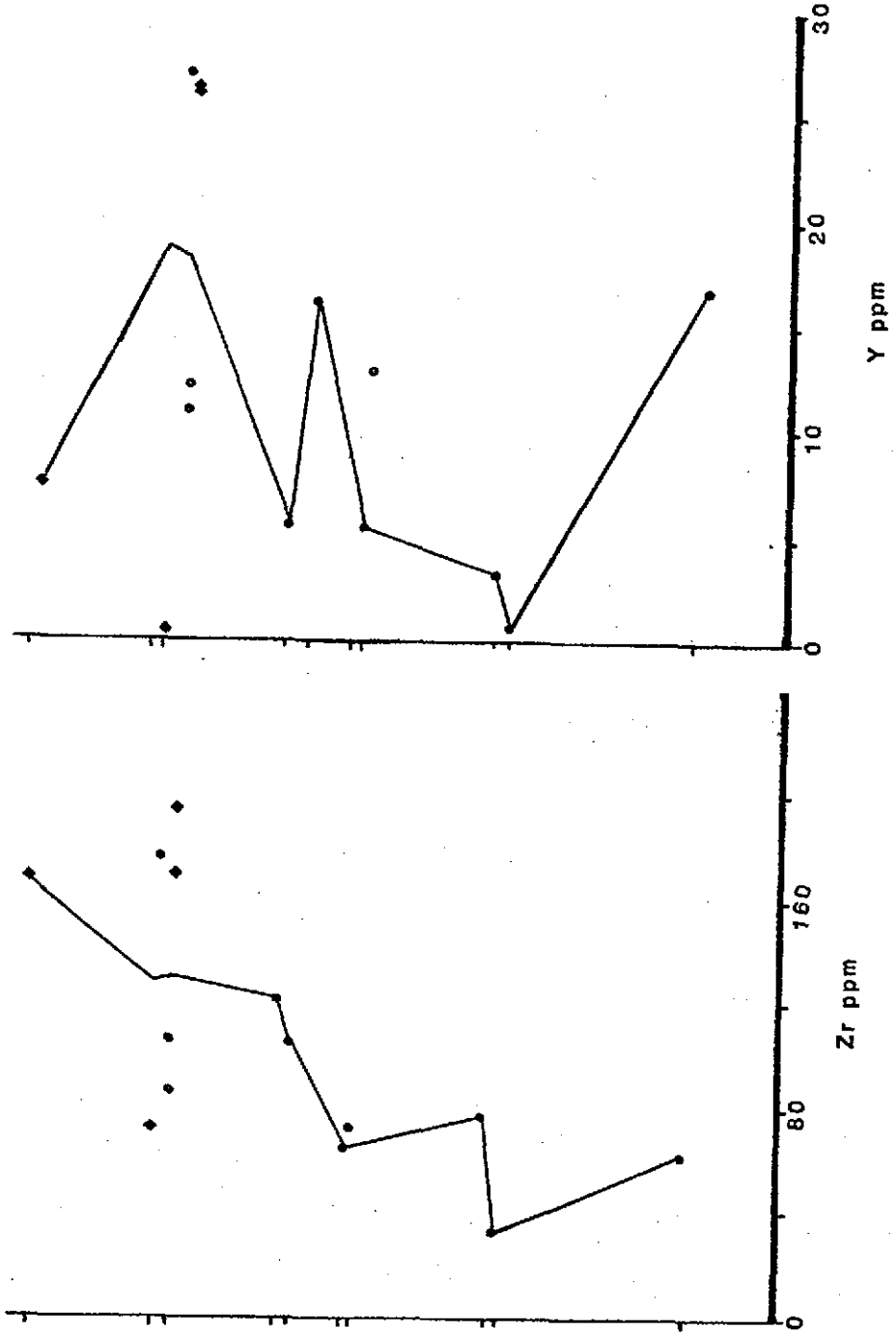
30
20
10
0
Y ppm
160
80
0
Zr ppm

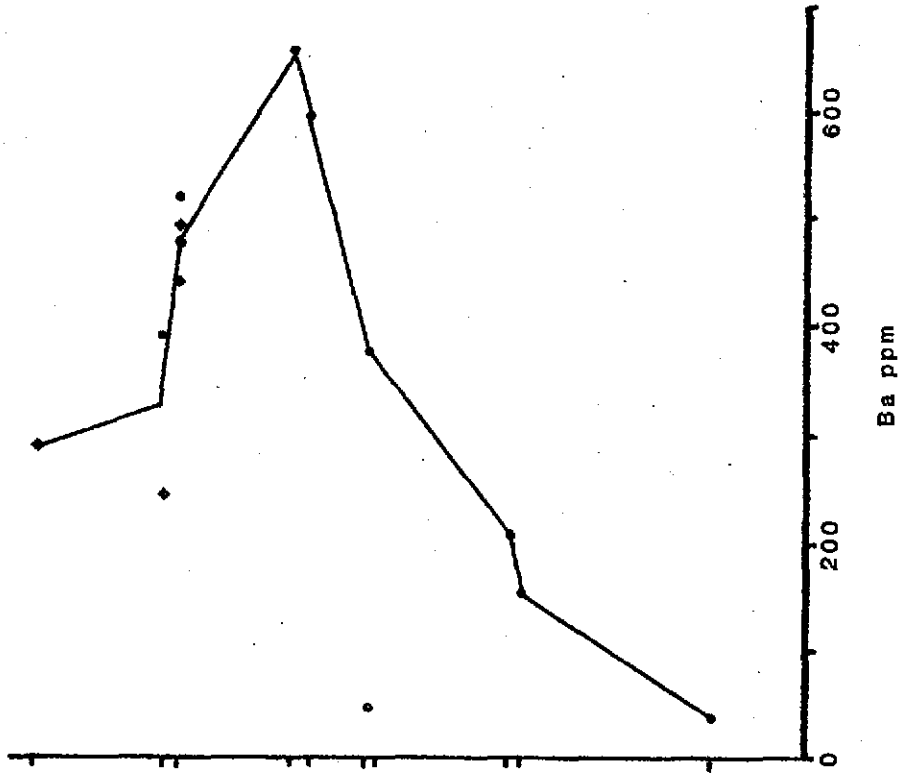
600
400
200
0
Ba ppm

APPENDIX C

DATA

Table 15 contains the XRF data and CIPW norms for the samples analyzed as part of this study. Table 16 contains the trace element data for the samples analyzed as part of this study. In each of the tables, the first number is the sample number. SHEU82-1 was analyzed as a veined and a less-veined separate, and these are designated "V" and "L", respectively.

TABLE 15 -- VERMILION MAJOR ELEMENT DATA

	KLV3-1	GL3-2	KH7-2	SFV14-1	GL16-1	SFV16-1	SFV17-1	GL18-1
SIO2	50.65	53.28	66.24	69.20	53.57	67.30	61.70	66.27
AL2O3	12.42	15.05	15.82	15.18	15.02	15.01	17.63	15.71
FE2O3	8.73	10.16	1.95	0.51	7.24	2.52	0.90	1.42
MGO	8.00	4.98	1.67	0.38	6.51	1.44	0.77	0.77
CAO	7.18	7.14	2.61	5.74	7.94	2.75	4.14	2.73
NA2O	3.58	2.10	6.45	6.42	2.90	7.83	4.20	7.09
K2O	0.94	0.79	1.73	0.63	0.30	0.70	2.82	3.35
TIO2	0.65	0.75	0.24	0.09	0.48	0.21	0.25	0.19
P2O5	0.33	0.11	0.07	0.02	0.09	0.04	0.07	0.06
MNO	0.12	0.08	0.03	0.02	0.12	0.03	0.01	0.03
TOTAL	92.60	94.44	96.81	98.19	94.17	97.83	92.49	97.62
QUARTZ	4.13	17.78	15.44	20.81	12.34	13.53	18.06	8.17
CORUNDUM	0.0	0.0	0.0	0.0	0.0	0.0	0.33	0.0
ZIRCON	0.0	0.0	0.0	0.0	0.0	0.0	0.0	0.0
ORTHOCLASE	6.00	4.94	10.56	3.79	1.88	4.23	18.06	20.28
ALBITE	32.71	18.82	56.38	55.33	26.06	67.72	38.52	61.46
ANORTHITE	16.24	31.03	9.40	10.94	28.76	3.82	21.77	1.18
LEUCITE	0.0	0.0	0.0	0.0	0.0	0.0	0.0	0.0
NEPHELINE	0.0	0.0	0.0	0.0	0.0	0.0	0.0	0.0
DIOPSIDE	13.98	2.55	2.15	2.08	8.70	7.18	0.0	4.24
WOLLASTONI	0.0	0.0	0.0	6.27	0.0	0.0	0.0	2.63
HEMATITE	9.43	10.76	2.01	0.52	7.69	2.58	0.98	1.45
SPHENE	1.36	1.71	0.52	0.17	0.90	0.44	0.0	0.39
PEROVSKITE	0.0	0.0	0.0	0.0	0.0	0.0	0.0	0.0
RUTILE	0.0	0.0	0.0	0.0	0.0	0.0	0.0	0.0
APATITE	0.83	0.27	0.17	0.05	0.22	0.10	0.18	0.14

TABLE 15 -- VERMILION MAJOR ELEMENT DATA

	LLGB21-1	LLGB23-1	SS29-1	SFV34-1	LLGB37-1	LLF39-1	ST40-1	ST41-1
SIO2	60.37	61.53	58.23	63.74	58.73	64.14	48.02	64.88
AL2O3	14.37	14.03	16.70	18.31	14.55	17.63	12.53	16.10
FE2O3	6.18	4.48	6.48	1.43	6.25	0.57	11.44	1.33
MGO	3.82	3.91	5.50	1.02	5.24	0.41	5.02	1.61
CAO	4.08	3.62	2.95	2.33	3.15	3.80	16.45	3.54
NA2O	3.08	3.42	3.53	4.62	3.46	4.25	2.79	5.33
K2O	1.87	2.12	2.18	2.50	2.02	1.83	0.0	1.03
TIO2	0.63	0.52	0.50	0.27	0.56	0.11	1.09	0.21
P2O5	0.20	0.23	0.09	0.08	0.15	0.03	0.05	0.10
MNO	0.09	0.06	0.10	0.02	0.10	0.02	0.29	0.02
TOTAL	94.69	93.92	96.26	94.32	94.21	92.79	97.68	94.15
QUARTZ	22.75	22.03	15.74	22.34	17.85	25.62	2.12	21.53
CORUNDUM	0.36	0.08	3.53	4.21	1.39	1.96	0.0	0.02
ZIRCON	0.0	0.0	0.0	0.0	0.0	0.0	0.0	0.0
ORTHOCLASE	11.74	13.40	13.44	15.70	12.73	11.67	0.0	6.48
ALBITE	27.68	30.96	31.16	41.56	31.22	38.79	24.17	48.00
ANORTHITE	20.11	17.61	14.65	11.73	15.62	20.12	22.18	18.00
LEUCITE	0.0	0.0	0.0	0.0	0.0	0.0	0.0	0.0
NEPHELINE	0.0	0.0	0.0	0.0	0.0	0.0	0.0	0.0
DIOPSIDE	0.0	0.0	0.0	0.0	0.0	0.0	27.61	0.0
WOLLASTONI	0.0	0.0	0.0	0.0	0.0	0.0	9.54	0.0
HEMATITE	6.56	4.79	6.76	1.52	6.67	0.61	11.71	1.42
SPHENE	0.0	0.0	0.0	0.0	0.0	0.0	1.92	0.0
PEROVSKITE	0.0	0.0	0.0	0.0	0.0	0.0	0.0	0.0
RUTILE	0.0	0.0	0.0	0.0	0.0	0.0	0.0	0.0
APATITE	0.49	0.57	0.22	0.20	0.37	0.08	0.12	0.25

TABLE 15 -- VERMILION MAJOR ELEMENT DATA

	TF42-1	SFV44-1	SFV46-1	SFV48-2	ST50-2	TFS51-1	TFS52-1	TFS52-2
SIO2	68.23	65.76	55.23	65.98	65.18	67.97	69.38	65.50
AL203	15.52	17.62	16.81	17.82	15.93	16.28	16.00	16.89
FE203	0.67	2.22	10.53	1.92	1.19	1.50	1.91	1.46
MGO	0.45	1.03	5.82	1.25	0.81	1.42	1.08	0.63
CAO	3.39	3.17	1.28	3.29	3.47	2.66	3.50	4.80
NA20	4.30	4.21	1.52	3.47	4.78	3.45	3.77	4.05
K20	0.98	1.39	1.66	2.06	2.35	1.72	1.06	0.46
TIO2	0.12	0.16	0.86	0.19	0.22	0.14	0.15	0.23
P205	0.03	0.04	0.07	0.04	0.08	0.04	0.04	0.05
MNO	0.03	0.04	0.07	0.04	0.04	0.03	0.03	0.04
TOTAL	93.72	95.64	93.85	96.06	94.05	95.21	96.92	94.11
QUARTZ	33.77	29.04	30.96	30.35	21.60	35.35	35.53	30.98
CORUNDUM	1.38	3.69	11.12	4.17	0.0	4.21	2.46	1.19
ZIRCON	0.0	0.0	0.0	0.0	0.0	0.0	0.0	0.0
ORTHOCLASE	6.18	8.60	10.54	12.69	14.77	10.69	6.47	2.89
ALBITE	38.86	37.29	13.82	30.61	43.01	30.70	32.95	36.49
ANORTHITE	17.75	16.19	6.33	16.74	16.02	13.60	17.67	25.01
LEUCITE	0.0	0.0	0.0	0.0	0.0	0.0	0.0	0.0
NEPHELINE	0.0	0.0	0.0	0.0	0.0	0.0	0.0	0.0
DIOPSIDE	0.0	0.0	0.0	0.0	0.84	0.0	0.0	0.0
WOLLASTONI	0.0	0.0	0.0	0.0	0.0	0.0	0.0	0.0
HEMATITE	0.72	2.32	11.31	2.00	1.27	1.58	1.97	1.55
SPHENE	0.0	0.0	0.0	0.0	0.46	0.0	0.0	0.0
PEROVSKITE	0.0	0.0	0.0	0.0	0.0	0.0	0.0	0.0
RUTILE	0.0	0.0	0.0	0.0	0.0	0.0	0.0	0.0
APATITE	0.07	0.10	0.17	0.10	0.20	0.10	0.10	0.12

TABLE 15 -- VERMILION MAJOR ELEMENT DATA

	TFS52-3	TGB56-1	TGB57-1	TGB59-1	ST60-1	SFV65-3	SFV65-4	SFV65-5A
SIO2	64.80	55.78	59.78	59.16	44.77	60.16	59.47	58.02
AL203	16.83	15.11	14.65	14.28	13.72	20.63	18.73	20.13
FE203	1.48	7.50	5.44	5.57	10.88	3.32	7.18	6.61
MGO	0.63	4.91	4.62	5.27	6.46	2.06	3.32	3.45
CAO	4.80	4.00	3.23	3.75	13.34	1.51	0.79	0.85
NA2O	3.87	3.13	4.00	3.67	4.72	2.58	1.68	1.91
K2O	0.46	2.66	2.28	2.11	0.0	4.04	3.38	3.74
TIO2	0.23	0.71	0.57	0.58	1.00	0.31	0.65	0.63
P2O5	0.06	0.34	0.22	0.21	0.06	0.04	0.13	0.12
MNO	0.04	0.12	0.07	0.07	0.20	0.04	0.07	0.06
TOTAL	93.20	94.26	94.86	94.67	95.15	94.69	95.40	95.52
QUARTZ	31.69	13.30	15.47	15.47	0.0	24.89	32.15	27.35
CORUNDUM	1.49	0.67	0.27	0.0	0.0	9.92	11.79	12.30
ZIRCON	0.0	0.0	0.0	0.0	0.0	0.0	0.0	0.0
ORTHOCLASE	2.92	16.78	14.28	13.17	0.0	25.28	21.06	23.27
ALBITE	35.21	28.27	35.87	32.80	20.31	23.12	14.99	17.02
ANORTHITE	25.18	18.81	15.46	17.17	17.08	7.66	3.24	3.62
LEUCITE	0.0	0.0	0.0	0.0	0.0	0.0	0.0	0.0
NEPHELINE	0.0	0.0	0.0	0.0	11.74	0.0	0.0	0.0
DIOPSIDE	0.0	0.0	0.0	0.0	36.47	0.0	0.0	0.0
WOLLASTONI	0.0	0.0	0.0	0.0	0.99	0.0	0.0	0.0
HEMATITE	1.59	8.01	5.76	5.88	11.43	3.52	7.57	6.96
SPHENE	0.0	0.0	0.0	0.72	0.0	0.0	0.0	0.0
PEROVSKITE	0.0	0.0	0.0	0.0	1.39	0.0	0.0	0.0
RUTILE	0.0	0.0	0.0	0.23	0.0	0.0	0.0	0.0
APATITE	0.15	0.84	0.54	0.52	0.15	0.10	0.32	0.29

TABLE 15 -- VERMILION MAJOR ELEMENT DATA

	SFV65-5B	SFV65-6A	SFV65-6B	ST68-1	TGC68-1	ST68-2	TEL69-1	TGB70-1
SIO2	60.36	71.84	59.74	68.60	59.56	67.68	62.57	55.30
AL203	19.22	13.57	18.36	15.21	14.53	16.80	15.41	13.80
FE203	2.75	0.38	7.21	1.61	3.98	1.66	1.69	6.31
MGO	1.64	0.21	3.55	0.78	3.62	1.67	1.85	4.75
CAO	2.58	2.42	0.93	3.04	4.28	2.44	4.00	5.89
NA2O	2.42	4.92	2.15	4.14	4.02	3.72	4.51	4.65
K2O	3.72	0.87	3.08	1.25	1.31	1.80	1.62	2.62
TIO2	0.25	0.17	0.65	0.22	0.39	0.16	0.21	0.67
P2O5	0.03	0.04	0.12	0.05	0.10	0.04	0.10	0.20
MNO	0.04	0.01	0.07	0.02	0.06	0.02	0.19	0.09
TOTAL	93.01	94.43	95.86	94.92	91.85	95.99	92.15	94.28
QUARTZ	26.03	36.60	29.91	33.99	19.05	32.91	21.23	3.36
CORUNDUM	7.10	0.24	10.58	1.73	0.0	4.58	0.0	0.0
ZIRCON	0.0	0.0	0.0	0.0	0.0	0.0	0.0	0.0
ORTHOCLASE	23.69	5.45	19.10	7.80	8.43	11.10	10.39	16.42
ALBITE	22.06	44.16	19.09	36.98	37.03	32.84	41.41	41.73
ANORTHITE	13.58	12.46	4.02	15.58	19.31	12.36	18.47	9.59
LEUCITE	0.0	0.0	0.0	0.0	0.0	0.0	0.0	0.0
NEPHELINE	0.0	0.0	0.0	0.0	0.0	0.0	0.0	0.0
DIOPSIDE	0.0	0.0	0.0	0.0	1.46	0.0	1.83	13.94
WOLLASTONI	0.0	0.0	0.0	0.0	0.0	0.0	0.0	0.0
HEMATITE	2.96	0.40	7.57	1.70	4.33	1.73	1.83	6.69
SPHENE	0.0	0.0	0.0	0.0	0.86	0.0	0.0	1.48
PEROVSKITE	0.0	0.0	0.0	0.0	0.0	0.0	0.0	0.0
RUTILE	0.0	0.0	0.0	0.0	0.0	0.0	0.0	0.0
APATITE	0.08	0.10	0.29	0.12	0.25	0.10	0.25	0.49

TABLE 15 -- VERMILION MAJOR ELEMENT DATA

	TGB72-1	TGB73-1	TGB75-1	BWWBM76-1	ST79-1	ENES80-1	SHEU82-1V	SHEU82-1L
SIO2	58.16	63.10	58.68	41.19	56.56	69.66	56.95	54.37
AL2O3	14.29	16.04	15.72	14.14	12.33	11.16	13.66	15.02
FE2O3	5.16	4.04	3.88	14.29	9.80	3.55	4.16	4.44
MGO	3.64	3.66	2.67	6.62	5.12	4.36	3.43	4.15
CAO	5.33	3.41	5.73	16.38	5.68	0.21	4.63	5.89
NA2O	2.97	2.68	3.90	2.26	2.23	4.68	4.94	7.11
K2O	2.69	2.94	1.79	0.41	0.0	0.23	1.40	1.31
TIO2	0.61	0.51	0.42	0.79	0.72	0.15	0.47	0.53
P2O5	0.23	0.21	0.11	0.03	0.06	0.07	0.23	0.24
MNO	0.09	0.05	0.05	0.35	0.17	0.04	0.12	0.12
TOTAL	93.17	96.64	92.95	96.46	92.67	94.11	89.99	93.18
QUARTZ	17.12	25.04	15.97	0.0	26.82	37.03	11.94	0.0
CORUNDUM	0.0	2.86	0.0	0.0	0.0	3.19	0.0	0.0
ZIRCON	0.0	0.0	0.0	0.0	0.0	0.0	0.0	0.0
ORTHOCLASE	17.06	18.06	11.38	2.51	0.0	1.45	9.19	8.31
ALBITE	26.97	23.58	35.50	5.16	20.36	42.13	46.45	54.81
ANORTHITE	19.01	16.16	21.63	28.22	25.50	0.62	12.18	5.58
LEUCITE	0.0	0.0	0.0	0.0	0.0	0.0	0.0	0.0
NEPHELINE	0.0	0.0	0.0	7.94	0.0	0.0	0.0	5.29
DIOPSIDE	4.56	0.0	5.31	36.87	1.94	0.0	8.08	17.61
WOLLASTONI	0.0	0.0	0.0	2.93	0.0	0.0	0.0	0.0
HEMATITE	5.54	4.20	4.17	14.81	10.57	3.78	4.62	4.76
SPHENE	1.34	0.0	0.96	0.0	1.40	0.0	0.91	0.0
PEROVSKITE	0.0	0.0	0.0	0.70	0.0	0.0	0.0	0.72
RUTILE	0.0	0.0	0.0	0.0	0.0	0.0	0.0	0.0
APATITE	0.57	0.51	0.28	0.07	0.15	0.17	0.59	0.60

TABLE 15 — VERMILION MAJOR ELEMENT DATA

	SHEU88-1	LLBM100-1	LLBM102-2	VGC105-1	VGC108-1	CKGB117-1	SSGB120-1	CKGB122-1
SIO2	65.58	48.88	42.89	59.58	60.38	58.49	57.31	62.18
AL203	15.03	12.15	12.04	15.39	14.39	15.68	14.66	15.89
FE203	1.53	10.42	11.86	7.53	3.70	5.17	6.52	4.11
MGO	1.29	4.20	5.55	3.74	2.37	3.40	5.63	3.64
CAO	2.76	11.17	12.89	2.70	1.08	2.71	4.28	3.48
NA2O	5.85	2.96	2.04	2.77	7.07	4.86	4.08	2.61
K2O	0.96	0.0	0.0	2.23	1.12	1.70	1.56	2.95
TIO2	0.22	0.95	0.99	0.45	0.41	0.45	0.62	0.52
P2O5	0.07	0.06	0.06	0.12	0.13	0.13	0.22	0.21
MNO	0.02	0.21	0.26	0.09	0.05	0.07	0.09	0.05
TOTAL	93.31	91.00	88.58	94.60	90.70	92.66	94.97	95.64
QUARTZ	22.00	10.14	4.41	25.37	10.53	14.31	11.85	24.61
CORUNDUM	0.0	0.0	0.0	4.03	0.0	1.33	0.0	2.71
ZIRCON	0.0	0.0	0.0	0.0	0.0	0.0	0.0	0.0
ORTHOCLASE	6.08	0.0	0.0	13.98	7.30	10.88	9.71	18.32
ALBITE	53.05	27.52	19.49	24.87	65.96	44.56	36.35	23.20
ANORTHITE	12.77	21.83	26.75	13.38	4.65	13.65	17.98	16.70
LEUCITE	0.0	0.0	0.0	0.0	0.0	0.0	0.0	0.0
NEPHELINE	0.0	0.0	0.0	0.0	0.0	0.0	0.0	0.0
DIOPSIDE	0.53	24.79	32.89	0.0	0.0	0.0	0.75	0.0
WOLLASTONI	0.0	1.69	0.0	0.0	0.0	0.0	0.0	0.0
HEMATITE	1.64	11.45	13.39	7.99	4.08	5.60	6.87	4.32
SPHENE	0.52	1.92	1.93	0.0	0.22	0.0	1.34	0.0
PEROVSKITE	0.0	0.0	0.0	0.0	0.0	0.0	0.0	0.0
RUTILE	0.0	0.0	0.0	0.0	0.30	0.0	0.0	0.0
APATITE	0.17	0.15	0.16	0.30	0.33	0.33	0.54	0.51

TABLE 15 -- VERMILION MAJOR ELEMENT DATA

	CKGB125-1	LGGB128-1	IDGB135-1	TMV146-1	SFV151-1	SFV152-1	SFV155-1	ENEL160-1
SIO2	59.79	61.05	65.52	51.43	62.17	63.68	58.21	62.36
AL203	16.01	15.45	14.45	11.75	16,67	16.17	19.04	14.84
FE203	6.03	4.69	3.40	8.34	1.01	1.48	7.66	3.77
MGO	3.42	3.36	2.76	9.03	1.20	1.49	3.95	5.29
CAO	2.36	4.90	3.27	7.19	4.93	3.06	0.82	3.67
NA2O	2.72	2.61	3.98	3.28	5.00	5.33	1.94	5.29
K2O	3.02	2.14	1.74	1.24	1.49	1.79	3.07	0.89
TIO2	0.53	0.53	0.45	0.64	0.20	0.21	0.62	0.33
P2O5	0.15	0.18	0.22	0.23	0.07	0.09	0.12	0.16
MNO	0.04	0.06	0.04	0.13	0.02	0.03	0.07	0.05
TOTAL	94.07	94.97	95.83	93.26	92.76	93.33	95.50	96.65
QUARTZ	24.23	24.00	26.42	4.09	17.67	18.57	29.35	14.01
CORUNDUM	4.63	0.38	0.63	0.0	0.0	0.12	11.92	0.0
ZIRCON	0.0	0.0	0.0	0.0	0.0	0.0	0.0	0.0
ORTHOCLASE	19.07	13.38	10.77	7.86	9.49	11.35	19.10	5.44
ALBITE	24.59	23.37	35.29	29.76	45.61	48.42	17.29	46.31
ANORTHITE	11.46	24.48	15.49	14.66	20.10	15.67	3.46	14.61
LEUCITE	0.0	0.0	0.0	0.0	0.0	0.0	0.0	0.0
NEPHELINE	0.0	0.0	0.0	0.0	0.0	0.0	0.0	0.0
DIOPSIDE	0.0	0.0	0.0	15.67	3.98	0.0	0.0	1.68
WOLLASTONI	0.0	0.0	0.0	0.0	0.0	0.0	0.0	0.0
HEMATITE	6.44	4.96	3.56	8.94	1.09	1.59	8.07	3.90
SPHENE	0.0	0.0	0.0	1.30	0.47	0.0	0.0	0.69
PEROVSKITE	0.0	0.0	0.0	0.0	0.0	0.0	0.0	0.0
RUTILE	0.0	0.0	0.0	0.0	0.0	0.0	0.0	0.0
APATITE	0.37	0.44	0.54	0.57	0.18	0.22	0.29	0.38

TABLE 15 — VERMILION MAJOR ELEMENT DATA

	ENEL163-1	SFVC177-1	SFV181-3	SFV183-1	TFV187-1	SXFV192-1	TFV195-1	TFV196-1
SIO2	65.21	72.28	54.32	61.64	63.44	61.34	74.20	74.12
AL203	14.40	13.62	16.32	13.68	16.40	14.74	12.86	12.52
FE203	2.44	1.00	10.19	6.37	1.43	4.21	0.41	0.29
MGO	2.39	0.78	5.85	4.27	0.98	3.85	0.21	0.18
CAO	3.24	1.24	2.66	3.35	2.41	3.55	1.91	3.03
NA2O	5.04	5.21	2.58	3.89	5.60	4.78	5.06	4.45
K2O	1.76	0.80	0.64	0.98	3.14	1.16	0.58	0.77
TIO2	0.29	0.15	0.71	0.46	0.22	0.38	0.14	0.14
P2O5	0.16	0.04	0.07	0.12	0.07	0.11	0.04	0.04
MNO	0.03	0.02	0.11	0.09	0.0	0.07	0.01	0.02
TOTAL	94.96	95.14	93.45	94.85	93.69	94.19	95.42	95.56
QUARTZ	20.93	37.05	24.38	23.34	13.53	17.41	40.15	41.08
CORUNDUM	0.0	2.13	7.23	0.44	0.0	0.0	0.56	0.0
ZIRCON	0.0	0.0	0.0	0.0	0.0	0.0	0.0	0.0
ORTHOCLASE	10.95	4.98	4.07	6.13	19.80	7.28	3.60	4.76
ALBITE	44.91	46.40	23.51	34.83	50.58	42.94	44.93	39.40
ANORTHITE	12.08	6.20	13.72	16.76	11.03	16.28	9.67	12.47
LEUCITE	0.0	0.0	0.0	0.0	0.0	0.0	0.0	0.0
NEPHELINE	0.0	0.0	0.0	0.0	0.0	0.0	0.0	0.0
DIOPSIDE	2.19	0.0	0.0	0.0	0.33	0.42	0.0	1.01
WOLLASTONI	0.0	0.0	0.0	0.0	0.0	0.0	0.0	0.53
HEMATITE	2.57	1.05	10.97	6.74	1.53	4.47	0.43	0.30
SPHENE	0.66	0.0	0.0	0.0	0.58	0.78	0.0	0.30
PEROVSKITE	0.0	0.0	0.0	0.0	0.0	0.0	0.0	0.0
RUTILE	0.0	0.0	0.0	0.0	0.0	0.0	0.0	0.0
APATITE	0.39	0.10	0.18	0.30	0.17	0.27	0.10	0.10

TABLE 15 -- VERMILION MAJOR ELEMENT DATA

	TFV196-2	TFV196-3	TFV197-1	TFV197-2	SEU200-1	TF204-2	SXF206-2	SXF210-1
SIO2	71.90	72.25	62.35	47.27	46.10	68.13	54.76	47.49
AL203	13.34	13.53	16.42	16.30	12.15	14.42	13.69	10.79
FE203	0.29	0.32	1.26	11.04	13.26	0.47	8.84	13.10
MGO	0.16	0.18	0.76	4.32	7.96	0.26	6.33	8.44
CAO	3.08	3.13	5.26	9.30	9.69	3.92	7.91	11.18
NA2O	4.68	4.55	4.71	3.12	2.16	4.73	4.09	0.39
K2O	0.86	0.95	1.69	1.34	0.0	0.56	1.15	0.0
TIO2	0.16	0.16	0.24	0.81	0.91	0.10	0.55	0.71
P2O5	0.04	0.03	0.09	0.05	0.05	0.02	0.10	0.04
MNO	0.03	0.03	0.03	0.17	0.21	0.02	0.14	0.26
TOTAL	94.54	95.13	92.81	93.72	92.49	92.63	97.56	92.40
QUARTZ	37.16	37.44	19.19	2.06	6.80	32.78	5.57	15.95
CORUNDUM	0.0	0.0	0.0	0.0	0.0	0.0	0.0	0.0
ZIRCON	0.0	0.0	0.0	0.0	0.0	0.0	0.0	0.0
ORTHOCLASE	5.38	5.90	10.76	8.45	0.0	3.57	6.97	0.0
ALBITE	41.89	40.47	42.94	28.17	19.76	43.21	35.47	3.57
ANORTHITE	13.59	14.39	20.12	28.29	25.36	17.77	15.99	29.97
LEUCITE	0.0	0.0	0.0	0.0	0.0	0.0	0.0	0.0
NEPHELINE	0.0	0.0	0.0	0.0	0.0	0.0	0.0	0.0
DIOPSIDE	0.91	0.99	4.40	14.24	18.47	1.51	17.25	21.95
WOLLASTONI	0.28	0.0	0.39	0.0	0.0	0.36	0.0	0.0
HEMATITE	0.31	0.34	1.36	11.78	14.34	0.51	9.06	14.18
SPHENE	0.33	0.33	0.55	1.62	1.79	0.21	0.99	1.11
PEROVSKITE	0.0	0.0	0.0	0.0	0.0	0.0	0.0	0.0
RUTILE	0.0	0.0	0.0	0.0	0.0	0.0	0.0	0.0
APATITE	0.10	0.07	0.23	0.12	0.13	0.05	0.24	0.10

TABLE 15 -- VERMILION MAJOR ELEMENT DATA

	SXF211-1	TMV213-1	TES214-1	EMMV217-1	SFV219-3
SIO2	58.68	62.63	60.73	49.00	46.86
AL203	15.45	18.67	15.78	14.82	12.96
FE203	6.00	2.16	2.00	8.30	12.46
MGO	4.76	1.12	2.26	7.27	5.00
CAO	3.81	4.19	4.91	6.84	14.28
NA2O	5.17	4.14	3.44	2.92	4.68
K2O	0.77	1.55	2.32	2.24	0.0
TIO2	0.51	0.31	0.20	0.66	1.05
P2O5	0.15	0.07	0.10	0.20	0.06
MNO	0.09	0.02	0.04	0.11	0.24
TOTAL	95.39	94.86	91.78	92.36	97.59
QUARTZ	11.63	23.44	20.56	1.18	0.0
CORUNDUM	0.0	2.89	0.0	0.0	0.0
ZIRCON	0.0	0.0	0.0	0.0	0.0
ORTHOCLASE	4.77	9.68	14.94	14.33	0.0
ALBITE	45.86	37.04	31.71	26.75	28.18
ANORTHITE	17.48	21.50	22.62	22.43	14.71
LEUCITE	0.0	0.0	0.0	0.0	0.0
NEPHELINE	0.0	0.0	0.0	0.0	6.72
DIOPSIDE	0.0	0.0	2.04	8.47	27.52
WOLLASTONI	0.0	0.0	0.0	0.0	8.07
HEMATITE	6.29	2.28	2.18	8.99	12.77
SPHENE	0.92	0.0	0.41	1.42	0.0
PEROVSKITE	0.0	0.0	0.0	0.0	1.36
RUTILE	0.05	0.0	0.0	0.0	0.0
APATITE	0.37	0.17	0.25	0.50	0.14

TABLE 16 -- VERMILION TRACE ELEMENT DATA

	KLV3-1	GL3-2	KH7-2	SFV14-1	SFV9-1	GL16-1	SFV16-1	SFV17-1
BA	408.00	173.60	380.90	152.70	434.20	132.20	203.60	670.90
CR	320.96	229.05	10.20	3.40	27.51	197.70	29.81	5.50
NI	31.20	15.00	7.90	8.10	11.80	39.60	9.50	6.40
RB	29.30	20.30	60.40	15.80	33.40	19.40	29.60	77.45
SR	286.47	938.08	327.23	470.59	556.95	206.95	344.50	441.29
V	711.10	976.60	0.0	0.0	114.50	570.50	85.70	0.0
Y	22.20	6.50	7.10	1.00	3.30	11.80	3.50	5.90
ZR	126.64	82.50	115.05	38.30	83.22	100.86	72.02	82.05

	GL18-1	LLGB21-1	LLGB23-1	SS29-1	SFV34-1	LLGB37-1	LLF39-1	ST40-1
BA	951.20	346.70	430.70	519.20	654.20	657.00	273.90	57.70
CR	5.80	175.21	125.80	151.48	7.20	194.34	8.10	328.05
NI	5.20	15.10	12.00	18.20	5.80	20.30	7.70	31.60
RB	99.87	51.00	58.00	59.50	84.46	55.50	42.30	0.0
SR	817.88	435.24	723.63	319.50	416.38	457.61	569.85	172.09
V	0.0	1072.00	348.20	532.60	0.0	517.70	0.0	1594.00
Y	9.00	9.80	9.40	12.20	5.90	10.00	3.50	17.20
ZR	111.21	101.45	104.57	97.67	100.73	83.35	40.20	54.25

TABLE 16 -- VERMILION TRACE ELEMENT DATA

	ST41-1	TF42-1	SFV44-1	SFV46-1	SFV48-2	ST50-2	TFS51-1	TFS52-1
BA	425.20	287.50	320.80	594.70	379.40	730.60	407.80	1243.00
CR	26.27	6.20	7.90	258.80	12.50	4.80	14.10	8.20
NI	8.60	9.50	12.00	27.00	7.20	10.50	7.50	5.70
RB	31.80	21.00	38.20	47.60	64.40	81.68	64.10	33.60
SR	689.88	499.64	501.47	165.64	427.76	496.18	374.27	396.08
V	0.0	0.0	0.0	993.80	133.20	0.0	38.00	0.0
Y	2.30	1.50	4.00	16.60	5.80	7.95	5.40	2.80
ZR	68.12	51.84	54.25	89.14	68.83	61.77	74.50	55.49

	TFS52-2	TFS52-3A	TGB56-1	TGB57-1	TGB59-1	ST60-1	SFV65-3	SFV65-4
BA	571.60	581.50	687.20	909.70	775.80	33.90	517.90	444.30
CR	9.60	10.50	133.94	151.83	225.50	376.57	80.81	217.36
NI	9.40	9.20	26.20	28.50	13.70	28.30	11.90	24.00
RB	14.10	13.50	79.33	67.50	57.70	0.0	114.23	103.55
SR	501.31	498.76	470.90	495.02	769.88	79.40	306.05	165.24
V	0.0	0.0	1085.75	1458.00	485.50	1937.00	208.60	639.30
Y	0.60	1.40	15.65	12.50	9.70	17.20	12.40	26.20
ZR	68.38	65.38	106.82	103.08	108.28	63.10	91.36	148.78

TABLE 16 -- VERMILION TRACE ELEMENT DATA

	SFV65-5A	SFV65-5B	SFV65-6A	SFV65-6B	TGC68-1	ST68-1	ST68-2	TEL69-1
BA	493.10	472.00	242.10	390.50	467.70	301.10	257.40	673.10
CR	196.11	60.80	6.90	203.72	73.73	11.00	9.80	51.33
NI	24.40	10.70	6.70	26.80	16.70	9.40	5.80	18.75
RB	114.72	106.11	23.90	101.19	24.20	43.90	49.20	50.00
SR	212.04	312.42	443.36	199.55	449.09	532.20	413.59	516.75
V	646.90	107.00	0.0	322.90	152.60	0.0	0.0	0.0
Y	26.90	11.10	0.60	27.30	4.60	4.70	3.60	5.65
ZR	130.42	75.73	68.70	135.82	78.60	57.51	73.00	69.13

	TGB70-1	TGB72-1	TGB73-1	TGB75-1	BWWBM76-1	ST79-1	ENES80-1	SHEU82-1V
BA	688.20	735.95	500.80	386.60	97.10	40.70	45.70	496.60
CR	158.92	159.09	96.40	46.46	389.32	221.61	46.28	153.25
NI	12.70	15.90	15.60	11.50	28.90	24.90	15.80	13.00
RB	62.60	84.46	96.74	39.90	12.50	1.20	14.60	41.30
SR	700.95	596.87	557.67	437.87	106.34	284.88	163.65	610.04
V	300.00	459.75	596.40	186.10	1541.00	1007.00	162.60	353.00
Y	9.60	11.90	14.50	5.60	15.05	13.40	0.0	12.50
ZR	105.48	97.18	112.91	75.80	35.65	63.30	63.04	165.44

TABLE 16 -- VERMILION TRACE ELEMENT DATA

	SHEU82-1L	SHEU88-1	LLBN100-1	LLBM102-2	VGC105-1	VGC108-1	CKGB117-1	SSGB120-1
BA	563.10	344.70	29.80	77.30	480.60	232.30	311.20	414.40
CR	166.18	9.50	268.89	212.58	113.93	97.82	177.16	166.88
NI	15.40	7.30	34.50	28.50	10.40	10.40	13.20	12.80
RB	39.90	30.50	0.15	1.90	79.60	37.80	60.00	48.20
SR	592.69	413.19	215.51	135.15	382.71	381.43	343.78	709.94
V	906.00	0.0	1315.50	1499.00	107.30	0.0	266.10	106.10
Y	13.10	4.00	20.10	17.00	9.40	6.00	11.20	8.40
ZR	184.19	84.59	63.01	56.20	124.88	117.66	133.09	102.49

	CKGB122-1	CKGB125-1	LGGB128-1	IDGB135-1	TMV146-1	SFV151-1	SFV152-1	SFV155-1
BA	495.10	747.10	413.80	361.30	411.10	509.50	614.60	596.80
CR	96.40	195.57	164.58	81.35	736.26	8.30	11.70	198.41
NI	16.30	14.80	22.35	15.00	30.70	12.90	14.20	25.50
RB	98.06	93.83	54.55	48.70	38.80	45.90	60.90	121.52
SR	558.54	343.78	542.42	552.97	450.21	499.56	498.76	238.71
V	178.50	720.60	1091.15	452.00	868.80	0.0	0.0	484.00
Y	14.50	12.80	9.85	9.70	10.50	4.30	6.50	31.40
ZR	114.73	108.48	101.84	102.10	98.19	63.17	67.07	130.55

TABLE 16 -- VERMILION TRACE ELEMENT DATA

	ENEL160-1	ENEL163-1	SFVC177-1	SFV181-3	SFV183-1	TFV187-1	SXFV192-1	TFV195-1
BA	613.80	761.70	237.40	226.20	287.80	298.80	316.45	153.40
CR	141.56	46.28	17.65	198.94	285.01	13.20	164.94	7.40
NI	32.60	18.90	7.20	30.50	17.60	8.50	11.65	6.10
RB	26.20	39.70	22.35	26.20	38.20	93.21	33.05	16.30
SR	525.43	535.06	364.88	272.86	333.51	304.06	391.94	422.03
V	507.90	0.0	0.0	1012.00	309.80	0.0	232.15	24.80
Y	5.50	5.70	2.05	15.20	7.30	9.60	5.00	0.90
ZR	68.77	71.70	66.42	94.55	129.64	81.33	106.23	58.48

	TFV196-1	TFV196-2	TFV196-3	TFV197-1	TFV197-2	SEU200-1	TF204-2	SXF206-2
BA	225.60	336.10	374.50	656.00	327.35	48.00	242.65	319.50
CR	10.60	8.50	9.80	6.80	244.54	300.24	5.80	352.84
NI	6.10	7.60	8.15	11.70	33.95	26.80	8.30	29.30
RB	18.10	18.40	19.45	53.60	38.60	0.0	17.10	41.60
SR	428.72	454.19	456.26	523.36	245.36	144.23	486.82	293.48
V	0.0	0.0	0.0	0.0	1462.00	1647.00	425.70	811.60
Y	0.60	1.10	1.20	7.70	21.40	16.10	0.40	16.70
ZR	57.77	66.10	65.64	75.15	66.07	55.68	44.25	97.48

TABLE 16 -- VERMILION TRACE ELEMENT DATA

	SXF210-1	SXF211-1	TMV213-1	TES214-1	EMMV217-1	SFV219-3
BA	35.30	279.30	392.10	619.90	687.70	96.50
CR	1084.79	301.48	58.32	73.73	256.32	230.29
NI	42.10	17.50	8.30	12.20	35.50	32.60
RB	0.0	21.60	55.00	66.20	47.50	0.0
SR	82.30	668.23	857.68	412.64	496.54	247.07
V	1039.00	431.60	0.0	355.40	2228.00	1666.00
Y	9.80	6.30	5.70	6.10	10.90	20.40
ZR	24.60	92.14	85.95	64.34	89.86	46.80

APPENDIX D

SAMPLE LOCATIONS

The abbreviations NE, NW, SE, and SW used below refer to the NE 1/4, NW 1/4, SE 1/4, and SW 1/4, respectively. The number following the quarters is the section number; these are followed by the township and range of that section.

The codes for rock types are as follows:

AD	Andesite
BGW	Biotitic graywacke
BS	Basalt
CGL	Conglomerate
CGW	Chloritic graywacke
DP	Dacite porphyry or porphyritic dacite
RD	Rhyodacite or rhyodacite porphyry
SL	Slate
VC	Volcaniclastic rocks (graywacke/tuffs of the felsic volcaniclastic member

The codes for formations and members are as follows:

EG	Ely Greenstone, member unknown
ELG	Lower member of Ely Greenstone
EUG	Upper member of Ely Greenstone
FV	Felsic volcaniclastic member of Lake Vermilion Formation
GW	Graywacke member of Lake Vermilion Formation
KLG	Knife Lake Group
LVF	Lake Vermilion Formation
MV	Mixed volcaniclastic member of Lake Vermilion Formation
NL	Newton Lake Formation
SEG	Soudan iron-formation member of Ely Greenstone

"Geologic Quadrangle Designation" applies only to samples within the Tower Geologic Quadrangle Map (Ojakangas, et al., 1978), the Soudan Geologic Quadrangle Map (Sims, et al., 1980), the Lost Lake Miscellaneous Map (Ojakangas, et al., 1977), and the Gabbro Lake Geologic Quadrangle Map (Green, et al., 1966), and refers to the rock unit's designation on whichever is the appropriate geologic map. The initial letter (or two letters) of all sample numbers stands for the USGS 7.5-minute quadrangle in which the sampled outcrop is located, except in the cases of sample KH7-2 (Shagawa Lake Quad), sample SS29-1 (Tower Quad), sample VGC108-1 (Lost Lake quad), and sample SXF211-1

(Tower quad).

The codes for the quadrangles are as follows:

BWW	Biwabik Northwest
CK	Cook
EN	Eagles Nest
GL	Gabbro Lake (15-minute quad)
ID	Idington
LG	Linden Grove
LL	Lost Lake
S	Soudan
SH	Shagawa Lake
SS	Sassas Creek
ST	Soudan
SX	Sioux Pine Island
T	Tower
V	Vermilion Dam

Sample Locations

Sample no.	Rock Type	Formtn/ Member	Geol. Quad. Designation	Location
GL3-2	SL	KLG	kvf	NE NW NW 10, 63N, 10W
	Massive argillaceous metagraywacke-tuff			
KH7-2	DP	EUG		SE SW SW 4, 62N, 12W
	Dacite porphyry			Harry Homer's lumberyard, Shagawa L. Quad
SFV9-1	DP	FV(LVF)	Avp	SW SE SE 28, 62N, 15W
	Dacite porphyry			
SFV14-1	VC	FV(LVF)	Avbt	NE SE NW 13, 62N, 15W
	Massive metagraywacke-tuff			(see fig. 25)
GL16-1	BS	EG	egs	NW NE NE 11, 63N, 10W
	Massive, variolitic metabasalt			Entrance to Jasper L. resort
SFV16-1	VC	FV(LVF)	Avbt	NW SW NE 13, 62N, 15W
	Massive metagraywacke-tuff			(see fig. 25)
SFV17-1	DP	FV(LVF)	Avbt	NE SE SW 13, 62N, 15W
	Dacite porphyry			(see fig. 25)
GL18-1	RD	EG	rp	NW NE SW 21, 63N, 10W
	Rhyodacite porphyry			S. shore Greenstone L.
LLGB21-1	BGW	GW(LVF)	vgs	SW NE SE 12, 61N, 16W
	Massive biotitic graywacke			
LLGB23-1	BGW	GW(LVF)	vgs	SW SE SW 4, 61N, 16W
	Graded biotitic graywacke			

SS29-1	CGW	GW(LVF)	Wvgc	NE 29, 62N, 15W
Bedded chloritic graywacke				N. of McKinley Park dock area, Tower Quad
SFV34-1	VC	FV(LVF)	Avbt	NW SE SW 12, 62N, 15W
Massive metagraywacke-tuff				(see fig. 25)
LLGB37-1	BGW	GW(LVF)	vgs	SW SE SE 4, 61N, 16W
Massive biotitic graywacke				
LLF39-1	VC	FV(LVF)	vfv	NW NE SE 32, 62N, 16W
Massive volcanic sandstone				Otcp. near dirt rd. to Lost Lake
ST40-1	BS	FV(LVF)	Avb	SW NE SW 16, 62N, 14W
Pillowed metabasalt				N. side of Hwy. 169-1
				(see fig. 25)
ST41-1	DP	FV(LVF)	Avft	SW NE SW 16, 62N, 14W
Porphyritic dacite				(see fig. 25)
TF42-1	VC	FV(LVF)	Wvfs	SW SW NW 3, 61N, 16W
Conglomerate or breccia				On County Rd. 77
SFV44-1	VC	FV(LVF)	Avbt	NW SE NE 15, 62N, 15W
Massive metagraywacke-tuff				On Ely Island
SFV46-1	VC	FV(LVF)	Avbt	SE SW 11, 62N, 15W
Slate				S. shore, Birch Island
				(see fig. 25)
SFV48-2	VC	FV(LVF)	Avft	SE SE SE 11, 62N, 15W
Massive metagraywacke-tuff				S. shore, Dog Island
				(see fig. 25)
ST50-2	DP	SEG	Aesi	NW NW 20, 62N, 14W
Dacite porphyry dike intruding fefmn.				Long roadcut, Hwy. 169-1
TFS51-1	VC	FV(LVF)	Wvfu	SW SW SW 32, 62N, 14W
Coarse-grained, cobbly, agglomerate				(Entrance to Tower Marina)
TFS52-1,2,3	VC	FV(LVF)	Wvfs	SW NE 1, 61N, 16W
Massive volcanic sandstone				Roadcut on Hwy 169-1
TGB56-1	BGW	GW(LVF)	Wvgb	NE SE SE 3, 61N, 16W
Bedded biotitic graywacke				Roadcut on Hwy 169-1
TGB57-1	BGW	GW(LVF)	Wvgb	NE NW SW 10, 61N, 16W
Massive biotitic graywacke				Roadcut on Hwy 169-1
TGB59-1	BGW	GW(LVF)	Wvgb	SW NW NW 15, 61N, 16W
Massive biotitic graywacke				Roadcut on Hwy 169-1
ST60-1	VC/BS	FV(LVF)	Avb	NW SE SW 18, 62N, 14W
Mafic tuff or basalt				Small otcp on dirt road

to Pavlich's cabin
(see fig. 25)

SFV65-3, 4, 5, 6 VC FV(LVF) Avbt NW NE SW 12, 62N, 15W (see fig. 25 and Table 10)
Interbedded metagraywacke-tuff and slate

ST68-1,2 VC FV(LVF) Wvfa SE NW SW 21, 62N, 15W
1:agglomerate clast 2:agglomerate matrix Swedetown Bay agglomerates

TGC68-1 CGW GW(LVF) Wvgs SE SW 19, 62N, 15W
Massive chloritic volcanic sandstone Keith Causin's place, Echo Pt.

TEL69-1 DP ELG Wel SW SW NE 5, 61N, 15W
Dacite porphyry Otcp along Hwy 135

TGB70-1 BGW GW(LVF) Wvgb On sectn. line, 1/4 mi. E
Massive biotitic graywacke of W. edge of 7, 61N, 15W

TGB72-1 BGW GW(LVF) Wvgb On sectn. line, 1/5 mi. E
Massive biotitic graywacke of W. edge of 13, 62N, 16W

TGB73-1 BGW GW(LVF) Wvgb NE corner 23, 62N, 16W on
Massive biotitic graywacke Co. Rd. 411

TGB75-1 BGW GW(LVF) Wvgb Jct. Co. Rds. 411 & 409,
Massive biotitic graywacke center of 23, 62N, 16W

BWWBM76-1 BS GW(LVF) SW NW 29, 61N, 16W
Sheared metabasalt End of Co. Rd. 367

ST79-1 VC FV(LVF) Avbt SW SE SW 12, 62N, 15W
Coarse clastic tuff/conglomerate Near USCGS marker between sections 12 and 13 (see fig. 25)

ENES80-1 DP SEG SW SW NE 14, 62N, 14W
Dacite porphyry dike

SHEU82-1 AD EUG Wqp NW NE SW 32, 63N, 12W
Andesite dike Power pole debris near 169-1

SHEU88-1 DP EUG SE SW SW 4, 62N, 12W
Dacite porphyry (Harry Homer's Lumberyard)

LLBM100-1 BS GW(LVF) vmb SW NW NW 9, 62N, 16W
Massive diabasic metabasalt

LLBM102-2 BS GW(LVF) vmb NE NE NE 9, 62N, 16W
Massive diabasic metabasalt

VGC105-1 CGW GW(LVF) SE SW 33, 63N, 16W
Massive, fine-grained chloritic graywacke (power pole debris)

VGC108-1	CGW	GW(LVF)	vgs	NE NE NE 12, 62N, 17W
Fine-grained chloritic graywacke				Lost Lake quad
CKGB117-1	BGW	GW(LVF)		SW SW SE 11, 62N, 19W
Bedded biotitic graywacke				
SSGB120-1	BGW	GW(LVF)		SE SW SE 8, 61N, 17W
Massive biotitic graywacke				
CKGB122-1	BGW	GW(LVF)		SW SE SW 9, 61N, 18W
Bedded metagraywacke				
CKGB125-1	BGW	GW(LVF)		NE SW NE 7, 61N, 18W
Bedded biotitic graywacke				
LGGB128-1	BGW	GW(LVF)		SE NE NW 20, 61N, 19W
Massive biotitic graywacke				
IDGB135-1	BGW	GW(LVF)		SE SW SW 20, 61N, 18W
Massive biotitic graywacke				
TMV146-1	BS	MV(LVF)	Wvm	NE NW SW 20, 61N, 15W
Massive metabasalt				
SFV151-1	DP	FV(LVF)	Aeup	SE SE SW 8, 62N, 14W
Massive dacite porphyry				On logging rd to LaRue Mine (see fig. 25)
SFV152-1	VC	FV(LVF)	Avbt	NW NW NE 17, 62N, 14W
Massive metagraywacke-tuff				On logging rd to LaRue Mine (see fig. 25)
SFV155-1	VC	FV(LVF)	Avbt	NE NW NW 16, 62N, 14W
Massive graywacke-tuff/slate				S. of logging rd to LaRue Mine (see fig. 25)
ENEL160-1	DP	ELG		SE NE NE 28, 62N, 14W
Dacite porphyry dike intruding fefmn				Railroad cut
ENEL163-1	DP	ELG		SW SW SE 22, 62N, 14W
Dacite porphyry dike intruding fefmn				Railroad cut
SFVC177-1	CGL	FV(LVF)	Avc	SW SE NW 22, 62N, 15W
"Stuntz Bay" conglomerate				
SFV181-3	VC	FV(LVF)	Avbt	SE SW 11, 62N, 15W
Massive metagraywacke-tuff				
SFV183-1	VC	FV(LVF)	Avbt	SW NE 11, 62N, 15W
Slate				(see fig. 25)
TFV187-1	VC	FV(LVF)	Wvft	SE NE NW 16, 62N, 15W
Massive metagraywacke-tuff				

SXFV192-1 CGW GW(LVF) SE SW 5, 62N, 15W
Slate

TFV197-1,2 GW GW(LVF) Wvgc SW SW SW 21, 62N, 15W
1:Volcanic sandstone 2:Volcanic sandstone

SEU200-1 BS EUG Aeub SE NW NW 11, 62N, 15W
Sheared basalt

TF204-2 VC FV(LVF) Wvfs NE SW SW 3, 61N, 16W
Volcanic sandstone/conglomerate

SXF206-2 CGW GW(LVF) NE SE SW 6, 62N, 15W
Chloritic graywacke

SXF210-1 BS NL NW NW SW 34, 63N, 16W
Massive metabasalt

SXF211-1 CGW GW(LVF) Wvgs NW SW SE 12, 62N, 16W
Chloritic graywacke Small is. off Comet Is., Tower quad.

TES214-1 DP FV(LVF) Wvfu NW NE NW 4, 61N, 15W
Dacite porphyry North American mine tailings

SFV219-3 BS FV(LVF) Avft NE NE NW 24, 62N, 15W
Massive, sheared basalt (see fig. 25)

BIBLIOGRAPHY

Abbey, S., 1980, Studies in "standard samples" for use in the general analysis of silicate rocks and minerals, Part 6: 1979 Edition of "Usable" Values: U. S. Geological Survey Paper 80-14.

Arth, J. G., and Hanson, G. N., 1972, Quartz diorites derived by partial melting of eclogite or amphibolite at mantle depths: Contributions to Mineralogy and Petrology v. 37, p. 161-174.

Arth, J. G., and Hanson, G. N., 1975, Geochemistry and origin of the early Precambrian crust of northeastern Minnesota: Geochimica Cosmochimica ACTA v. 39, p. 325-362.

Aumento, F., Mitchell, W. S., and Fratta, M., 1976, Interaction between seawater and oceanic layer two as a function of time and depth -- I. Field evidence: Canadian Mineralogist v. 14, p. 269-290.

Ayres, L. D., 1983, Bimodal volcanism in Archean greenstone belts exemplified by greywacke composition, Lake Superior Park, Ontario: Canadian Journal of Earth Sciences v. 20, p. 1168-1194.

Baker, P. E., 1968, Petrology of Mt. Misery volcano, St. Kitts, West Indies: Lithos v. 1, p. 124-150.

Baragar, W. R. A., Plant, A. G., Pringle, G. J., and Schau, Mikkel, 1979, Diagenetic and postdiagenetic changes in the composition of an Archean pillow: Canadian Journal of Earth Sciences v. 16, p. 2102-2121.

Barker, F., Millard, H. T., Jr., and Knight, R. J., 1979, Reconnaissance geochemistry of Devonian island arc volcanic intrusive rocks, West Shasta District, California, in: Barker, F., ed., Trondhjemites, Dacites, and Related Rocks, Developments in Petrology 6, Amsterdam, Elsevier, p. 517-530.

Battey, M. H., 1955, Alkali metasomatism and the petrology of some keratophyres: Geological Magazine v. 92, p. 104-126.

Bauer, R. L., 1985, Correlation of early recumbent and younger upright folding across the boundary between an Archean gneiss belt and greenstone terrane, northeastern Minnesota: Geology v. 13, p. 57-660.

Beccaluva, L., Ohnenstetter, D., and Ohnenstetter, O., 1979, Geochemical discrimination between ocean-floor and island arc tholeiites: Canadian Journal of Earth Sciences v. 16, p. 1874-1882.

Bell, R. T., and Jolly, W. T., 1975, Archean graywackes: petrology and lithogenesis: Geotraverse Workshop 1975, Precambrian Research Group, University of Toronto, p. 186-195.

Beswick, A. E., and Soucie, G., 1978, A correction procedure for metasomatism in an Archean greenstone belt: Precambrian Research v. 6, p. 235-248.

Bickford, M. E., and Boardman, S. J., 1984, A Proterozoic volcano-plutonic terrane, Gunnison and Salida areas, Colorado: Journal of Geology v. 92, p. 657-666.

Bloxam, J. W., and Lewis, A. D., 1972, Ti, Zr and Cr in some British pillow lavas and their petrogenetic affinities: Nature Phys. Sci., v. 237, p. 134-136.

Brouwer, H. A., 1942, Geological expedition of the University of Amsterdam to the Lesser Sunda Islands in the south eastern part of the Netherlands East Indies 1937, part IV, Amsterdam, 237 p.

Brown, G. M., Holland, J. G., Sigurdsson, H., Tomblin, J. F., and Arculus, R. J., 1977, Geochemistry of the Lesser Antilles volcanic island arc: Geochimica Cosmochimica ACTA v. 41, p. 785-801.

Cann, J. R., 1970, Rb, Sr, Y, Zr, and Nb in some ocean floor basaltic rocks: Earth and Planetary Science Letters v. 10, p. 7-11.

Chow, T. J., Stern, R. J., and Dixon, T. H., 1980, Absolute and relative abundances of K, Rb, Sr, and Ba in circumPacific island arc magmas, with special reference to the Marianas: Chemical Geology v. 28, p. 111-121.

Coleman, R. G., and Donato, M. M., 1979, Oceanic plagiogranite revisited, in Barker, R. ed., Trondhjemites, Dacites, and Related Rocks, Developments in Petrology 6, Elsevier, Holland, p. 149-168.

Condie, K. C., 1980, Origin and early development of the earth's crust: Precambrian Research v. 11, p. 183-197.

Condie, K. C., Macke, S. E., and Reimer, T. O., 1970, Petrology and geochemistry of Early Precambrian greywackes from the Fig Tree Group, South Africa: Geological Society of America Bulletin, v. 81, p. 2759-2776.

Condie, K. C., and Moore, J. M., 1977, Geochemistry of Proterozoic volcanic rocks from the Grenville Province, eastern Ontario, in Geological Association of Canada Special Paper No. 16, p. 147-168.

Condie, K. C., and Shadel, C. A., 1984, An Early Proterozoic volcanic arc succession in southeastern Wyoming: Canadian Journal of Earth Sciences v. 21, p. 415-427.

Cordani, U. G., and Sato, K., 1985, The geologic evolution of the ancient granite-greenstone terrane of central-southern Bahia,

Brazil: Precambrian Research v. 27, p. 187-213.

Coulon, C., Dostal, J. and Dupuy, C., 1978, Petrology and geochemistry of the ignimbrites and associated lava domes from northwestern Sardinia: Contributions to Mineralogy and Petrology v. 68, p. 89-98.

Criss, J. W., Birks, L. S., and Gilfrich, J. V., 1978, A versatile X-Ray analysis program combining fundamental parameters and empirical coefficients: Analytical Chemistry v 50, p. 33.

Csejtey, B., Jr., Cox, Dennis P., and Everits, Russel C., 1982: The Cenozoic Denali Fault System and the Cretaceous accretionary development of Southern Alaska: Journal of Geophysical Research v. 87, p. 3741-3754.

Davies, J. R., Grant, R. W. E., and Whitehead, R. E. S., 1979, Immobile trace elements and Archean volcanic stratigraphy in the Timmins mining area, Ontario: Canadian Journal of Earth Sciences v. 16, p. 305-311.

Deer, W. A., Howie, R. A., and Zussman, J., 1978, An Introduction to the Rock-Forming Minerals: Halsted Press, U. S. A., 528 p.

Dimroth, Erich, and Lichtblau, Andreas P., 1979, Metamorphic evolution of Archean hyaloclastites, Noranda area, Quebec, Canada. Part I: Comparison of Archean and Cenozoic sea-floor metamorphism: Canadian Journal of Earth Sciences v. 16, p. 1315-1340.

Dixon, T. H., and Batiza, R., 1979, Petrology and chemistry of Recent lavas in the Northern Marianas: Implications for the origin of island arc basalts: Contributions to Mineralogy and Petrology v. 70, p. 167-181.

Donnelly, T. W. and Rogers, J. J. W., 1980, Igneous series in island arcs: the northeastern Caribbean compared with world wide island arc assemblages: Bulletin of Volcanology v. 43, p. 347-382.

Donnelly, T. W., Rogers, J. J. W., Pushkar, P., and Armstrong, R. L., 1971, Chemical evolution of the igneous rocks of the eastern West Indies: An investigation of Thorium, Uranium, and Potassium distributions, and Lead and Strontium isotopic ratios: Geological Society of America Memoir no. 130, p. 181-224.

Dostal, J., and Strong, D. F., 1983, Trace-element mobility during low-grade metamorphism and silicification of basaltic rocks from St. John, New Brunswick: Canadian Journal of Earth Sciences v. 20, p. 431-435.

Ewart, A., 1979, A review of the mineralogy and chemicstry of Tertiary-Recent dacitic, latitic, rhyolitic, and related salic volcanic rocks, in: Barker, F., ed., Trondhjemites, Dacites, and Related Rocks, Developments in Petrology 6, Amsterdam, Elsevier, p. 13-121.

Ewart, A., Bryan, W. B., and Gill, J. B., 1973, Mineralogy and geochemistry of the younger volcanic islands of Tonga, Southwestern Pacific: J. Petrol. v. 14, p. 429-465.

Fahrig, W. F., and Eade, K. E., 1968, The chemical evolution of the Canadian Shield: Canadian Journal of Earth Sciences v. 5, p. 1247-1252.

Feirn, W. C., 1977, The geology of the early Precambrian rocks of the Jasper Lake area, Cook County, northeastern Minnesota: unpublished Master's thesis, Univ. of Minnesota, Duluth, 146 p.

Flood, T. P., 1981, Geology of the Cypress, Hanson, and South Arm of Knife Lake area, Boundary Waters Canoe Area, eastern Vermilion District, northeastern Minnesota: unpublished Master's thesis, Univ. of Minnesota, Duluth, 142 p.

Floyd, P. A., and Winchester, S. A., 1975, Magma type and tectonic setting discrimination using immobile elements: Earth and Planetary Science Letters v. 27, p. 211-218

Frey, F. A., Haskin, M. A., Poetz, J. A., and Haskin, L. A., 1968, RE abundances in some basic rocks: Journal of Geophysical Research v. 73, p. 6085-6098.

Garcia, M. O., 1978, Criteria for identification of ancient volcanic arcs: E. Sci. Rev. v. 14, p. 147-165.

Gelinas, L., Brooks, C., Perrault, G., Carignan, J., Trudel, P., and Grasso, F., 1977, Chemo-stratigraphic divisions within the Abitibi volcano belt, Rouyn-Noranda district, Quebec: in Geological Association of Canada Special Paper no. 16, p. 265-295.

Gelinas, L., Mellinger, M., and Trudel, P., 1982, Archean mafic metavolcanics from the Rouyn-Noranda district, Abitibi Greenstone Belt, Quebec. I. Mobility of major elements: Canadian Journal of Earth Sciences v. 19, p. 2258-2275.

Gill, J. B., 1970, Geochemistry of Viti Levu, Fiji, and its evolution as an island arc: Contributions to Mineralogy and Petrology v. 27, p. 179-203.

Gill, J. B., 1981, Orogenic andesites and Plate Tectonics, Minerals and Rocks series no. 16, Springer-Verlag, Berlin, 390 p.

Goldich, S. S., 1972, Geochronology in Minnesota, in: Sims, P. K., and Morey, G. B., eds., Geology of Minnesota: A Centennial Volume, Minnesota Geological Survey, St. Paul, Minnesota, p. 27-37.

Goldich, S. S., Hanson, B. N., Hallford, C. R., and Mudrey, M. G., Jr., 1972, Early Precambrian rocks in the Saganaga Lake - Northern Light Lake area, Minnesota-Ontario, Part I. Petrology and Structure, in: Geological Society of America Memoir no. 135, Gruner Volume, p. 151-178.

Goodwin, A. E. M., 1977, Archean Volcanism in Superior Province, Canadian Shield, in: Geological Association of Canada Special Paper No. 16, p. 205-241.

Green, J. C., Phinney, W. C., and P. W. Weiblen, 1966, Gabbro Lake Quadrangle, Lake County, Minnesota: scale 1:31680, Minnesota Geological Survey Misc. Map Series Map M-2.

Green, J. C., 1970, Lower Precambrian rocks of the Gabbro Lake Quadrangle, northeastern Minnesota: Minnesota Geological Survey Special Publication SP-13, 96 p.

Grescens, R., 1967, Composition-volume relationships of metasomatism: Chemical Geology v. 2, p. 7-65.

Griffin, W. L., and Morey, G. B., 1969, Geology of the Isaac Lake Quadrangle, St. Louis County, Minnesota: Minnesota Geological Survey Special Publication SP-8, 57 p.

Grout, F. F., 1926, The geology and magnetite deposits of northern St. Louis County, Minnesota: Minnesota Geological Survey Bulletin 21, 220 p.

Grout, F. F., 1933, Contact metamorphism of the slates of Minnesota by granite and by gabbro magmas: Geological Society of America Bulletin v. 44, p. 989-1040.

Gruner, J. W., 1941, Structural geology of the Knife Lake area of Northeastern Minnesota: Geological Society of America Bulletin v. 52, p. 1576-1642.

Gunn, B. M., and Roobol, M. J., 1976, Metasomatic alteration of the predominantly island arc igneous suite of the Limestone Caribbees (East Caribbean): Geologisches Rundschau v. 65, p. 1078-1108.

Hanson, G. N., and Goldich, S. S., 1972, Early Precambrian rocks in the Saganaga Lake-Northern Light Lake area, Minnesota-Ontario Part II: Petrogenesis: Geological Society of America Memoir no. 135, p. 179-192.

Hargraves, R. B., 1981, Precambrian tectonic style: a liberal uniformitarian interpretation, in: Kroner, A., ed., Precambrian Plate Tectonics, Elsevier, Amsterdam, p. 21-56.

Hart, S. R., 1969, K, Rb, Cs contents and K/Rb, K/Cs ratios of fresh and altered submarine basalts: Earth and Planetary Science Letters v. 6, p. 295-303.

Hart, R., 1970, Chemical exchange between seawater and deep ocean basalts: Earth and Planetary Science Letters v. 9, p. 269-279.

Hart, S. R., Erlank, A. J., and Kable, E. J. D., 1974, Sea floor basalt alteration: some chemical and Sr isotopic effects: Contributions to Mineralogy and Petrology v. 44, p. 219-230.

Hart, S. R., and Nalwalk, A. J., 1970, K, Rb, Cs and Sr relationships in submarine basalts from the Puerto Rico trench; Geochimica Cosmochimica ACTA v. 34, p. 145-155.

Hellman, P. L., Smith, R. E., and Anderson, P., 1977, Rare earth element investigation of the Cliefden Outcrop, N. S. W., Australia: Contributions to Mineralogy and Petrology v. 65, p. 155-164.

Hellman, P. L., Smith, R. E., and Anderson, P., 1979, The mobility of rare earth elements: Evidence and implications from selected terrains affected by burial metamorphism: Contributions to Mineralogy and Petrology v. 71, p. 23-44.

Henderson, J. B., 1972, Sedimentology of Archean turbidites at Yellowknife, Northwest Territories: Canadian Journal of Earth Sciences v. 9, p. 882-902.

Holm, P. E., 1982, Non-recognition of continental tholeiites using the Ti-Y-Zr diagram: Contributions to Mineralogy and Petrology v. 79, p. 308-310.

Hooper, P. R., and Ojakangas, R. W., 1971, Multiple deformation in Archean rocks of the Vermilion district, northeastern Minnesota: Canadian Journal of Earth Sciences v. 8, p. 423-434.

Hudleston, P. J., 1976, Early deformational history of Archean rocks in the Vermilion District, northeastern Minnesota: Canadian Journal of Earth Sciences v. 13, p. 579-592.

Hughes, C. J., 1972, Spilites, keratophyres, and the igneous spectrum: Geological Magazine v. 109, p. 513-527.

Humphris, Susan E., and Thompson, Geoffrey, 1978, Hydrothermal alteration of oceanic basalts by seawater: Geochimica Cosmochimica ACTA v. 42, p. 107-125.

Humphris, Susan E., and Thompson, Geoffrey, 1978b, Trace element mobility during hydrothermal alteration of oceanic basalts: Geochimica Cosmochimica ACTA v. 42, p. 127-136.

Irvine, T. N., and Baragar, W. R. A., 1971, A guide to the chemical classification of the common volcanic rocks: Canadian Journal of Earth Sciences v. 8, p. 523-548.

Jahn, B., 1972, Trace element and Sr isotope studies of the lower Precambrian rocks from the Vermilion district, northeastern Minnesota: unpublished Ph. D. Disseration, University of Minnesota, 132 p.

Jahn, B., and Murthy, V. R., 1975, Rb-Sr ages of the Archean rocks of the Vermilion district, northeastern Minnesota: Geochimica Cosmochimica ACTA v. 39, p. 1679-1689.

Jahn, B., Shih, C., and Murthy, V. R., 1974, Trace element geochemistry

of Archean volcanic rocks: Geochimica Cosmochimica ACTA v. 38, p. 611-627.

Jakes, P., and Gill, J. B., 1970, Rare earth elements and the island arc tholeitic series: Earth and Planetary Science Letters v. 9, p. 17-28.

Jakes, P., and Smith, I. E., 1970, High-K Calc-alkaline rocks from Cape Nelson, eastern Papua: Contributions to Mineralogy and Petrology v. 28, p. 259-271.

Jakes, P., and White, A. J. R., 1972, Major and trace element abundances in rocks of orogenic areas: Geological Society of America Bulletin v. 83, p. 29-40.

Jensen, L. S., 1976, A new cation plot for classifying subalkalic volcanic rocks: Ontario Division of Mines Miscellaneous Paper no. 66, 22 p.

Jolly, W. T., 1970, Zeolite and prehnite-pumpellyite facies in south Puerto Rico: Contributions to Mineralogy and Petrology v. 27, p. 204-224.

Kay, R. W., Hubbard, N. J., and Gast, P. W., 1970, Chemical characteristics and origins of oceanic ridge volcanic rocks: Journal of Geophysical Research v. 75, p. 1585-1613.

Korringa, M. K., and Noble, D. C., 1971, Distribution of Sr and Ba between natural feldspar and igneous melt: Earth and Planetary Science Letters v. 11, p. 147-151.

Kroner, A., 1981, Precambrian plate tectonics, in: Kroner, A., ed., Precambrian Plate Tectonics, Elsevier, Amsterdam, p. 57-90.

Kroner, A., 1985, Ophiolites and the evolution of tectonic boundries in the late Proterozoic Arabian-Nubian Shield of northeast Africa and Arabia: Precambrian Research v. 27, p. 277-300.

Lambert, R. St. J., and Holland, J. G., 1974, Yttrium geochemistry applied to petrogenesis utilizing calcium-yttrium relationships in minerals and rocks: Geochimica Cosmochimica ACTA v. 38, p. 1393-1414.

Lambert, R. St. J., Holland, J. G., and Owen, P. F., 1974, Chemical petrology of a suite of calc - alkaline lavas from Mount Ararat, Turkey: Journal of Geology v. 82, p. 419-438.

Langford, F. F., and Morin, J. A., 1976, The development of the Superior Province of northwestern Ontario by merging island arcs: American Journal of Science v. 276, p. 1023-1034.

LeFevre, C., Dupuy, C., and Coulon, C., 1974, Le volcanisme Andesitique: Revue de la Haute-Auvergne, v. 44, Imprimeur Gerbert 15000, Aurillac, France, p. 313-355.

Lowe, D. R., Byerty, G. R., Ransom, B. L., and Nocita, B. W., 1985, Stratigraphic and sedimentological evidence bearing on structural repetition in early Archean rocks of the Barberton Greenstone Belt, South Africa: Precambrian Research v. 27, p. 165-186.

Ludden, J., Gelinas, L., and Trudel, P., 1982, Archean metavolcanics from the Rouyn - Noranda district, Abitibi Greenstone Belt, Quebec. 2. Mobility of trace elements and petrogenetic constraints: Canadian Journal of Earth Sciences v. 19, p. 2276-2287.

MacKenzie, D. E., and Chappell, B. W., 1972, Shoshonitic and calc - alkaline lavas from the highlands of Papua New Guinea: Contributions to Mineralogy and Petrology v. 35, p. 50-62.

Masuda, Y., Nishimura, S., Ikeda, T., and Katsui, Y., 1975, Rare-earth and trace elements in the Quaternary rocks of Hokkaido, Japan: Chemical Geology v. 15, p. 251-271.

McLennan, S. M., Taylor, S. R., and Eriksson, K. A., 1983a, Geochemistry of Archean shales from the Pilbara Supergroup, Western Australia: Geochimica Cosmochimica ACTA v. 47, p. 1211-1222.

McLennan, S. M., Taylor, S. R., and Kroner, A., 1983b, Geochemistry and evolution of Archean shales from South Africa. I. The Swaziland and Pongola Supergroups: Precambrian Research v. 2, p. :93-124.

McLimans, R. K., 1972, Granite-bearing conglomerates of the Lower Precambrian in the Vermilion District, northeastern Minnesota: unpublished Master's thesis, Univ. of Minnesota, Duluth, 130 p.

Melson, W. G., 1973, Basaltic glasses from the Deep Sea Drilling Project: chemical characteristics, compositions of alteration products, and fission track "ages": EOS Transactions, AGU v. 54, p. 1011-1014.

Mertzman, S. A., 1984, Initial chemical and Nd and Sr isotopic results from the Mount Shasta region of northern California: Eos, v. 65, p. 299.

Mitchell, A. H. G., and Reading, H. G., 1971, Evolution of island arcs: Journal of Geology v. 79, p. 253-284.

Miyashiro, A., and Shido, F., 1975, Tholeiitic and calc - alkalic series in relation to the behaviors of titanium, chromium, and nickel: American Jouurnal of Science v. 275, p. 267-277.

Miyashiro, A., Shido, F., and Ewing, M., 1969, Diversity and origin of abyssal tholeiite from the Mid - Atlantic Ridge near 24* and 30* N latitude: Contributions to Mineralogy and Petrology v. 23, p. 38-52.

Morey, G. B., Green, J. C., Ojakangas, R. W., and Sims, P. K., 1970, Stratigraphy of the Lower Precambrian rocks in the Vermilion

district, northeastern Minnesota: Minnesota Geological Survey Reports of Investigations 14, 33 p.

Morrison, M. A., 1978, The use of "immobile" trace elements to distinguish the paleotectonic affinities of metabasalts; applications to the Paleocene basalts of Mull and Skye, northwest Scotland: Earth and Planetary Science Letters v. 39, p. 407-416.

Mottl, M. J., 1983, Metabasalts, axial hot springs, and the structure of hydrothermal systems at mid - ocean ridges: Geological Society of America Bulletin v. 94, p. 161-180.

Mueller, P. A., 1970, TiO2 and K - Ar age: A covariation in the mafic rocks of the southern Beartooth Mountains of Montana and Wyoming: Earth and Planetary Science Letters v. 9, p. 427-430.

Naqvi, S. M., Condie, K. C., and Allen, P., 1983, Geochemistry of some unusual Early Archean sediments from Dharwar Craton, India: Precambrian Research v. 22, p. 125-147.

Nicholls, G. D., and Islam, M. R., 1971, Geochemical investigations of basalts and associated rocks from the ocean floor and their implications: Philosophical Transactions of the Royal Society of London A v. 268, p. 469-486.

Nicholls, I. A., and Whitford, D. A., 1976, Primary magmas associated with Quaternary volcanism in the western Sunda Arc, Indonesia, in: Johnson, R. W., ed., Volcanism in Australasia, Elsevier, p. 77-90.

Nokleberg, W. A., 1983, Wall rocks of the Central Sierra Nevada Batholith, California: A collage of accreted tectono-stratigraphic terranes: USGS Prof. Pap. 1255, 28 p.

Nur, A., and Ben - Avraham, A., 1982, Oceanic plateaus, the fragmentation of continents, and mountain building: Journal of Geophysical Research v. 87, p. 3644-3662.

Ojakangas, R. W., 1972a, Archean volcanogenic graywackes of the Vermilion district, northeastern Minnesota: Geological Society of America Bulletin v. 83, p. 429-442.

Ojakangas, R. W., 1972b, Graywackes and related rocks of the Knife Lake Group and the Lake Vermilion Formation, Vermilion district, in: Sims, P. K., and Morey, G. B., eds., Geology of Minnesota: A Centennial Volume: Minnesota Geological Survey, p. 82-90.

Ojakangas, R. W., 1985, Review of Archean clastic sedimentation, Canadian Shield: Major felsic volcanic contributions to turbidite and alluvial fan-fluvial facies associations, in: Ayres, L. D., Thurston, P. C., Card, K. D., and Weber, W., eds., Evolution of Archean Supracrustal Sequences, Geological Association of Canada Special Paper no. 28, p. 23-47.

Ojakangas, R. W., and Sims, P. K., 1977, Geologic Map of Lost Lake

Quadrangle, St. Louis County, Minnesota: scale 1:24000, Minnesota Geological Survey Miscellaneous Map M-17.

Ojakangas, R. W., Sims, P. K., and Hooper, P. R., 1978, Geologic Map of the Tower Quadrangle, St. Louis County, Minnesota: scale 1:24000, Minnesota Geological Survey Geologic Quadrangle Map GQ-1457.

Ondrick, C. W., and Griffiths, J. C., 1969, Frequency distribution of elements in Rensselaer graywacke, Troy, New York: Geological Society of America Bulletin v. 80, p. 509-518.

Payne, J. G., and Strong, D. F., 1979, Origin of the Twillingate Trondhjemite, north - central Newfoundland: Partial melting in the roots of an island arc, in: Barker, F., ed., Trondhjemites, Dacites, and Related Rocks, Developments in Petrology 6, Amsterdam, Elsevier, p. 465-488.

Pearce, J. A., 1975, Basalt geochemistry used to investigate past tectonic environments on Cyprus: Tectonophys. v. 25, p. 41-67.

Pearce, J. A., and Cann, J. R., 1973, Tectonic setting of basic volcanic rocks determined using trace element analysis: Earth and Planetary Science Letters v. 19, p. 290-300.

Pearce, J. A., and Norry, M. J., 1979, Petrogenetic implications of Ti, Zr, Y and Nb variations in volcanic rocks: Contributions to Mineralogy and Petrology v. 69, p. 33-47.

Pettijohn, F. J., 1963, Data of geochemistry: Chapter S., Chemical composition of sandstones - excluding carbonate and volcanic sands: USGS Prof. Pap. 440-S, 19 p.

Renmin, W., Shuyan, H., Zhenzhen, C., Pingfan, L., and Fengyan, D., 1985, Geochemical evolution and metamorphic development of the Early Precambrian in eastern Hebei, China: Precambrian Research v. 27, p. 111-129.

Rogers, J. J. W., and McKay, S. M., 1972, Chemical evolution of geosynclinal material, in: Studies in Mineralogy and Precambrian Geology, J. W. Gruner Volume, Geological Society of America Memoir no. 135, p. 3-28.

Rogers, J. J. W., Suayah, I. B., and Edwards, J. M., 1985, Trace elements in continental - margin magmatism: Part IV. Geochemical criteria for recognition of two volcanic assemblies near Auburn, Western Sierra Nevadas, California: Geological Society of America Bulletin v. 95, p. 1437-1445.

Schermer, E. R., Howell, D. G., and Jones, D. L., 1984, The origin of allochthonous terranes: Perspectives on the growth and shaping of continents: Annual Reviews of Earth and Planetary Sciences v. 12, p. 107-131.

Schulz, K. J., 1977, The petrology and geochemistry of Archean

volcanics, west Vermilion district, northeastern Minnesota: unpub. Ph. D. Thesis, University of Minnesota, 349 p.

Schulz, K. J., 1980, The magmatic evolution of the Vermilion greenstone belt, northeastern Minnesota: Precambrian Research v. 11, p. 215-245.

Seiders, V. M., 1978, A chemically bimodal, calc-alkaline suite of volcanic rocks, Carolina Volcanic Slate Belt, central North Carolina: Southeastern Geology v. 19, p. 241-265.

Siegers, A., Pichler, H., and Zeil, W., 1969, Trace element abundances in the 'Andesite' formation of Northern Chile: Geochimica Cosmochimica ACTA v. 33, p. 882-887.

Sims, P. K., 1972a, Vermilion district and adjacent areas, in: Sims, P. K., and Morey, G. B., eds., Geology of Minnesota: A Centennial Volume, Minnesota Geological Survey, St. Paul, Minnesota, p. 49-62.

Sims, P. K., 1972b, Metavolcanic and associated synvolcanic rocks in the Vermilion district, in: Sims, P. K., and Morey, G. B., eds., Geology of Minnesota: A Centennial Volume, Minnesota Geological Survey, St. Paul, Minnesota, p. 63-75.

Sims, P. K., 1973, Geological Map of the western part of the Vermilion district, northeastern Minnesota: Minnesota Geological Survey Misc. Map Ser. Map M - 13, scale 1:48,000.

Sims, P. K., 1976, Early Precambrian tectonic - igneous evolution in the Vermilion district, northeastern Minnesota: Geological Society of America Bulletin v. 87, p. 379-389.

Sims, P. K., and Morey, G. B., eds., 1972, Geology of Minnesota: A Centennial Volume, Minnesota Geological Survey, St. Paul, Minnesota, 510 p.

Sims, P. K., and Southwick, D. L., 1980, Geologic Map of the Soudan Quadrangle, St. Louis County, Minnesota: scale 1:24000, Minnesota Geological Survey Geologic Quadrangle Map GQ-1540.

Smith, R. E., and Smith, S. E., 1976, Comments on the use of Ti, Zr, Y, Sr, K, P and Nb in classification of basaltic magmas: Earth and Planetary Science Letters v. 32, p. 114-120.

Stern, R. J., 1981, Petrogenesis and tectonic setting of Late Precambrian ensimatic volcanic rocks, Central Eastern Desert of Egypt: Precambrian Research v. 16, p. 195-230.

Stone, D. B., Panuska, B. C., and Packer, D. R., 1982, Paleolatitudes versus time for southern Alaska: Journal of Geophysical Research v. 87, p. 3697-3707.

Strong, D. F., 1977, Volcanic regimes of the Newfoundland Appalachians:

in Baragar W. R. A., Coleman, L. C., and Hall, J. M., eds., Volcanic Regimes in Canada, Geological Association of Canada Special Paper no. 16, p. 61-90.

Strong, D. F., Dickson, W. L., and Pickerill, R. K., 1979, Chemistry and prehnite-pumpellyite facies metamorphism of calc-alkaline carboniferous volcanic rocks of southeastern New Brunswick: Canadian Journal of Earth Sciences v. 16, p. 1071-1085.

Thompson, G., 1973, A geochemical study of low-temperature interaction of seawater and oceanic igneous rock: EOS Transactions , AGU v. 54, p. 1015-1019.

Turner, C. C., and Walker, R. G., 1973, Sedimentology, stratigraphy, and crustal evolution of the Archean greenstone belt near Sioux Lookout, Ontario: Canadian Journal of Earth Sciences v. 10, p. 817-845.

Vinje, S. P., 1978, Archean geology of an area between Knife Lake and Kekekabic Lake, eastern Vermilion District, northeastern Minnesota: unpublished Master's thesis, Univ. of Minnesota, Duluth, 176 p.

Walker, R. G., 1984, Facies models 2nd Ed., Turbidites and associated coarser clastic deposits: Geoscience Canada, Reprint Series 1, p. 171-188.

White, C. M., and McBirney, A. R., 1977, Some quantitative aspects of orogenic volcanism in the Oregon Cascades: Geological Society of America Memoir no. 152, p. 369-388.

Whitehead, R. E. S., and Goodfellow, W. D., 1978, Geochemistry of volcanic rocks from the Tetagouche Group, Bathurst, New Brunswick, Canada: Canadian Journal of Earth Sciences v. 15, p. 207-219.

Whitney, J. A., Paris, T. A., Carpenter, R. H., and Hartley, M. E. III, 1978, Volcanic evolution of the southern Slate Belt of Georgia and South Carolina: a primitive oceanic island arc: Journal of Geology v. 86, p. 173-192.

Winchester, J. A., and Floyd, P. A., 1977, Geochemical discrimination of different magma series and their differentiation products using immobile elements: Chemical Geology v. 20, p. 325-343.

Windley, B. F., 1981, Precambrian rocks in the light of the plate-tectonic concept, in: Kroner, A., ed., Precambrian Plate Tectonics, Elsevier, N. Y., p. 1-20.

Wood, D. A., Gibson, I. L., and Thompson, R. N., 1976, Elemental mobility during zeolite facies metamorphism of the Tertiary basalts of eastern Iceland: Contributions to Mineralogy and Petrology v. 55, p. 241-254.

Zhang, G.-W., Bai, Y.-B., Sen, Y., Guo, A.-L., Zhou, D.-W., and Li,

T.-H., 1985, Composition and evolution of the Archean crust in central Henan, China: Precambrian Research v. 27, p. 7-35.